UAB
Universitat Autònoma de Barcelona

Immunosenescence and the prognosis of patients with respiratory infections

Immunophenotyping of elders with community acquired pneumonia and patients with common variable immunodeficiency

Teresa Franco Leyva

ADVERTIMENT. L'accés als continguts d'aquesta tesi queda condicionat a l'acceptació de les condicions d'ús establertes per la següent llicència Creative Commons:  https://creativecommons.org/licenses/?lang=ca

ADVERTENCIA. El acceso a los contenidos de esta tesis queda condicionado a la aceptación de las condiciones de uso establecidas por la siguiente licencia Creative Commons:  https://creativecommons.org/licenses/?lang=es

WARNING. The access to the contents of this doctoral thesis it is limited to the acceptance of the use conditions set by the following Creative Commons license:  https://creativecommons.org/licenses/?lang=en

Universitat Autònoma de Barcelona

Immunosenescence and the prognosis of patients with respiratory infections

Immunophenotyping of elders with community acquired pneumonia and patients with common variable immunodeficiency

Doctorate in Advanced Immunology

June 2026

Teresa Franco Leyva

DIRECTORS:

Laura Martínez Martínez, PhD

Olga H. Torres Bonafonte, PhD

Oscar de la Calle Martín, PhD

TUTOR:

Oscar de la Calle Martín, PhD

Department of Immunology

Hospital de la Santa Creu I Sant Pau

HOSPITAL DE LA SANTA CREU I SANT PAU

FUNDACIÓ DE GESTIÓ SANITÀRIA

UNIVERSITAT AUTÒNOMA DE BARCELONA

AKNODLEDGMENTS

Un viaje así de largo raramente se hace en solitario y yo he tenido la buena suerte de estar muy bien acompañada.

Primero, este trabajo existe por mis directores, Oscar, Laura y Olga. A Oscar, quien me convenció de entrar en el emocionante mundo de la inmunología y las inmunodeficiencias, por ser la persona ideal con quien filosofar de fisiopatología de la inmunología y emocionarnos juntos con las ideas nuevas. A Olga, por haber tenido el interés y el esfuerzo de estudiar a estos pacientes (qué suerte tienen contigo), por tu confianza en mí, por aportar tu visión de médico clínico y por tu comprensión siempre. Y especialmente a Laura, por tu confianza desde el primer momento, antes de que esto fuera un proyecto de tesis, por meterte en el mundo de la inmunosenescencia con Olga y contar conmigo para acompañarte, por ser faro del orden (que persigo con un éxito *relativo*) y por mantener la calma cuando el caos acontece para siempre llegar a puerto.

A Manuela, Vero, Gemma y Dani, porque no hubiera sido posible si no hubiera podido contar con vosotros acompañándome en el citómetro. A todas las técnicos del laboratorio por las sonrisas al saludar cada día, però especialment a la Eli, que és qui em va ensenyar a buscar mostres per primer cop, i a la Yoli, per les abraçades, els ànims i la fe. Cap a Galícia.

A las compañeras de despacho en estos últimos años, además de Laura: Anaís, Carmen y Esther. Los días son mejores por poder empezarlos con vosotras

También a todos los que fueron resis conmigo: Andrés, porque he agradecido ver a un amigo en cada seguimiento de tesis; a Leti, por el ejemplo de que el camino acaba; a Lio y Andi, por perseguir todo lo que es importante en la vida. Molt especialment a les resis a qui he tingut el privilegi de poder ensenyar alguna cosa com a adjunta i de les que he après encara més: Anna, Angi i Melisa, literalment no hauria pogut acabar això sense vosaltres i sabent que podía confiar en vosaltres.

A Nico, por enseñarme a usar R y sobre todo por recordarme a no tenerle miedo a no saber del todo cómo funciona la tecnología, porque siempre se puede aprender. Te debo ya como 5 desayunos al menos.

A Iván, porque no esperaba hacer un amigo fuera del laboratorio, y ahora te echo de menos. Gracias por los ánimos navegando esto y por tu honestidad siempre.

A Tania, porque le importa de verdad que consigamos llegar a buen puerto.

A mis amigos, por ser fuente de felicidad. A la Laura i la Júlia, per ser-hi sempre, sou dos sols a la meva vida. Ja ho sabeu però sempre em teniu també. A Edu y Guillem, por preguntarme si estoy haciendo tesis, y porque me dolería decepcionaros, igual que en el AOE. Al resto del team AOE: Wilhelm, Grifé, Cefe y Álvaro por el tiempo de alegría y de frustración a partes iguales. A los dos últimos y Ferran, Maria y Natalia, doctores del grupo, porque vuestro ejemplo siempre me motiva y por el acompañamiento

sabiendo como es el camino. A Lluís, por su alegría y por ser lo mejor de Madrid, aunque le echemos de menos. També pels amics IQS que em va adoptar com una més: Marga, Toni y Enric, per ser motivació i pels ànims, i a la Laura, que ha estat la més llesta de tots al no deixar-se enganyar. A Silvia, Sara e Ilana, porque me encanta ver la distinta forma de hacer medicina de cada una y porque cuando por fin nos vemos parece que no haya pasado el tiempo. A Julia R (de Reina), por las conversaciones infinitas, por recordarme la *sunk cost fallacy*, y por maravillarnos de todas nuestras etapas y evoluciones. A Noelia y Oscar, por seguir probando sitios y celebrando vida, ahora con Vicky. A Luisa y Artur, por las cenas que se alargan arreglando el mundo. A todos, por los ánimos siempre y porque nadie dudó en ningún momento, o por lo menos lo pareció.

A mi familia: al yayo, por sonreír cuando me ve aunque haya pasado demasiado tiempo. A mis tíos, por las velitas y por la ilusión que les hace mi dedicación a la ciencia; y a mis primas, que les daría igual pero lo celebran con toda la ilusión igualmente. A Ricard, por cuánto cree y apoya nuestro futuro, y a Ana, por evitarnos cocinar y encima comer de lujo, haciendo la vida más fácil.

Pero sobre todo, a mis padres y mis hermanos, Germán y Cristina, porque su preocupación no es que lo consiga o no, ya que no lo dudan, sino que no me pierda en el camino, y porque las cosas buenas que pueda tener en mí es gracias a vosotros. Gracias por ser refugio y la base en la que recargar, como dice Carlos.

A Marc, no podría tener más suerte. Fíjate que estás en todas las cajas y podría haber dicho tu nombre varias veces ya, en la de los amigos, los AOE, los IQS, los doctores y la de familia. Gracias por ser el mejor compañero de vida, por ver las luces y las sombras, porque sabes cuándo animarme a descansar o a apretar, porque sé que nos podemos turnar en tirar del carro según necesitemos y gracias por hacerlo tanto hacia el final de este camino. Gracias por la ilusión de las aventuras que nos quedan.

ABBREVIATIONS

ANOVA:	Analysis of Variance
APRIL:	A Proliferation-Inducing Ligand
AUC:	Area Under the Curve
BAFF:	B Cell Activating Factor
BCR:	B Cell Receptor
CAP:	Community-Acquired Pneumonia
CBA:	Cytometric Bead Array
CCR:	C-C Chemokine Receptor
CD:	Cluster of Differentiation
CI:	Confidence Intervals/Concordance Index
CM:	Central Memory
CMV:	Cytomegalovirus
CT:	Computed Tomography
CTLA:	Cytotoxic T-Lymphocyte–Associated Protein
CVID:	Common Variable Immunodeficiency
DCs:	Dendritic Cells
EBV:	Epstein–Barr virus
EDTA:	Ethylenediaminetetraacetic Acid
EM:	Effector Memory
ESID:	European Society for Immunodeficiencies
FOXP:	Forkhead box P
GLILD:	Granulomatous Lymphocytic Interstitial Lung Disease
HAP:	Hospital-Acquired Pneumonia
HCAP:	Healthcare-Associated Pneumonia
HEp:	Human Epithelial
HEXA	Sexagenarians
HIV:	Human Immunodeficiency Virus
HLA:	Human Leukocyte Antigen
IBD:	Inflammatory Bowel Disease
IEI:	Inborn Error Of Immunity
IFNγ:	Interferon Gamma
Ig:	Immunoglobulin
IL:	Interleukin
ILD:	Interstitial Lung Disease
IQR:	Interquartile Range
IRP:	Immune Risk Phenotype
IRT	Immunoglobulin Replacement Therapy
ITP:	Immune Thrombocytopenia
JAK:	Janus Kinase

LOCID:	Late-Onset Combined Immunodeficiency
LRBA:	Lipopolysaccharide-Responsive Beige-Like Anchor Protein
LWA:	Lyse Wash Assistant
MAIT:	Mucosal-Associated Invariant T Cells
MALT:	Mucosa-Associated Lymphoid Tissues
MHC:	Major Histocompatibility Complex
NF-κB:	Nuclear factor kappa B
NK:	Natural Killer
NLR:	Neutrophil-To-Lymphocyte Ratio
NONA:	Nonagenarians
OCTO:	Octogenarians
OR:	Odds Ratio
PBS:	Phosphate-Buffered Saline
PCA:	Principal Component Analysis
PCR:	Polymerase Chain Reaction
PD1:	Programmed Cell Death Protein 1
PI3K:	Phosphoinositide 3-Kinase
PSVD:	Porto-Sinusoidal Vascular Disease
RNH:	Regenerative Nodular Hyperplasia
ROC:	Receiver Operating Characteristic
RORγT:	*Retinoic Acid–Related Orphan Receptor Gamma T*
SASP:	Senescent Associated Secretory Phenotype
SA-T:	Senescence-Associated T cells
SD:	Standard Deviation
STAT:	Signal Transducer and Activator of Transcription
TACI:	TNF Receptor Superfamily Member 13B (TNFRSF13B)
Tc:	Cytotoxic T Cell
TCR:	T-Cell Receptor
TECs:	Thymic Epithelial Cells
TEMRA:	Effector Memory T Cells re-expressing CD45-RA
TGF:	Transforming Growth Factor
Th:	T-helper
TLR:	Toll-Like Receptor
TNF:	Tumor Necrosis Factor
TNFRSF:	Tumor Necrosis Factor Receptor Superfamily
TNFSF:	Tumor Necrosis Factor Superfamily
VAP:	Ventilator-Associated Pneumonia

1. CONTENT

AKNODLEDGMENTS II
ABBREVIATIONS V
INDEX OF FIGURES AND TABLES X
Index of Figures X
Index of Tables XII
Index of Supplementary Tables XIII
ABSTRACT XIV
RESUMEN XVI
RESUM XVIII
1. INTRODUCTION 1
1.1. Hallmarks of aging 1
1.2. The immune system 2
1.2.1. The organs 2
1.2.2. Cellular and soluble components 2
1.2.3. The innate and the adaptive immune system 3
1.3. Immunosenescence 4
1.3.1. Thymic involution 4
1.3.2. Late differentiated T cells 5
1.3.3. Immune Risk Phenotype 6
1.3.4. T-helper changes 6
1.3.5. B-cell and humoral function 9
1.3.6. Innate system 9
1.4. Community acquired pneumonia 9
1.5. Common Variable Immunodeficiency 11
1.5.1. Description and Epidemiological Context 11
1.5.2. Diagnosis 11
1.5.3. Clinical Manifestations 11
1.5.4. Etiology and the Genetic Landscape 14
1.5.5. Immunophenotyping and Patient Stratification 15
1.5.6. Treatment options 15
2. HYPOTHESIS AND OBJECTIVES 16
3. MATERIALS AND METHODS 18
3.1. PART I - CAP in aged people 18

3.1.1. Study design 18
3.1.2. Serum analysis 18
3.1.3. Flow cytometry analysis 19
3.1.4. Immune Risk Phenotype (IRP) 22
3.1.5. Data analysis and statistics 23
3.2. PART II - CVID 24
3.2.1. Study design 24
3.2.2. Flow cytometry analysis 24
3.2.3. Data analysis and statistics 30
4. RESULTS 31
4.1. PART I - CAP in aged people 31
4.1.1. Demographics 31
4.1.2. Immunoglobulin and complement 32
4.1.3. Leukocyte subpopulations 32
4.1.4. Lymphocytic subpopulations 36
4.1.5. Differentiated T cell subpopulations 40
4.1.6. Immune Risk Phenotype Markers 48
4.1.7. T-helper phenotype 50
4.1.8. Serum cytokines 52
4.2. PART II – Common Variable Immunodeficiency 54
4.2.1. Demographics 54
4.2.2. Clinical characteristics 54
4.2.3. Differentiated phenotype 56
4.2.4. Immune Risk Phenotype 57
4.2.5. T-helper phenotype 57
4.2.6. Individual variable correlation to clinical score 58
4.2.1. Phenotype clustering – Derivation cohort 59
4.2.2. Confirmation cohort 61
4.2.3. Genetic background 62
5. DISCUSSION 64
5.1. PART 1 - CAP 64
5.1.1. Humoral immune system 64
5.1.2. Myeloid – lymphoid axis 64
5.1.3. Lymphocyte subpopulations 65

5.1.4. The differentiated phenotype and the IRP 66
5.1.5. Etiology and specific immune response 68
5.1.6. Immune exhaustion vs immune resilience 69
5.2. Part II – CVID 69
5.2.1. Clinical phenotype 69
5.2.2. Differentiated T cells and IRP 70
5.2.3. Expanded lymphocytic phenotype complicated CVID vs LOCID 70
5.2.4. The complexity of CVID phenotypes 71
6. Conclusions 73
7. Bibliography 75
8. Annex 89

INDEX OF FIGURES AND TABLES

Index of Figures

Figure 1. The hallmarks of aging. Reference: Lopez-Otin et al 2023[3]. 2
Figure 2. T cell differentiation states. Figure made with ChatGPT (GPT-5.5) by the author, based on Strioga et al [36]. 6
Figure 3. T-helper subsets, their function, cytokine profile and characteristic surface cytokine receptors. Created with ChatGPT (GPT-5.5) by the author based on Sallusto et al, Kim et al, Aldrige et al [56,57,60]. 8
Figure 4. Clinical manifestations of Common Variable Immunodeficiency. Patients present typically with infections but up to 70% of them also present some form of non-infectious complication. Figure based on: Baumann et al [103]. 12
Figure 5. Genes in which defects have been described in Common Variable Immunodeficiency patients. From: Cunningham-Rundles et al [101]. 14
Figure 6. Gating strategy for the stages of differentiation of T lymphocyte populations. Lymphocytes were gated using forward scatter versus side scatter based on size and granularity. Afterwards, T cells were selected using CD3 positivity. Extended lymphocyte exhaustion phenotype subpopulations were assessed with different panels according to CD28 and CD27 expression as described Table 2. 21
Figure 7. Designed gating protocol for the T-helper analysis. Lymphocytes were gated using forward scatter versus side scatter based on size and granularity. Afterwards, T-helper cells were selected using CD4 positivity. Extended lymphocyte subpopulations were assessed with different panels as described in Table 2. 22
Figure 8. Designed gating protocol for the differentiated and memory T cell analysis. Lymphocytes were gated using forward scatter versus side scatter based on size and granularity after singlet gating over all events. Afterwards, T cells were selected using CD3 positivity. Extended lymphocyte subpopulations were assessed with different panels as described in Table 3. 27
Figure 9. Designed gating protocol for the T-helper analysis. Lymphocytes were gated using forward scatter versus side scatter based on size and granularity. Afterwards, T-helper cells were selected using CD4 positivity. Extended lymphocyte subpopulations were assessed with different panels as described in Table 2. 28
Figure 10. Designed gating protocol for the Tregs and Teffs cells analysis. Lymphocytes were gated using forward scatter versus side scatter based on size and granularity. Afterwards, $CD4^+$T cells were selected using CD4 positivity. Subpopulations were assessed with the CD45R0, CD25 and CD127 as described in Table 3. Tregs=regulator T cells, Teffs=effector T cells. 28
Figure 11. Designed gating protocol for the activated T cell analysis. Lymphocytes were gated using forward scatter versus side scatter based on size and granularity after singlet gating over all events. Extended lymphocyte subpopulations were assessed with different panels as described in Table 3. 28
Figure 12. Designed gating protocol for the B cell subpopulations analysis. Lymphocytes were gated using CD45 versus side scatter after singlet gating over all events. Afterwards, B cells were selected using CD19 positivity. Extended lymphocyte subpopulations were assessed with different panels as described in Table 3. 29

Figure 13. Sex stratified analysis of survival. T0: men (54%) vs women (38%). Log-rang test p=0.09 **(A)**; Fisher's exact test p=0.12 **(B)**. T1: men (39.6%) and women (19.5%). Log-rang test p<0.05 **(C)**; Fisher's exact test p<0.05 **(D)** 31
Figure 14. Blood cell count in the T0 cohort **(A)** and leukocyte distribution **(C)**. Grey bands indicate reference ranges for healthy individuals. Proportion of monocytopenia (<300 cells/μL) **(B)** and lymphopenia **(D)**.*p<0.05, **p<0.01, ***p<0.001, ns=non-significant. 33
Figure 15 ROC curve for total lymphocytes for two-year survival. AUC = 0.67. 33
Figure 16. Sex-stratified analysis from T0 cohort of lymphocytes **(A)** and neutrophil-to-lymphocyte ratio (NLR) **(B)**. *p<0.05, ***p<0.001, ns=non-significant. 34
Figure 17. Blood cell counts from T1 cohort **(A)** and percentage of leukocytes **(B)**. The grey bands indicate reference ranges for healthy individuals. *p<0.05, **p<0.01, ***p<0.001, ****p<0.0001, ns=non-significant. 35
Figure 18. Sex and sex-survival stratified analysis of total lymphocytes **(A)** and neutrophils **(B)** from T1 cohort. *p<0.05, **p<0.01, ns=non-significant. 35
Figure 19. Paired neutrophil absolute counts of survivors and non-survivors **(A)** and men and women **(B).** 36
Figure 20. Lymphocyte subsets in the T0 cohort, by cell counts **(A)**, and by percentage **(B)**. Grey bands indicate reference ranges for healthy individuals. *p<0.05, ***p<0.001, ns=non-significant. 37
Figure 21. Sex and survival stratified subanalysis of the lymphocyte subsets in the T0 cohort. Grey bands indicate reference ranges for healthy individuals. *p<0.05, **<0.01, ***p<0.001, ns=non-significant. 37
Figure 22. Paired analysis of lymphocytic subpopulations in total **(A)**, by survival **(B)** and by sex stratification **(C)**. 39
Figure 23**.** Early differentiated (EaT) ($CD27^+$ $CD28^+$), intermediate (InT) ($CD28^+$ $CD27^{neg}$), and late T cells (LaT) ($CD28^{neg}$ $CD2^{neg}$) at T0 (green) and at T1 (pink) in percentage over total T cells **(A)** and by cells/μL **(B)**. *** <0.0001. 40
Figure 24. $CD4^+$ and $CD8^+$ early ($CD27^+$ $CD28^+$) and late T cells ($CD28^{neg}$ $CD27^{neg}$) at T0 (green) and at T1 (pink) in percentage over total $CD4^+$ or $CD8^+$ T cells **(A)** and in cells/μL **(B)**. 41
Figure 25. Paired analysis of absolute counts of early, intermediate and late $CD4^+$T cells and $CD8^+$ T cells. Int=Intermediate, LaT=Late. *p<0.05, **p<0.01. 41
Figure 26**.** Sex-stratified analysis of early ($CD27^+$ $CD28^+$) and late T cells ($CD28^{neg}$ $CD27^{neg}$) at T0 and T1, in cells/μL for total $CD3^+$ T cells **(A)**, $CD4^+$ T cells **(C)**, $CD8^+$ T cells **(E)** and percentage over total $CD3^+$ T cells **(B)**, $CD4^+$ T cells **(D)** and $CD8^+$ T cells **(F)**. 43
Figure 27. Survival-stratified analysis of early and late T cell counts at T0. Green=survivors; Red=non-survivors. **<0.01, ***p<0.001 44
Figure 28. Survival-stratified analysis of early and late T cell counts at T1. Green=survivors; Red=non-survivors. **<0.01, ***p<0.001 44
Figure 29. Survival-stratified analysis of paired data of late T cell subpopulations. Green=survivors; red=non-survivors. *p<0.05 **<0.01, ns=non-significant. 45
Figure 30**.** Univariate Cox regression and concordance index (C-index) for early differentiated (early) ($CD27^+$ $CD28^+$) and late T cells (ExT) ($CD28^{neg}$ $CD27^{neg}$) at T0 **(A)** and T1 **(B)**. 47

Figure 31. ROC curves for predicting 2-year mortality by early T subpopulations. $CD8^+$T cells at T0 **(A)** and T1 **(B)**, $CD4^+$T cells at T0 **(C)** and at T1 **(D)**, and total early T cells at T0 **(E)** and T1 **(F)**. 48
Figure 32. Kaplan-Meier survival curves by immune-risk phenotype (IRP) positivity at T0 **(A)** and T1 **(B)**. No differences were found between patients with or without IRP at neither time-point. 49
Figure 33**.** Kaplan-Meier survival curves for the 5 clusters of patients with CAP based on their T-helper profiles (95% CI shown as dotted line). No significant differences were found between the clusters' survival curves. 52
Figure 34**.** Cytokines of each of the 5 clusters defined by T-helper profiles. Only significant finding was in IL-4 between cluster 1 and 4 ($p<0.05$). * = $p<0.05$. 53
Figure 35. Ages of men and women from the derivation and the confirmation cohorts. 54
Figure 36. Clinical score in our derivation and confirmation cohorts. No differences were found between cohorts. 55
Figure 37. Spearman's correlation of the cell phenotype cell count **(A)** and percentual **(B)** variables with the clinical score. *$p<0.05$. 59
Figure 38. Principal component analysis (PCA) showing the distribution of patients according to the k-means clustering solution. Shaded ellipses represent the 95% confidence region for each cluster. 60
Figure 39. ROC curve for defining the clinical score that distinguished the 2 phenotypic clusters. Cut-off point was established at 6.5, with 100% sensitivity and 77.8% specificity. AUC = 0.917. 60
Figure 40. Principal component analysis (PCA) showing the distribution of patients according to the k-means clustering solution. Shaded ellipses represent the 95% confidence region for each cluster. 61

Index of Tables

Table 1. Clinical criteria for a probable diagnosis of Common Variable Immunodeficiency, as defined by the European Society for Immunodeficiencies (ESID)[99]. 11
Table 2. Analyzed populations in the flow-cytometry assays. Lymphocytic subpopulations, T-helper and T differentiated studies "Diff."=differentiated 20
Table 3. Analyzed populations in the extended phenotype flow-cytometry assays. 27
Table 4**.** Lymphocytic subpopulations of men, women, survivors and non-survivors at T0. *$p<0.05$, **<0.01, ***$p<0.001$, ns=non-significant. 38
Table 5. IRP cell-count criteria on the paired cohort. Patients met 0, 1, 2 or 3 criteria at T0 (column) or T1 (row). Expressed as n(%), percentage relative to the overall paired cohort (n=46). 50
Table 6. Microbiological etiology of community acquired pneumonia in our cohort. Most were unknown. Out of the identified, Streptococcus pneumoniae and gram-negative bacteria (GNB) were the most prevalent. 50
Table 7**.** K-means clustering of patients with CAP based on T-helper profiles (A) and their mean values for each variable (B). 51
Table 8**.** Heatmap of the prevalence of the clinical characteristics of both derivation cohort and confirmation cohorts, and stratified by sex. PSVD: Porto-sinusoidal vascular disease. ILD: interstitial lung disease. IBD: inflammatory bowel disease. 55

Table 9. Heatmap of the prevalence of the clinical characteristics of complicated (≥9) and non-complicated (<9) CVID in the derivation and confirmation cohorts. PSVD: Porto-sinusoidal vascular disease. ILD: interstitial lung disease. IBD: inflammatory bowel disease. CVID: common variable immunodeficiency. *<0.05, **<0.01. ns=non-significant. 56
Table 10. T-helper subpopulations distribution within the derivation and confirmation cohorts. No differences were found between the cohorts. 57

Index of Supplementary Tables

Supplementary Table 1. Immunoglobulin and complement values from T0 and T1 by survival and sex stratification, expressed as mean and standard deviation. Significant p values are highlighted in green. 89
Supplementary Table 2. Leukocytes values from T0 by survival and sex stratification, expressed as median and interquartile range (IQR). Significant p values are highlighted in green. 89
Supplementary Table 3. Leukocytes values from T1 by survival and sex stratification, expressed as median and interquartile range (IQR). Significant p values are highlighted in green. 90
Supplementary Table 4. Paired analysis of leukocytes by survival and sex stratification, expressed as median and interquartile range (IQR). Significant p values are highlighted in green. 90
Supplementary Table 5. T differentiated cell values by T-helper clusters. 91
Supplementary Table 6. Cytokine median and interquartilic range of each of the 5 clusters defined by T-helper profiles.. *p<0.05, ns=non-significant 91
Supplementary Table 7. Cytokine levels of men, women, survivors and non-survivors. *p<0.05, **<0.01, ***p<0.001, ns=non-significant 91
Supplementary Table 8. Gender-stratified analysis of differentiated T cell subpopulations at T0. 92
Supplementary Table 9. Gender-stratified analysis of differentiated T cell subpopulations at T1. 93
Supplementary Table 10. Mean and U-Mann Whitney test for each variable included in CVID derivation cohort clustering. 94

ABSTRACT

As the world's population is aging, it becomes more relevant to understand its mechanisms. Aging is defined as a time-dependent functional decline. When aging affects the immune system specifically, it is referred to as immunosenescence, a process of progressive decline caused by age-related changes to both the innate and adaptive immunity and their balance. Ultimately, it causes a less efficient immune response to infection or vaccine responses, among others. Some of its characteristics include: a shift towards innate and myeloid responses at the expense of the adaptive responses, or the accumulation of $CD27^{neg}$ $CD28^{neg}$ late differentiated T cells, which arise from repeated antigen-restricted proliferation. Related to that, studies described an Immune Risk Phenotype (IRP) that predicted mortality in aged patients. It was defined by positive CMV serology and at least one of the following: CD4/CD8 ratio <1, $CD8^+$ T cells >600 cells/μL or $CD28^{neg}$ T cells >300 cells/μL. Since respiratory infections, mainly pneumonia, are one of the main burdens of disease in older people, we aimed to understand the impact of immunosenescence in patients with respiratory infections.

Common variable immunodeficiency (CVID) is the most prevalent symptomatic inborn error of immunity (IEI) and it is characterized by their humoral defect, with hypogammaglobulinemia, failed vaccine responses and recurrent respiratory infections. Therefore, they share many clinical characteristics to immunosenescent patients so we aimed to study them as a model for patients at risk ok respiratory infections. To that end, in this thesis we performed our studies in two parts.

In Part I, 162 patients older than 65 years-old hospitalized for community-acquired pneumonia (CAP) at the Hospital de la Santa Creu i Sant Pau between May 2019 and July 2021 were included prospectively. Blood count, lymphogram, immunoglobulins, complement factors, T helper distribution profiles, T cell differentiation phenotype and IRP were collected at two time-points: during CAP (T0), and at a 1-2 months follow-up (T1). Then, we followed-up their 2-year survival and compared the immune characteristics of survivors vs non survivors. A gendered stratified sub-analysis was also performed. We found that at T0, non-survivors presented higher neutrophil and lower lymphocyte percentages, with reduced T and B cell counts but comparable NK cells, consistent with the innate shift described in immunosenescence. Monocytopenia emerged as a particularly high-risk factor, while the neutrophil-to-lymphocyte ratio (NLR) was not informative at this timepoint. At T1, survivors recovered normal neutrophil counts and increased $CD8^+$ T and NK cell counts, whereas non-survivors failed to do so, confirming impaired immunoresilience; NLR became informative only at T1. The $CD4^+$ and $CD8^+$ compartments showed fundamentally different differentiation states. At both time-points, $CD4^+$ T cells were predominantly early differentiated, while $CD8^+$ T cells showed comparable proportions of early and late phenotypes. The absolute number of early differentiated T cells was the strongest predictor of 2-year all-cause mortality: proposed cut-offs were 532 cells/μL (total early T cells) or 416 cells/μL (early $CD4^+$ T cells) at T0; and 666 cells/μL (total early T cells) or 523 cells/μL (early $CD4^+$ T cells) at T1. Sex-stratified analysis was essential, as survivor women and non-survivor men drove the majority of differences across lymphocyte populations. Finally, the IRP was

not useful in this context, as lymphopenia in higher-risk patients prevented them from meeting cell-count criteria, thus reducing sensitivity precisely in those who needed it most.

In Part II, CVID patients were studied as a potential model for aged patients at risk of respiratory infections. First, 13 long-known patients with CVID were included for the creation of a clinical score and 9 new-diagnosis patients from 2022-2025 were included as a confirmation cohort. T, B and NK cells, B cell subpopulations and several T cell subset: memory T cell, T-helper subsets, Treg, activated T cells; differentiated T cell subsets were analyzed. We developed a clinical scoring system based on the presence or absence of: bronchiectasis, unusual infections, cytopenias, lmyphadenopathy, splenomegaly, porto-sinusoidal vascular disease, inflammatory bowel disease, interstitial lung disease and hematological or solid organ malignancy. A virtual panel for IEI over in-house clinical exome was performed to rule-out other IEI. The developed clinical scoring system discriminated complicated CVID at a threshold of 9 points. In the derivation cohort, complicated CVID showed a specific reduction in late-differentiated $CD4^+$ T cells compared to non-complicated CVID, suggesting a more prevalent immunosenescent state in the non-complicated group. The $CD4^+$ and $CD8^+$ differentiation pattern was comparable to that observed in the CAP cohort, with $CD4^+$ cells predominantly early differentiated and $CD8^+$ cells showing a balanced early/late distribution. The IRP did not discriminate between complicated and non-complicated CVID. Non-complicated patients showed a less activated T cell profile, with higher Th0 and lower HLA-DR^+CD38^+ $CD8^+$ T cell percentages. Naive and effector memory T cell subsets, activated T cell subsets, and naive and non-switched memory B cell subsets correlated independently with the clinical score. Unsupervised clustering identified two CVID clusters defined by the percentage of: NK cells, T helper subsets, Teff/Treg ratio, naive and intermediate $CD4^+$ T cells, and $CD21^{low}$ and transitional B cells. Cluster 1 showed a pro-inflammatory phenotype consistent with LOCID findings, but clustering failed to identify complicated CVID driven by immune dysregulation mutations, potentially placing these patients alongside a premature senescent-phenotype subgroup. No specific molecular defect underlying both CVID and an increased immunosenescent phenotype was identified in our cohort.

Taken together, these findings highlight the early differentiated T cell subset as a clinically actionable marker of immune competence across two distinct but physiologically related conditions, and highlight the value of immunophenotyping as a practical tool in the management of both elderly patients with infection and patients with CVID.

RESUMEN

A medida que la población mundial envejece, se va haciendo esencial comprender los mecanismos subyacentes a este proceso. El envejecimiento se define como un deterioro funcional progresivo a lo largo del tiempo. Cuando éste afecta específicamente al sistema inmunitario, se denomina inmunosenescencia, un proceso de deterioro causado por la edad que afecta tanto a la inmunidad innata como a la adaptativa y a su equilibrio. Poco a poco esto conduce a una respuesta inmune menos eficaz ante las infecciones o las vacunas, entre otros. Algunas de las características de la inmunosenescencia incluyen: un sesgo hacia una respuesta innata o mieloide en detrimento de la respuesta adaptativa, o la acumulación de linfocitos T tardíamente diferenciados $CD27^{neg}$ $CD28^{neg}$ por la proliferación repetida por reexposición a un mismo antígeno. De hecho, varios estudios han descrito un inmunofenotipo de riesgo (IFR) que predice la mortalidad en pacientes de edad avanzada. Se definió como: seropositividad a CMV y al menos uno de los siguientes criterios: ratio CD4/CD8 < 1, linfocitos T $CD8^+$ > 600 células/µL o linfocitos T $CD28^{neg}$ > 300 células/µL. Dado que las infecciones respiratorias, principalmente la neumonía, constituyen una de las principales causas de morbi-mortalidad en las personas mayores, nuestro objetivo fue comprender el impacto de la inmunosenescencia en estos pacientes.

En consonancia, la inmunodeficiencia común variable (IDCV) es el error innato de la inmunidad (EII) sintomático más prevalente y se caracteriza por su defecto humoral, con hipogammaglobulinemia, ausencia de respuesta vacunal e infecciones respiratorias recurrentes. Es decir, comparte varias características clínicas con los pacientes inmunosenescentes, por lo que nos propusimos estudiarla como modelo de pacientes con riesgo de infecciones respiratorias. Con este fin, en la presente tesis realizamos nuestros estudios en dos partes.

En la Parte I se incluyeron prospectivamente 162 pacientes mayores de 65 años hospitalizados por neumonía adquirida en la comunidad (NAC) en el Hospital de la Santa Creu i Sant Pau entre mayo de 2019 y julio de 2021. Se recogieron: hemograma, linfograma, inmunoglobulinas, factores de complemento, perfiles de linfocitos T-*helper*, fenotipo de diferenciación de linfocitos T e IFR en dos momentos: durante la NAC (T0) y en una visita de seguimiento 1-2 meses posterior (T1). Después, se realizó un seguimiento de su supervivencia a 2 años y se compararon las características inmunológicas de supervivientes y no supervivientes. También se llevó a cabo un subanálisis estratificado por sexo. Observamos que en T0, los no supervivientes presentaban porcentajes más elevados de neutrófilos y más bajos de linfocitos, con disminución de linfocitos T y B pero células NK comparables, hallazgos compatibles con el sesgo hacia la inmunidad innata descrito en la inmunosenescencia. La monocitopenia mostró ser un factor de riesgo especialmente elevado, mientras que el cociente neutrófilo-linfocito (CNL) no aportaba información en T0. En T1, los supervivientes volvieron a recuentos normales de neutrófilos y aumentaron su número de linfocitos T $CD8^+$ y NK, mientras que los no supervivientes no lo lograron, lo que confirmó una inmunorresiliencia deteriorada; el CNL únicamente mostró utilidad en T1. Los compartimentos de $CD4^+$ y $CD8^+$ mostraron estados de diferenciación fundamentalmente distintos. En ambos momentos, los linfocitos T $CD4^+$ eran predominantemente tempranos, mientras que los linfocitos T $CD8^+$ mostraron proporciones comparables de fenotipos tempranos y tardíos. El número absoluto de linfocitos T tempranamente diferenciados fue el predictor más potente de mortalidad por cualquier causa

a 2 años: se propusieron puntos de corte de 532 células/μL (linfocitos T tempranos totales) o 416 células/μL (linfocitos T $CD4^+$ tempranos) en T0; y 666 células/μL (linfocitos T tempranos totales) o 523 células/μL (CD4+ T tempranos) en T1. El análisis estratificado por sexo resultó esencial, ya que las mujeres supervivientes y los hombres no supervivientes explicaban la mayor parte de las diferencias observadas en las poblaciones linfocitarias. Por último, el IFR no resultó útil en este contexto, dado que la linfopenia presente en los pacientes de mayor riesgo les impedía cumplir los criterios de contaje celular, reduciendo así la sensibilidad precisamente en quienes más la necesitaban.

En la Parte II, los pacientes con IDCV fueron estudiados como posible modelo de pacientes de edad avanzada con riesgo de infecciones respiratorias. En primer lugar, se incluyeron 13 pacientes con IDCV de larga evolución para la creación de una escala clínica, y 9 pacientes diagnosticados entre 2022 y 2025 se incluyeron como cohorte de confirmación. Se analizaron linfocitos T, B y NK, subpoblaciones de linfocitos B y diversos subconjuntos de linfocitos T: linfocitos T de memoria, subpoblaciones T-helper, Treg, linfocitos T activados y linfocitos T diferenciados. Se desarrolló un sistema de puntuación clínica basado en la presencia o ausencia de: bronquiectasias, infecciones atípicas, citopenias, adenopatías, esplenomegalia, enfermedad vascular porto-sinusoidal, enfermedad inflamatoria intestinal, enfermedad pulmonar intersticial y neoplasias hematológicas o de órgano sólido. Se realizó un panel virtual para EII sobre exoma clínico casero para descartar otros EII. El sistema de puntuación clínica desarrollado discriminó la IDCV complicada con un umbral de 9 puntos. En la cohorte de derivación, la IDCV complicada mostró una reducción específica de los linfocitos T $CD4^+$ tardíamente diferenciados en comparación con la IDCV no complicada, lo que sugiere un estado inmunosenescente más prevalente en el grupo no complicado. El patrón de diferenciación $CD4^+$ y $CD8^+$ fue comparable al observado en la cohorte de NAC, con linfocitos T $CD4^+$ predominantemente tempranos y linfocitos T $CD8^+$ con una distribución equiparable de tempranos y tardíos. El IFR no discriminó entre IDCV complicada y no complicada. Los pacientes con IDCV no complicada mostraron menor activación de linfocito T, con mayor porcentaje de Th0 y menor porcentaje de células T $CD8^+$ $HLA\text{-}DR^+$ $CD38^+$. Los linfocitos T naïve y de memoria efectora, los linfocitos T activados y los linfocitos B naïve y de memoria sin cambio de clase se correlacionaron de forma independiente con la puntuación clínica. El análisis de clusterización no supervisado identificó dos grupos de IDCV definidos por el porcentaje de: células NK, subpoblaciones T-helper, cociente Teff/Treg, linfocitos T $CD4^+$ naïve e intermedios, y células B $CD21^{low}$ y transicionales. El cluster 1 mostró un fenotipo proinflamatorio compatible con LOCID, pero la clusterización no logró identificar la IDCV complicada causada por mutaciones de disregulación inmune, situando a estos pacientes junto al subgrupo que potencialmente presentaba un fenotipo de senescencia prematura. No se identificó ningún defecto molecular específico causante tanto de IDCV como de un fenotipo inmunosenescente en nuestra cohorte.

En conjunto, estos hallazgos destacan el papel de los linfocitos T tempranamente diferenciados como un marcador de inmunocompetencia clínicamente útil en dos entidades distintas pero fisiopatológicamente relacionadas, y resaltan el valor del inmunofenotipado como herramienta práctica en el manejo tanto de pacientes de edad avanzada con infecciones como de pacientes con IDCV.

RESUM

A mesura que la població mundial envelleix, comprendre'n els mecanismes esdevé cada vegada més rellevant. L'envelliment es defineix com un deteriorament funcional dependent del temps. Quan afecta específicament al sistema immunitari, en diem immunosenescència: un procés de declivi progressiu causat per canvis relacionats amb l'edat que afecten tant a la immunitat innata com a l'adaptativa i a l'equilibri entre totes dues. En darrer terme, provoca una resposta immunitària menys eficient enfront infeccions o vacunes, entre d'altres aspectes. Algunes de les característiques de la immunosenescència inclouen un biaix cap a una resposta innata i mieloide a expenses de la resposta adaptativa, o també l'acumulació de limfòcits T tardanament diferenciats $CD27^{neg}$ $CD28^{neg}$, que sorgeixen d'una proliferació per la reexposició enfront un mateix antigen de forma repetida. En relació amb això, diversos estudis van descriure un immunofenotip de risc (IFR) que predia la mortalitat en pacients d'edat avançada. Aquest fenotip es definia per serologia positiva per a CMV i almenys un dels criteris següents: quocient CD4/CD8<1, limfòcits T $CD8^+$ >600 cèl·lules/μL o limfòcits T $CD28^{neg}$ >300 cèl·lules/μL. Donat que les infeccions respiratòries, principalment la pneumònia, constitueixen una de les principals causes de morbi-mortalitat en les persones grans, ens vam proposar comprendre l'impacte de la immunosenescència en pacients amb infeccions respiratòries.

La immunodeficiència comuna variable (IDCV) és l'error innat de la immunitat (EII) simptomàtic més prevalent i es caracteritza pel seu defecte humoral, amb hipogammaglobulinèmia, resposta vacunal absent i infeccions respiratòries recurrents. Per tant, comparteix diverses característiques clíniques amb els pacients immunosenescents, i per això ens vam proposar estudiar-la com a model de pacients amb risc d'infeccions respiratòries. Amb aquesta finalitat, en la present tesi vam realitzar els nostres estudis en dues parts.

A la Part I, es van incloure prospectivament 162 pacients majors de 65 anys hospitalitzats per pneumònia adquirida a la comunitat (PAC) a l'Hospital de la Santa Creu i Sant Pau entre el maig del 2019 i el juliol del 2021. Es van recollir: hemograma, limfograma, immunoglobulines, factors de complement, perfils de limfòcits T-*helper*, fenotip de diferenciació de limfòcits T i IFR en dos moments: durant la PAC (T0) i en una visita de seguiment a 1-2 mesos després (T1). Posteriorment, es va realitzar un seguiment de la seva supervivència a 2 anys i es van comparar les característiques immunològiques de supervivents i no supervivents. També es va dur a terme una subanalisi estratificada per sexe. Vam observar que en T0, els no supervivents presentaven percentatges més elevats de neutròfils i més baixos de limfòcits, amb nombre reduït de limfòcits T i B però cèl·lules NK comparables, resultats compatibles amb el biaix cap a la immunitat innata descrit en la immunosenescència. La monocitopènia va mostrar ser un factor de risc especialment important, mentre que el quocient neutròfil-limfòcit (QNL) no va resultar discriminatori en aquest moment. En T1, els supervivents van tornar a valors normals de neutròfils i van augmentar el nombre de limfòcits T $CD8^+$ i NK, mentre que els no supervivents no ho van aconseguir, confirmant una immunoresiliència deteriorada; el QNL únicament va resultar útil en T1. Els compartiments T $CD4^+$ i $CD8^+$ van mostrar estats de diferenciació fonamentalment diferents. En tots dos moments, els limfòcits T $CD4^+$ eren predominantment primerencs, mentre que els limfòcits T $CD8^+$ mostraven proporcions comparables de fenotips primerencs i tardans. El nombre absolut de limfòcits T primerencs

va ser el predictor més potent de mortalitat per qualsevol causa a 2 anys: es van proposar punts de tall de 532 cèl·lules/μL (limfòcits T primerencs totals) o 416 cèl·lules/μL (limfòcits T $CD4^+$ primerencs) en T0; i 666 cèl·lules/μL (limfòcits T primerencs totals) o 523 cèl·lules/μL (limfòcits T $CD4^+$ primerencs) en T1. L'anàlisi estratificada per sexe va resultar essencial, ja que les dones supervivents i els homes no supervivents explicaven la major part de les diferències observades en les poblacions limfocitàries. Finalment, l'IFR no va resultar útil en aquest context, donat que la limfopènia present en els pacients de major risc els impedia complir els criteris de recompte cel·lular, reduint així la sensibilitat precisament en aquells que més la necessitaven.

A la Part II, els pacients amb IDCV van ser estudiats com a possible model de pacients d'edat avançada amb risc d'infeccions respiratòries. En primer lloc, es van incloure 13 pacients amb IDCV de llarga evolució per a la creació d'una escala clínica, i 9 pacients diagnosticats entre el 2022 i el 2025 es van incloure com a cohort de confirmació. Es van analitzar limfòcits T, B i NK, subpoblacions de limfòcits B i diversos subconjunts de limfòcits T: limfòcits T de memòria, subpoblacions T-*helper*, Treg, limfòcits T activats i limfòcits T diferenciats. Es va desenvolupar un sistema de puntuació clínica basat en la presència o absència de: bronquièctasis, infeccions atípiques, citopènies, adenopaties, esplenomegàlia, malaltia vascular porto-sinusoidal, malaltia inflamatòria intestinal, malaltia pulmonar intersticial i neoplàsies hematològiques o d'òrgan sòlid. Es va realitzar un panell virtual per a EII sobre exoma clínic intern per a descartar altres EII. El sistema de puntuació clínica desenvolupat va discriminar la IDCV complicada amb un llindar de 9 punts. En la cohort de derivació, la IDCV complicada va mostrar una reducció específica dels limfòcits T $CD4^+$ tardans en comparació amb la IDCV no complicada, la qual cosa suggereix un estat immunosenescent més prevalent en el grup no complicat. El patró de diferenciació dels limfòcits $CD4^+$ i $CD8^+$ va ser comparable a l'observat en la cohort de PAC, amb limfòcits T $CD4^+$ predominantment primerencs i limfòcits T $CD8^+$ amb una distribució equilibrada entre fenotips primerencs i tardans. L'IFR no va discriminar entre IDCV complicada i no complicada. Els pacients no complicats van mostrar un perfil amb menys activació de limfòcits T, amb percentatges més elevats de Th0 i més baixos de limfòcits T $CD8^+$ HLA-DR^+CD38^+. Els limfòcits T naïve i de memòria efectora, els limfòcits T activats i els limfòcits B naïve i de memòria sense canvi de classe es van correlacionar de manera independent amb la puntuació clínica. L'anàlisi de clusterització no supervisat va identificar dos grups d'IDCV definits pel percentatge de: cèl·lules NK, subpoblacions de limfòcits T-*helper*, quocient Teff/Treg, limfòcits T $CD4^+$ naïve i intermedis, i limfòcits B $CD21^{low}$ i transicionals. El cluster 1 va mostrar un fenotip proinflamatori compatible amb troballes descrites en LOCID. No obstant, la clusterització no va aconseguir identificar la IDCV complicada causada per mutacions de disregulació immunitària, situant aquests pacients en el mateix cluster que el potencial subgrup amb fenotip de senescència prematura. No es va identificar cap defecte molecular específic causant de la IDCV com de un fenotip immunosenescent prematur en la nostra cohort.

En conjunt, els nostres resultats destaquen els limfòcits T primerencs com un marcador de competència immunitària clínicament aplicable en dues entitats diferents però fisipatològicament relacionades, i subratllen el valor de l'immunofenotip com a eina pràctica en el maneig tant de pacients d'edat avançada amb infecció com de pacients amb IDCV.

1. INTRODUCTION

1.1.Hallmarks of aging

The world's population is aging. As the United Nations reports in their 2024 Revision of World Population Prospects, by 2080, people aged 65 or older will outnumber children under 18; by the mid 2030's they're expected to reach 265 million people aged 65 or older[1]. This demographic shift carries substantial implications for morbidity and for healthcare systems. Therefore, it is relevant to understand the underlying biological mechanisms associated with aging.

Aging is defined as a time-dependent functional decline that leads to a progressive loss of physiological integrity and increased vulnerability to human pathologies[2,3]. Hallmarks of aging must occur during normal aging, and its experimental reversal should delay it and promote a longer healthspan. Research has identified twelve hallmarks of aging that serve as common denominators across mammalian species: genomic instability, telomere attrition, epigenetic alterations, loss of proteostasis, disabled macroautophagy, deregulated nutrient-sensing, mitochondrial dysfunction, cellular senescence, stem cell exhaustion, altered intercellular communication, chronic inflammation and dysbiosis. These hallmarks are functionally grouped into:

- Primary hallmarks: the initiating causes of damage. They're comprised by genomic instability, telomere attrition, epigenetic alterations, loss of proteostasis and disabled macroautophagy.
- Antagonistic hallmarks: the compensatory responses that become deleterious when chronic. They include deregulated nutrient-sensing, mitochondrial dysfunction and cellular senescence.
- Integrative hallmarks: the end results ultimately responsible for the aging phenotype, which are stem cell exhaustion, altered intercellular communication, chronic inflammation and dysbiosis.

These hallmarks are interdependent and influence each other and yet, age-related human diseases are statistically more likely to co-occur and share genomic characteristics when they are causally linked to the same hallmark, rather than to different hallmarks[4]. Then, it is relevant to understand that aging is a complex process that has to be conceived as a whole.

Cellular senescence, specifically, is a key tumor-suppressive mechanism characterized by irreversible cell-cycle arrest, macromolecular damage, deregulated metabolism and a secretory phenotype[5]. It can be elicited by acute or chronic damage and is a major contributor to age-related changes across tissues as an antagonistic hallmark of aging[2,3]. Although, in humans, it mainly affects fibroblasts, endothelial cells, and immune cells, all cell types can undergo senescence during aging. The accumulation of senescent cells in the same tissue contributes to a loss of its functionality and integrity.

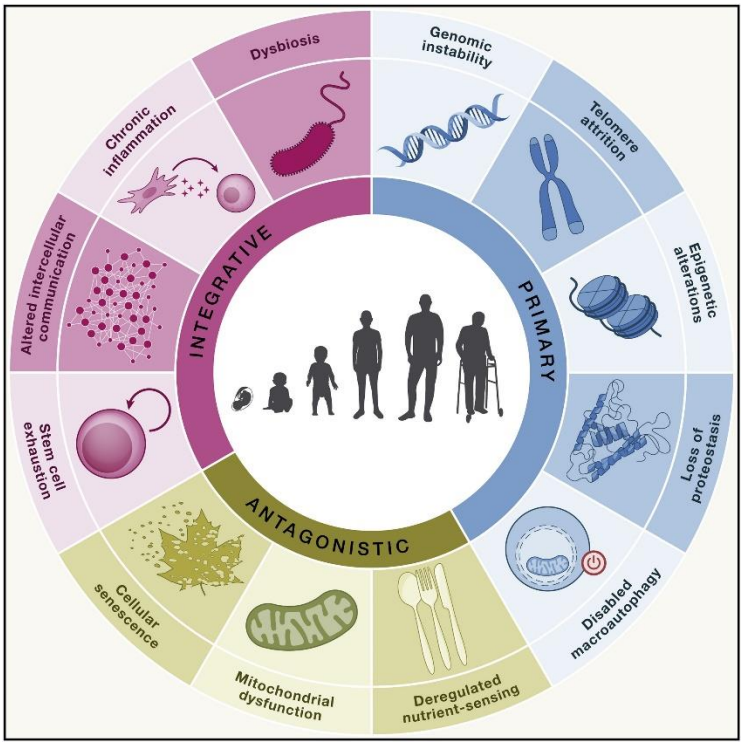


Figure 1. The hallmarks of aging. Reference: Lopez-Otin et al 2023[3].

1.2.The immune system

As every other tissue, the immune system ages too. The immune system is a highly coordinated network of organs, cells, and soluble molecules that protects the body against infections, eliminates damaged or abnormal cells, and contributes to tissue repair and homeostasis[6]. To achieve these functions, it must distinguish between self and non-self while maintaining tolerance to harmless antigens and the body's own tissues. Dysregulation of this balance can result in immunodeficiency, autoimmunity, allergy, or chronic inflammation[6].

1.2.1. The organs

The immune system is organized into specialized primary and secondary lymphoid organs. Primary lymphoid organs are responsible for the development and maturation of lymphocytes and include the bone marrow, where all blood cells originate and B cells mature, and the thymus, where T cells undergo selection and maturation. Secondary lymphoid organs, including the lymph nodes, spleen, and mucosa-associated lymphoid tissues (MALT) such as the tonsils and Peyer's patches, provide sites where immune cells encounter antigens and initiate adaptive immune responses. These organs are interconnected by the blood and lymphatic circulation, allowing efficient surveillance of pathogens throughout the body [6].

1.2.2. Cellular and soluble components

The immune response can be broadly divided into cellular and humoral components. The cellular components include neutrophils, macrophages, natural killer (NK) cells, and lymphocytes, which recognize and eliminate pathogens or infected cells. Humoral immunity is mediated by soluble factors

circulating in body fluids, antibodies produced by B lymphocytes and proteins of the complement system. These molecules facilitate pathogen neutralization, opsonization, and clearance, often acting in close cooperation with immune cells. Cytokines are also small soluble proteins that act as the primary communication signals of the immune system. Their secretion is dynamic and depends on the type of immune response that is triggered. They contribute to the initiation and amplification of the response because they allow immune cells that are physically distant from one another to exchange information thereby coordinating their activation, proliferation, differentiation, and migration. This ensures an effective and regulated immune response. In addition to mediating communication between immune cells, cytokines also facilitate interactions between the immune system and other tissues, including endothelial, epithelial, stromal, and parenchymal cells, linking immune responses to tissue homeostasis, repair, and inflammation[6].

1.2.3. The innate and the adaptive immune system

From a functional perspective, the immune system can be understood as two big categories: the innate and the adaptive immunity. Innate immunity provides a rapid, non-specific first line of defense through physical barriers, phagocytic cells, NK cells, and inflammatory mediators. In contrast, adaptive immunity is slower to develop but is highly specific and capable of generating immunological memory. Adaptive responses are mediated by B and T lymphocytes, allowing a more efficient response upon re-exposure to the same pathogen[6].

T lymphocytes play a central role in adaptive immunity. Each T cell expresses a unique T-cell receptor (TCR) capable of recognizing specific peptide antigens presented by major histocompatibility complex (MHC, or HLA in humans) molecules. Following antigen encounter, T cells undergo differentiation into distinct maturation stages that can be identified by their phenotype and function. Naive T cells ($CCR7^+$ $CD45RA^+$) have not yet encountered their cognate antigen and circulate between blood and secondary lymphoid organs[7–9]. Antigen presentation by professional antigen-presenting cells activates naive T cells, leading to their clonal expansion and differentiation into specialized subsets. $CD4^+$ T-helper cells coordinate immune responses through cytokine secretion, while $CD8^+$ cytotoxic T cells directly eliminate infected or malignant cells. Upon activation, some cells differentiate into central memory T cells ($CCR7^+$ $CD45RA^{neg}$) (CM), which retain high proliferative capacity and preferentially home to lymphoid tissues, providing long-term immunological memory. Others become effector memory T cells ($CCR7^{neg}$ $CD45RA^{neg}$)(EM), which migrate to peripheral tissues and can rapidly exert effector functions upon antigen re-encounter. The most differentiated subset, terminally differentiated effector memory cells re-expressing CD45RA ($CCR7^{neg}$ $CD45RA^+$) (TEMRA), displays immediate cytotoxic potential, reduced proliferative capacity, and is often expanded during chronic infections, aging, and persistent antigenic stimulation[7–10].

A specialized subset of $CD4^+$ T lymphocytes are regulatory T cells (Tregs), which play a central role in maintaining immune homeostasis and self-tolerance. Their function is to suppress excessive immune responses through direct cell-cell interactions and the production of inhibitory cytokines such as IL-10 and TGF-β[11]. By limiting the activation and proliferation of effector T cells, Tregs prevent autoimmunity and control tissue damage during inflammation. They are characterized by the expression of the transcription

factor FOXP3, and surface markers $CD25^+$ $CD127^{low/neg}$ [12]. Alterations in Treg number or function have been implicated in aging, autoimmunity, and primary immunodeficiencies[13–15].

B cells also undergo differentiation into distinct subsets that contribute to humoral immunity. Naive B cells (IgD^+ $CD27^{neg}$) are mature lymphocytes that have not yet encountered their specific antigen and continuously recirculate through secondary lymphoid organs. Following antigen recognition and activation, they can differentiate into antibody-secreting plasma cells and memory B cells, which can be divided into non-switched memory B cells (IgD^+ $CD27^+$) and switched memory B cells (IgD^{neg} $CD27^+$). Memory B cells persist long-term after antigen exposure and can rapidly reactivate upon re-encounter with the same antigen, generating a faster and more effective antibody response[16,17]. This immunological memory constitutes the basis for long-lasting protection after infection or vaccination[16–18].

1.3. Immunosenescence

When aging affects the immune system specifically, it is referred to as immunosenescence. As defined by Pawelec et al: “Immunosenescence is the impairment in immunity as a result of age-associated changes in function in a variety of cells: it is a phenomenon of decreased function, involving changes to both innate and adaptive immunity and a dysbalance between the two arms” [19]. Franceschi et al. add that immunesenescence is accompanied by “inflamm-aging”, a "low-grade chronic inflammation that consists of raised serum levels of pro-inflammatory cytokines (TNF-α, IL-6, IL-1β) in older adults”[20,21]. This inflammaging relates to the secretory phenotype of senescent cells and has also been identified as “SASP” Senescent Associated Secretory Phenotype [5]. The accumulated alterations can derive in a less efficient immune response to infection, but also to cancer and reduced vaccine responses [22–24]. Beyond its impact on host defense, immunosenescence acts as a driver for the senescence of solid organs by two main mechanisms. First, chronic SASP causes direct tissues damage. Second, the impaired immune system function results in a significant decline of the immune surveillance of tissues[25,26].

Immunosenescence, therefore, is the result of a gradual process that occurs throughout life and involves all components and cells of the immune system, and its study may help us understand or predict overall health. The first of these processes to appear is thymic involution.

1.3.1. Thymic involution

Thymic involution is one of the better-known processes the immune system undergoes with aging. In fact, at adolescence the thymic T-cell output is already half the rate at birth [27]. Although thymic involution’s primary cause was originally thought to result from the decreased capacity of T-cell progenitors to home and develop in the thymus, growing evidence support that age-dependent deterioration of the thymic epithelial cells (TECs) also plays an important part, as well as fibroblast compensation and accumulation of proinflammatory mature T cells [28–30]. Nonetheless, T cell numbers in healthy adults’ peripheral blood are maintained thanks to homeostatic proliferation, an autonomous antigen-independent proliferation of naive T cells. This process had already been observed in moderately lymphopenic patients that suffered thymectomy or γ-ray irradiation [28,31]. Homeostatic proliferation highly depends on the cytokines in the microenvironment but is different from antigen-derived proliferation since it is largely non-clonal and slow[28].

The progress of thymic involution and homeostatic proliferation may also increase the potential risk for the breakdown of self-tolerance and the development of autoimmunity [8,28] since they may cause a biased increase in the T-cell population bearing higher intrinsic affinity to self-HLA molecules [28,32].

In thymectomized mice, naive $CD8^+$ T cells with an elevated homeostatic proliferation have an increased capacity for TCR-mediated Interferon (IFN)γ and tumor necrosis factor (TNF)α production, as shown by Kato et al. This was attributed to an increase in $CXCR3^+$ cells in the naive $CD8^+$ T cell population and it lead to a predisposition to become Tc1 cytotoxic / inflammatory T cells [33]. On the contrary, naive $CD4^+$ T cells that endure persistent homeostatic proliferation become progressively dysfunctional after extensive cell divisions. It results in a reduced capacity to proliferate and differentiate even via optimal TCR signaling but also with an enhanced pro-inflammatory cytokine secretion [34]. This process is reminiscent of "inflammaging" and made the dysfunctional $CD4^+$ earn the name of "senescence-associated T cells (SA-T) [28].

However, thymic involution assessment has long been considered either highly invasive or inaccurate for routine clinical practice. Only very recently a study by Bernatz *et al* used machine learning to assess thymic involution by fatty degeneration in CT scans [35]. Therefore, multiple groups have focused on identifying peripheral immune biomarkers of biological aging.

1.3.2. Late differentiated T cells

Antigen-derived proliferation also appears to have an impact on aging. First, it is important to remember that the activation of T cells depends on the interaction of the TCR with a peptide bound to an HLA molecule. However, for this interaction to be effective, it needs the co-stimulating signal of CD28 interaction with CD80/86 [36]. An effective activation leads to antigen-restricted clonal proliferation and, in $CD8^+$ T cells, differentiation into cytotoxic or memory $CD8^+$ T cells. With reestimulation by the same antigen the cycle repeats, but, with each stimulation/proliferation round, CD28 expression is progressively and irreversibly down-regulated on the surface of $CD8^+$ T cells, eventually leading to the accumulation of highly antigen-experienced $CD8^+$ $CD28^{neg}$ T cells with critically shortened telomeres [36,37]. Thus, $CD8^+$ $CD28^{neg}$ T cells are defined as antigen-specific, highly oligoclonally expanded, terminally differentiated lymphocytes. This population only proliferate under specific conditions so they cannot be considered truly senescent but "exhausted" [36,38].

Second, CD27 is another costimulatory receptor that belongs to the tumor necrosis factor receptor superfamily (TNFRSF). It is constitutively expressed by several T-cell subsets, including naive $CD4^+$ and $CD8^+$ αβ T cells and regulatory T cells (Tregs), suggesting a role during the early stages of T-cell priming. However, its expression has also been shown to be progressively modulated during T-cell differentiation, with terminally differentiated effector populations showing reduced expression [39,40].

Therefore, it has been shown that with the combination of CD27 and CD28 expression, the $CD28^{neg}$ T cell population could be divided into more specific subpopulations, defining a pathway of T cell differentiation [36,38] : **$CD27^+$ $CD28^+$ early differentiated**, **$CD28^+$ $CD27^{neg}$ intermediate differentiated** and **$CD28^{neg}$ $CD27^{neg}$ late differentiated.**

The late differentiated subset is apoptosis-resistant and it accumulates with time. As a result, it is this particular subgroup of $CD28^{neg}$ T cells, rather than all of them, that behave as senescent T cells[41,42]. Consequently, in chronic viral infections, such as CMV or EBV but also HIV, where the T cells undergo many cycles of stimulation and proliferation as the ones described, the number of $CD8^{+}CD28^{neg}$ T cells are increased[36,43,44] (Figure 2). And yet, the total number of peripheral T cells is maintained, both by homeostatic proliferation and through regulated thymic feedback mechanism [36,44]. So, this accumulated $CD8^{+}$ $CD28^{neg}$ T cells end up taking up space from naive T cells, effectively reducing the person's TCR repertoire and worsening immunocompetence [36,44]. Therefore, they result in reduced overall immune response to novel pathogens, tumor cells and vaccines [45–49].

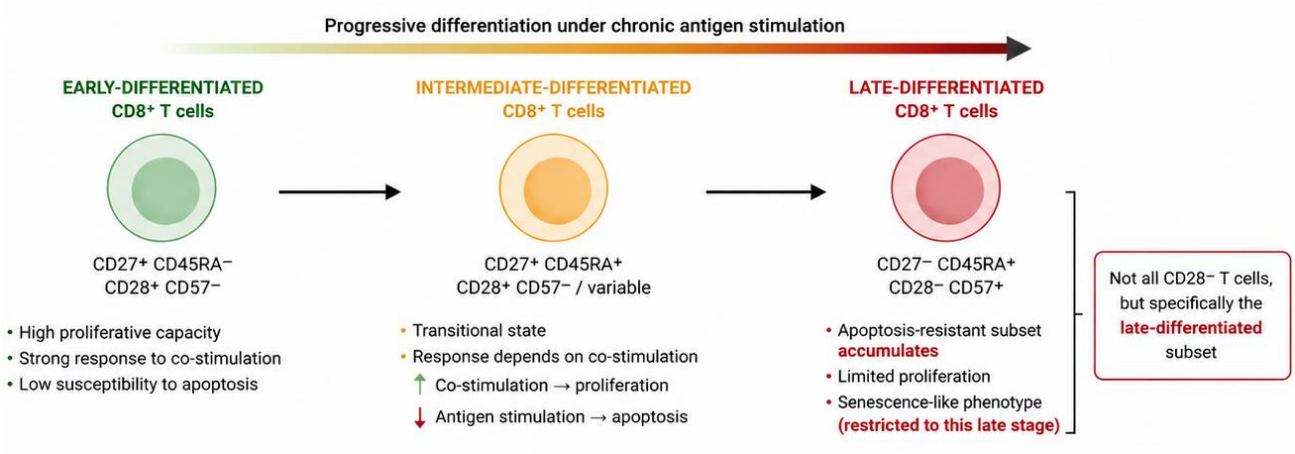


Figure 2. T cell differentiation states. Figure made with ChatGPT (GPT-5.5) by the author, based on Strioga et al [36].

1.3.3. Immune Risk Phenotype

Some of the earliest studies that tried to identify peripheral immune biomarkers of biological aging were performed by Wikby et al. through the 90's and early 2000's in Sweden. The Swedish OCTO, NONA and the later HEXA longitudinal studies considered different aspects of frailty focusing in octo, nona and sexagenarians. From their studies, they defined an Immune Risk Phenotype (IRP) that predicted increased 2-to-4-year mortality. IRP was characterized by high levels of $CD8^{+}$ T cells, low levels of $CD4^{+}$ T cells, a ratio of CD4/CD8<1 as a result, and poor proliferation responses [45,46,50]. Further characterization of the IRP linked this phenotype to the accumulation of $CD8^{+}$ $CD28^{neg}$ T cells and to persistent viral infections, particularly by CMV [47]. Thus, in clinical settings, the IRP has been operationally defined as positive CMV serology plus at least one of the following: CD4/CD8 ratio <1, $CD8^{+}$ T cells >600 cells/μL or $CD28^{neg}$ T cells >300 cells/μL [46,51]. The specific subpopulation of $CD8^{+}CD28^{neg}$ T cells links to the late differentiated T lymphocyte phenotype.

1.3.4. T-helper changes

Although, more pronounced in $CD8^{+}$ T cells, the loss of CD28 described above has also been observed in $CD4^{+}$ T cells. However, $CD4^{+}$ $CD28^{neg}$ T cells accumulate at a much slower rate, are less frequent in peripheral blood [36,44] and have been overall less studied. Other age-related changes have also been

reported within the $CD4^+$ T cell population, mainly involving shifts in the T-helper (Th) subset distribution. To frame these changes, Th subsets will first be briefly described. Although strictly defined by their cytokine secretory profile, the work of Federica Sallusto and colleagues have enabled their indirect identification by the expression of the surface cytokine receptors CXCR3, CCR4, CCR6 and CCR10 [52–55](Figure 3).

- Undifferentiated Th cells have been considered **Th0**. They are naive $CD4^+$ T cells that have yet to be stimulated and have not shown a secretory cytokine profile nor specific surface markers usually related to other subsets [56].
- The **Th1** subset is critical for the clearance of intracellular pathogens. Their differentiation is triggered by IL-12 and IFNγ through the induction of transcription factor T-bet. They are characterized by the production of IFNγ and by the expression of the surface cytokine receptor CXCR3, which is crucial for the recruitment of Th1 cells in the inflamed tissue and also expressed in $CD8^+$ T cells [55,57].
- The **Th2** subset is important for the elimination of helmintic parasites and is highly involved in atopia and allergy. Their differentiation is triggered by IL-4 through the transcription factor GATA3. They are characterized by the production of IL-4 as well as the expression of the surface cytokine receptor CCR4, which is also expressed in the thymus and the spleen so it may be related to the process of T-cell education and differentiation in the thymus [57].
- **Th17** cells are strong inducers of local tissue inflammation and seem to be critical in the response against infection but also in autoimmunity. Their differentiation is triggered by IL-6, low levels of TGF-β and IL-23, through the induction of the transcription factor RORγT [57]. They are characterized by the production of IL-17 and they can be identified by the expression of the surface cytokine receptor CCR6 and CCR4 [58].
- There seems to be an intermediate **Th1/Th17** hybrid subset. It is induced by IL-12 and IFNγ, and it expresses T-bet as well as RORγT, IL-23R and surface markers CXCR3 and CCR6. It also produces IFNγ [58]. Since Th17 are a highly plastic subset it has been suggested that, in humans, a developmental or functional relationship between Th17 and Th1 may exist [54,58].
- Although less explored, an intermediate **Th1/Th2** subset has also been described. They have been named “non-classical Th2” and they are characterized by dual expression of surface markers CXCR3 and CCR4, as well as the production of both IFNγ and IL-4 [59].
- Other minor Th subsets, such as Th9 or Th22, have been described. However, they are mainly found in tissues and seem to be poorly represented in peripheral blood [57,58,60].

T-helper subsets are fairly stable but they retain some plasticity that allows them to transition between phenotypes. The Th1/17 subset described may be an example, as well as the T cells co-expressing Th1 and Th2 surface cytokines and co-secretion of IFNγ and IL-4, especially early after the initial stimulation of naive T cells [61].

So, aging is associated with shifts from Th1 to Th2 cytokine profiles in response to immune stimulation [22,62]. However, the number of circulating Th1 and Th2 seem to be maintained while the Th17 population diminished [21,63]. The changes in the Th17 population are controversial since two other groups reported

that Th17 responses were increased in the elderly [21,64]. At the same time, Th17 cells have also been associated with Treg balance and inflammaging [22,65].

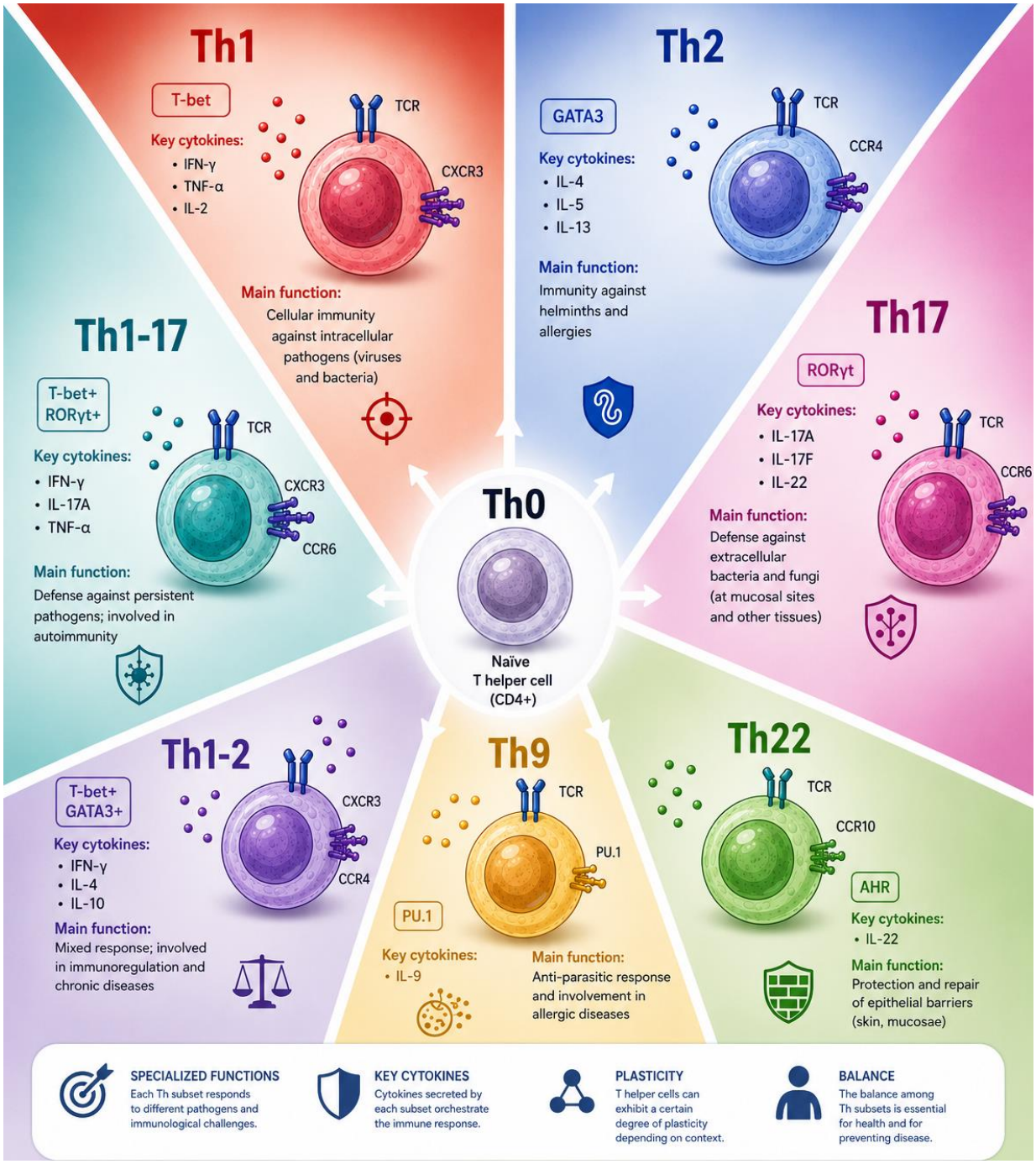


Figure 3. T-helper subsets, their function, cytokine profile and characteristic surface cytokine receptors. Created with ChatGPT (GPT-5.5) by the author based on Sallusto et al, Kim et al, Aldrige et al [55,56,59].

1.3.5. B-cell and humoral function

Not only T cells are affected by age. Global lymphocytic decrease in peripheral blood has been reported in relation to a progressive decline in regenerative capacity of hematopoietic stem cells and a shift toward myeloid-biased differentiation [22]. Thus, B cells and the humoral immune function are also affected. Multiple studies show that, with age, there is a decrease in the number and percentage of circulating B cells [23]. Not only that, but this reduction is also accompanied by a loss of naive B-cells and an increase in memory cells with age [22], as well as a diminished BCR repertoire. This decline is further exacerbated by a continuous decrease in peripheral maintenance factors essential for naive cell survival, such as B cell activating factor (BAFF) and APRIL, which correlate with reduced B cell longevity in older adults [66]. As a result, there is an impaired response to novel antigens decreased antibody responses, a reduced production of high-affinity antibodies and a shift toward the production of low-affinity IgM and self-recognizing (autoreactive) antibodies [22,23,67]. In fact, impaired B-cell homeostatic regulation, together with their interactions with senescence-associated T cells within germinal centers, contributes to the systemic pro-inflammatory state (inflamm-aging) and the heightened risk of autoimmunity observed in older individuals [67]. Furthermore, while memory B cell frequencies may appear stable, there is a distinct defect in their ability to differentiate into antibody-secreting plasma cells [66]. This is reflected in poor response to vaccination apparent in elderly people [23,49,67,68]. Notably, however, memory cells produced early in life remain normal [22].

1.3.6. Innate system

As described before, due to progressive decline of bone-marrow hematopoietic stem cells, aging seems to favor the production of myeloid cells in peripheral blood [24,48,69]. Thus, the number of macrophages, dendritic cells (DCs) and neutrophils but also of NK cells, increases [21–23].

The degree of such myeloid/lymphoid dysbalance has been reflected on the neutrophil-to-lymphocyte ratio (NLR). This ratio has been explored as non-specific prognostic factor across many settings, including sepsis and cancer [70–73].

While the number of myeloid cells increases, their function paradoxically declines [21–23]. For example, TLR functionality is reduced: TLR1 responses are significantly impaired when measured in older individuals as compared to younger adults; and TLR4 expression, essential for the response to *Streptococcus pneumoniae*, has also been described to be diminished among the elderly and during infection [22,74]. Moreover, macrophages have shown a reduced ability to secrete TNF and a reduced phagocytic activity**,** neutrophils migrate less and DCs have impaired antigenic presentation [22,23,68].

1.4.Community acquired pneumonia

We established that aging and immunosenescence could cause a worse response to infection and new pathogens. This reality was starkly illustrated by the COVID-19 pandemic, where elderly individuals were disproportionately affected by severe respiratory disease and mortality [75,76]. But even before it, the

World Health Organization registered that in 2000-2016, lower respiratory infections - mainly pneumonia - have been one of the leading causes of mortality worldwide in adults of 60 years or older [23,66,77].

Pneumonia is an infection of pulmonary parenchyma and the most severe form of respiratory infection. It is typically classified as: community acquired (CAP), hospital acquired (HAP), ventilator-associated (VAP) and health care–associated pneumonia (HCAP) [78]. CAP is the most frequent among them. In Spain in 2023, 5.0 cases of pneumonia per 1,000 inhabitants were recorded excluding COVID19 cases, (men: 4.9 and women: 5.0%), with the highest incidence in children and the elderly, even reaching over 1% in elders >80 years-old[79]. Although there are many potential etiological pathogens for pneumonia, most cases of CAP are produced only by a few of them. Those are usually classified as "typical" (*Streptococcus pneumonia, Haemophilus influenzae, Staphylococcus aureus, Klebsiella pneumoniae* and *Pseudomonas aeruginosa*) and "atypical" (*Mycoplasma pneumoniae, Chlamydia pneumoniae*, Legionella species and respiratory viruses such as influenza viruses, SARS-CoV-2, adenoviruses, human metapneumovirus, and respiratory syncytial viruses) [78].

The clinical presentation of CAP may include: fatigue, confusion, headache, myalgia, arthralgia, fever, tachycardia, chills, sweats, cough either productive or nonproductive, shortness of breath (dyspnea), or pleuritic chest pain. Up to 20% of patients may have gastrointestinal symptoms such as nausea, vomiting, and/or diarrhea [78].

The diagnosis of CAP is based on clinical history, physical examination with abnormal auscultation and opacities or other alterations in the chest radiography. The etiologic diagnosis includes Gram's stain, culture of the sputum and urinary antigen tests. The studies may be broadened, if needed, with serology or PCR tests for the suspected pathogens. Although clinical, epidemiologic and risk factors may suggest certain pathogens, unfortunately, the pathogen at fault in a case of CAP is difficult to establish with certainty; in more than one-half of cases, a specific etiology is never determined [78]. Since the COVID-19 pandemic, greater emphasis has been made to establish an accurate etiological diagnosis, expanding everyday screening to viral pathogens, often with bedside tests [80,81].

The susceptibility of elderly people to pneumonia is likely multifaceted. It may involve an impaired mucosal barrier, reduced mucociliary clearance, and blunted airway immune and inflammatory responses on exposure to potentially pathogenic microorganisms [22,82]. On the immunological aspect, lymphopenic pneumonia has been linked to higher mortality [83,84]. Many of these alterations are part of the development of frailty. Frailty is the "geriatric state associated with increased vulnerability to internal and external stressors resulting from a significant loss of physiological reserve" [67]. Many pathophysiological factors underlie the frailty syndrome, including some of the defined hallmarks of aging such as dysregulation of inflammatory processes, oxidative stress, mitochondrial dysfunction and cellular senescence [67,85]. However, it is a holistic syndrome also influenced by several other factors, including sociodemographic characteristics, psychological conditions, sedentariness, comorbidities and nutritional status [67,86]. In fact, low intake of certain micronutrients such as vitamin B6, B12, folate, or zinc is associated with a higher risk of developing frailty [67,87].

1.5.Common Variable Immunodeficiency

1.5.1. Description and Epidemiological Context

Common Variable Immunodeficiency (CVID) is an inborn error of immunity (IEI). It has an estimated prevalence of 1:10,000 and 1:50,000 worldwide, making it the most frequent clinically relevant IEI [88]. While it can manifest at any age, it typically manifests in adulthood between the second and fourth decades of life [89]. It is characterized by significant hypogammaglobulinemia, and a profound failure in specific antibody production following vaccination or natural infection, and, as the name states, it shows with many variable clinical presentations.

1.5.2. Diagnosis

In contrast with the majority of IEI, where a monogenic defect defines the diagnosis, only 20-30% of patients with CVID reach a definitive molecular and genetic diagnosis, and it is thought to be caused by polygenic defects [90–92]. Thus, the diagnosis is met by clinical criteria. Clinical criteria for a probable diagnosis of Common Variable Immunodeficiency, as defined by the European Society for Immunodeficiencies (ESID) are [93]:

At least one of the following: • increased susceptibility to infection • autoimmune manifestations • granulomatous disease • unexplained polyclonal lymphoproliferation • affected family member with antibody deficiency
AND marked decrease of IgG and marked decrease of IgA with or without low IgM levels (measured at least twice; < 2SD of the normal levels for their age);
AND at least one of the following: • poor antibody response to vaccines (and/or absent isohemagglutinins); i.e., absence of protective levels despite vaccination where defined • low switched memory B cells (<70% of age-related normal value)
AND secondary causes of hypogammaglobulinemia have been excluded (e.g., infection, protein loss, medication, malignancy)

Table 1. Clinical criteria for a probable diagnosis of Common Variable Immunodeficiency, as defined by the European Society for Immunodeficiencies (ESID)[93].

While useful for clinical practice, those criteria are still broad enough to make the CVID diagnosis an umbrella term under which probably encompasses many different molecular defects. This is underscored by the heterogeneity of the clinical evolution and complications of these patients.

1.5.3. Clinical Manifestations

As the “variable” part of the name reflects, clinical presentation is highly heterogeneous and is represented in Figure 4.

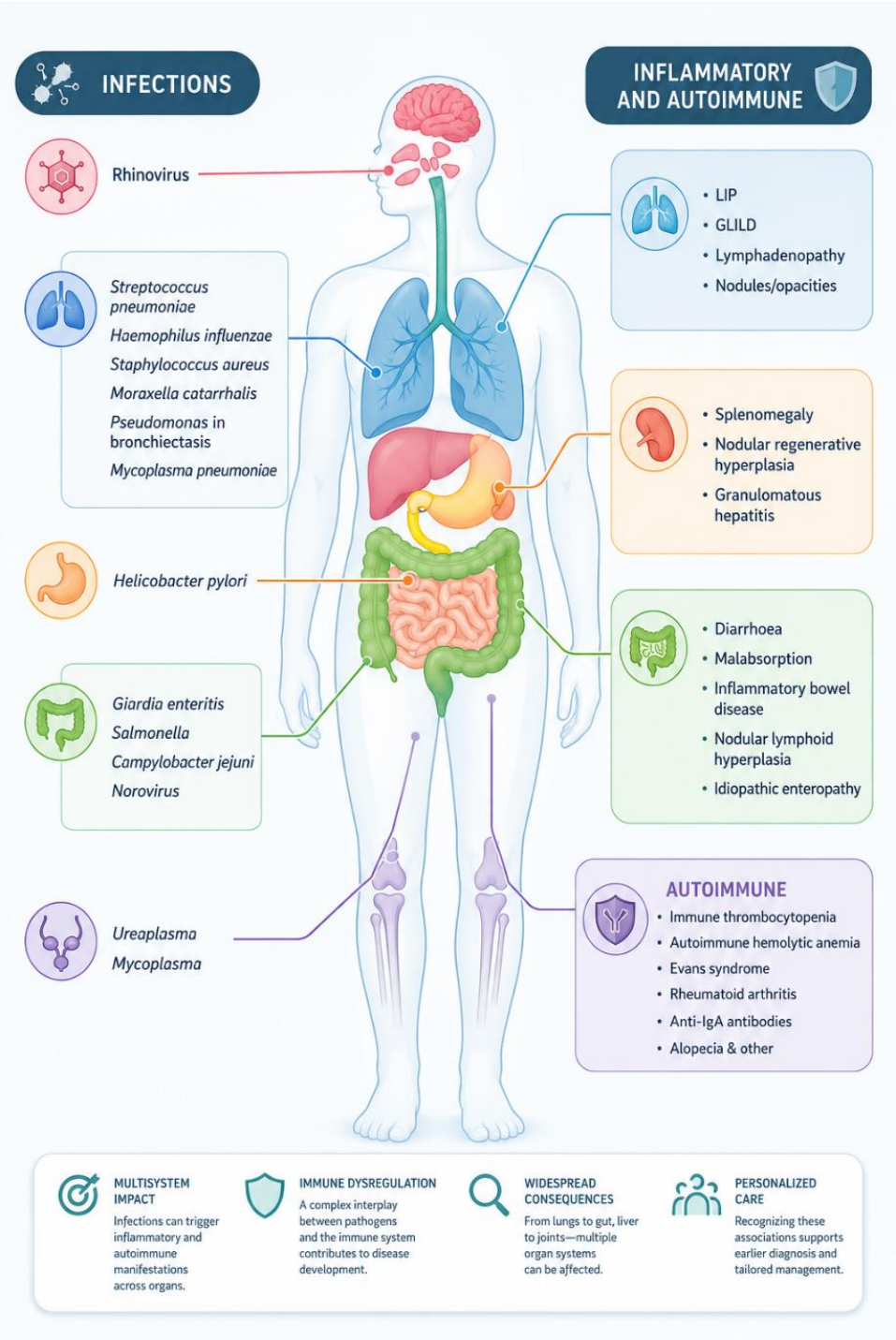


Figure 4. Clinical manifestations of Common Variable Immunodeficiency. Patients present typically with infections but up to 70% of them also present some form of non-infectious complication. Figure based on: Baumann et al [94].

Patients present typically with recurrent infections, the most common being respiratory infections manifesting as sinusitis, bronchitis, pneumonia and, ultimately, chronic bronchiectasis [88,89,95,96]. The most common pathogens include bacteria such as *Streptococcus pneumoniae* and *Haemophilus influenza* [91,94,97]. The second most common target is the gastrointestinal tract in the form of gastritis or enteritis. In this case the pathogens involved are more diverse, including bacteria like *Helicobacter pylori*, parasites

such as *Giardia enteritis* or virus like norovirus. Over 90% of patients suffer from upper and lower respiratory tract infections and/or gastrointestinal infections [89,94].

However, the clinical spectrum is expanded by the non-infectious complications. Approximately 70% of CVID patients exhibit symptoms of immune dysregulation, including autoimmunity, lymphoid hyperplasia, and malignancy. These patients generally have poorer prognosis and require more intensive, often invasive, management compared to those with an "infection-only" phenotype, who typically respond well to immunoglobulin replacement therapy (IRT) [88,89,94].

Autoimmunity can be found in 20-30% of patients, of which the most frequent manifestations are autoimmune cytopenias, such as immune thrombocytopenia (ITP) and Evans syndrome. Autoimmunity can even be the presenting feature of CVID, sometimes occurring before the development of hypogammaglobulinemia [88].

Lymphoid proliferation in the form of lymphadenopathy or splenomegaly are also common findings within CVID patients, present in 20%. Although generally avoided, some patients might even need splenectomy due to uncontrolled cytopenias, hypersplenism or to rule-out splenic lymphoma [88,96,98].

Granulomatous disease has been described to affect up to 9.3% of patients in some cohorts, although it is suspected to be underdiagnosed given that is a histologic finding and patients do not undergo routine biopsies. It typically consists of well-formed non-caseating granulomas and can sometimes be mistaken by sarcoidosis, delaying the diagnosis of CVID [88]. Its lung presentation is granulomatous lymphocytic interstitial lung disease (GLILD) and is one of the most severe forms of granulomatous disease [88,99–101]. It is characterized by profound pulmonary infiltration of T and B cells, occurs in approximately one-third of CVID patients with lung complications and significantly shortens survival. Research has highlighted the role of the IFNγ:STAT1:BAFF axis in driving pulmonary B-cell hyperplasia, and indeed B-cell depletive therapies like Rituximab are being used effectively in managing these complications [95,102,103].

Up to 30% of patients may show chronic lung disease, including the aforementioned bronchiectasis and GLILD but also lymphoid interstitial pneumonia or other interstitial lung disease (ILD) with ground glass opacities, pulmonary nodules or mediastinal lymphadenopathy [88,104].

Similarly, patients may show many non-infectious complications of the gastrointestinal tract that may include: autoimmune gastritis or enteropathy, inflammatory bowel disease, nodular lymphoid hyperplasia of the intestine, or malabsorption syndromes [88,96,105]. Not only that, but at least 10% of patients present with liver involvement in the form of granulomas, autoimmune hepatitis, fibrosis, and porto-sinusoidal vascular disorder (PSVD), the latter usually associated with the histological finding of regenerative nodular hyperplasia (RNH) [88,96,106–108]. Furthermore, CVID patients have a heightened risk of gastric adenocarcinoma that also occurs at a significantly younger age (median 43 years) compared to non-CVID patients (median 75 years). Pathogenesis is closely linked to Helicobacter pylori infection and the dysfunctional immune microenvironment in the gastric mucosa [109].

CVID patients face a 10 to 47-fold increased risk of malignancy compared to the general population and is reported to present in 10-15% of patients [88,96,109]. Lymphoma is been reported to affect around 6-

8% of patients, depending on the cohort [88,96,110,111]. Most cases are non-Hodgkin lymphoma, followed by Hodgkin lymphoma. Solid-organ cancers are also prevalent overall, but without a specific preference for any of them, which probably reflects a defect of immunovigilance more than a specific solid-organ defect [88,96,109,111].

1.5.4. Etiology and the Genetic Landscape

The pathogenesis of CVID is rooted in defective B-cell differentiation, specifically the inability of B cells to mature into memory B cells and immunoglobulin-secreting plasma cells. While the defining trait is humoral deficiency and B cell altered phenotype, it is increasingly recognized that many patients also harbor significant defects in the T cell compartment and innate immunity, contributing to the complex clinical landscape [89,96,112,113].

Although most patients never reach a definitive molecular diagnosis, more than 60 monogenic causes have been identified to date [92,96,98,114,115]. The identified mutations are found in genes codifying for proteins essential for:

- B-cell maturation and costimulation: CD19, CD20, CD21, and CD81 [92,96].
- TNFSF receptors and ligands: TACI (TNFRSF13B), where monoallelic or biallelic mutations are found in 5-10% of patients, and BAFF-R (TNFRSF13C) [92,95].
- Signaling and metabolic regulators: PI3K (leading to APDS), NF-κB1, and NF-κB2 [92,96,98].

In some patients presenting with CVID, the identification of genetic and molecular defects led to a reclassification of their disease. This occurred, for example, with defects related to dysregulation pathways and Treg cells, such as LRBA deficiency, CTLA4 haploinsufficiency or STAT3 gain-of-function defects [92,96,116]. The wide spectrum of genetic diseases is illustrated in Figure 5.

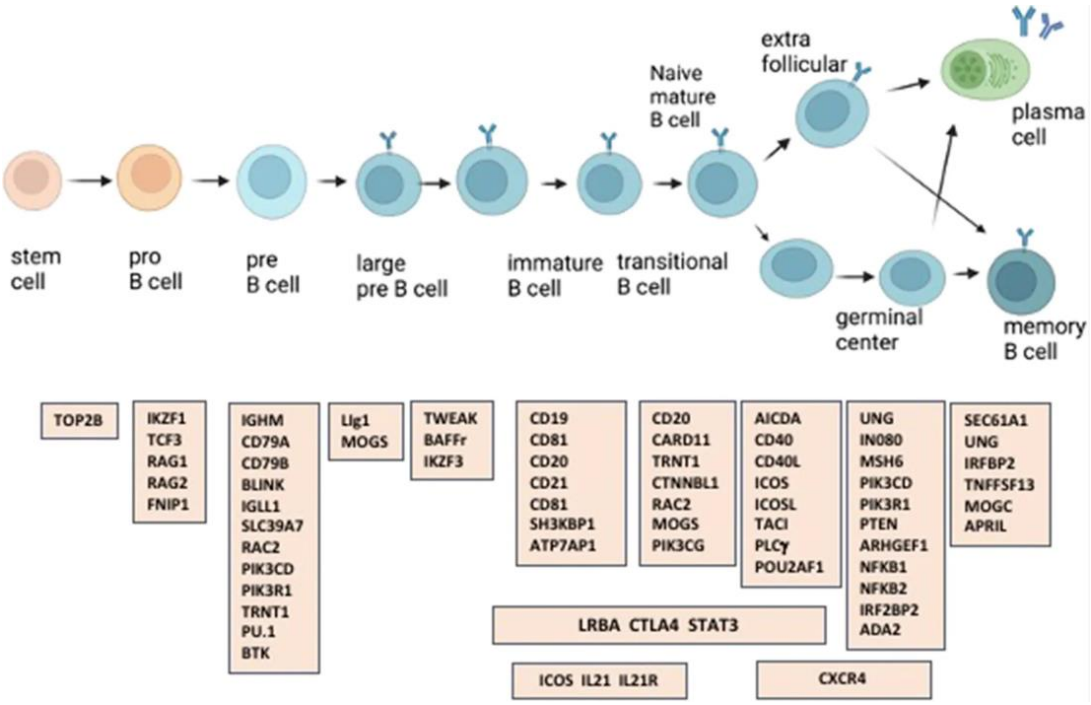


Figure 5. Genes in which defects have been described in Common Variable Immunodeficiency patients. From: Cunningham-Rundles et al [96].

1.5.5. Immunophenotyping and Patient Stratification

Given the heterogeneity and complexity of CVID, the major clinical challenge that arises is predicting the prognosis of patients. Since clinical features are either too generic or too heterogeneous and genetic findings are limited, several classification schemes have been developed based on B-cell and T-cell phenotypes:

Approximately 75% of CVID patients exhibit a profound loss of class-switched memory B cells ($CD19^+$ $CD27^+$ IgD^-). Reduced numbers of non-switched memory B cells ($CD19^+$ $CD27^+$ IgD^+) are also frequently observed [96,117]. A significant subset of patients shows an expansion of $CD21^{low}$ B cells ($CD19^+$ $CD38^{low}$ $CD21^{low}$). These cells are considered pre-activated, partially autoreactive, and prone to homing into peripheral tissues. An expansion of $CD21^{low}$ B cells is strongly associated with autoimmunity, splenomegaly, and GLILD [89,117,118]. Furthermore, increased frequencies of transitional B cells ($CD19^+$ $CD24^{high}$ $CD38^{high}$) have been noted, regardless of whether the patient presented with autoimmunity [118].

Changes in the T cell compartment have also been described. First, patients with immune dysregulation often show an extreme depletion of naive $CD4^+$ T cells (often below 10%) with predominance of $CCR7^{neg}$ effector-memory T cells, and reduced percentages of Tregs ($CD4^+$ $CD25^+$ $CD127^{low}$). The remaining Tregs may also show reduced suppressive capacity [96,109,119,120]. Moreover, many patients exhibit a skewing toward a Th1 profile, characterized by increased IFNγ production [95,117,118].

Thus, schemes like Freiburg, Paris, and EUROClass relied on the quantification of switched memory B cells and $CD21^{low}$ B cells to classify patients [121–123], while the loss of naive T cells have sparked debate over whether these patients should be reclassified as late-onset combined immunodeficiency (LOCID) [124].

1.5.6. Treatment options

The cornerstone of treatment for CVID is immunoglobulin replacement therapy, which effectively compensates for their humoral deficiency and reduces the frequency and severity of infections [125,126]. Additional management may include antimicrobial prophylaxis and specific treatment of the multiple non-infectious complications [100,103,127]. Although, as established, the majority of patients never reach a definitive molecular diagnosis, it is clinically relevant to still try to identify them since some of these patients may benefit from precision medicine approaches. That is, there are some targeted therapies directed at specific dysregulated pathways, such as CTLA4-Ig (Abatacept) for CTLA4 or LRBA deficiencies, PI3Kδ inhibitors for activated PI3Kδ syndrome, or JAK inhibitors for disorders involving aberrant JAK-STAT signaling [128–133]. Therefore, a molecular diagnosis can have significant therapeutic implications beyond conventional immunoglobulin replacement therapy and should always be pursued.

2. HYPOTHESIS AND OBJECTIVES

First, we hypothesized that the immune risk phenotype (IRP) would be a useful marker to predict prognosis in aged patients with community acquired pneumonia (CAP) and that the accumulated late differentiated $CD27^{neg}$ $CD28^{neg}$ T cells would accurately identify patients with worse prognosis after CAP, defined as higher all-cause mortality during subsequent follow-up.

Second, we hypothesized that patients with a non-complicated course of common variable immunodeficiency (CVID) actually exhibited a process comparable to immunosenescence, but at an earlier stage, and that they would have particularly high levels of late differentiated $CD27^{neg}$ $CD28^{neg}$ T cells as a sign of this process. We also hypothesized that patients with complicated CVID, accompanied by numerous manifestations of dysregulation, would exhibit a distinctive lymphocytic phenotype which could be used for screening and risk stratification.

To prove these hypotheses, we set the following objectives:

Part I:

Our main objective was identifying senescent-related biomarkers that predicted prognosis in patients with CAP. In order to do that, we set the following secondary objectives:

1. To correlate immunoglobulins, complement factors, leukocyte subpopulations and lymphocytic subpopulations of aged patients with CAP to the patients' outcome.
2. To describe the differentiated state of the T cells of aged patients with CAP based on their expression of CD27 and CD28, and to describe these cell subpopulations stratified by sex.
3. To analyze the association of the T cell differentiation states with final 2-year all cause survival.
4. To identify whether the late differentiated T cell phenotype is a useful biomarker to predict patients' long-term survival after CAP.
5. To analyze the T-helper phenotype in aged patients with CAP and test their predictive value.
6. To test the predictive value of the IRP in aged patients with CAP.

Part II:

We also aimed to see if the immunosenescent phenotype of CVID patients was similar to that of CAP patients. For this, we set the following secondary objectives:

1. To differentiate complicated from non-complicated CVID.

2. To describe and compare the immunosenescent state of T lymphocytes by the expression of CD27 and CD28 and the IRP in CVID patients, and their similarities to the CAP cohort.
3. To describe and compare the T-helper phenotype in complicated vs non-complicated CVID.
4. To identify a lymphocytic phenotype to discriminate complicated from non-complicated CVID.
5. To identify if the CVID patients with a molecular diagnosis had a particular immunosenescent state that might suggest a potential role for that molecular pathway in healthy aging in general.

3. MATERIALS AND METHODS

3.1. PART I - CAP in aged people

3.1.1. Study design

A prospective observational cohort, single-center study was conducted at the Hospital de la Santa Creu i Sant Pau, a tertiary university hospital in Barcelona, Spain. Patients older than 65 years old hospitalized for pneumonia between May 2019 and July 2021 were invited to participate; 162 patients were finally included. Pneumonia cases were defined by presence of an infiltrate in the chest radiography and one or more of the following symptoms: fever, shivering, cough, expectoration or malaise. The exclusion criteria were: patients moved from another hospital, patients that were HIV positive, patients who had neutropenia (<1000/mL) or chronic lymphocytic leukemia, transplanted patients, patients who were in end-of-life situation, COVID19 cases and those who didn't sign the consent form.

This study was approved by the hospital ethics committee of the Hospital Sant Pau and was part of a project of the Instituto de Salud Carlos III (PI18/00684, ClinicalTrials.gov; No.: NCT0462799). All study-related procedures were performed in accordance with the 1964 Helsinki declaration and its later amendments.

We aimed to study the patients at two consecutive time points: within 3 - 5 days after admission (during CAP: T0) and 1-2 months after admission (at follow-up: T1). However, recruitment and sample processing were impacted by the COVID-19 pandemic so, the final sample was comprised of 114 specimens obtained at T0 and 94 samples that were obtained at T1. Of note, 18 patients (15.8%) died between T0 and T1, and only 46 patients were assessed at both T0 and T1. Therefore, each time point was analyzed independently, and longitudinal dynamics between T0 and T1 were examined exclusively in the 46 patients with paired data. The main outcome was all-cause mortality at 2 years after the CAP episode. Mortality data were obtained from review of medical records and/or telephonic contact. Time to death was defined as the interval between the date of pneumonia diagnosis and the date of death. Patients who were alive were censored at 2 years. The outcome of all patients was successfully determined, with no losses.

The following blood analytical studies were performed to samples retrieved at both time points:

- Hematimetry: leukocytes, neutrophils, monocytes and lymphocytes count.
- Microbiology: Cytomegalovirus serology.
- Immunological study: immunoglobulin IgG, IgA, IgM and IgE, study of complement including C3, C4 and functionality with CH50 and cytokines (IL-2, IL-4, IL-6, IL-10, IL-17A, TNF and IFNγ). Lymphocytic subpopulations (T, B, NK), T-helper subpopulations (Th0, Th1, Th1/Th2, Th2, Th17, Th1/Th17) and differentiated T cell subpopulations (early, intermediate and late differentiated).

3.1.2. Serum analysis

The following analyses studies were performed in serum from centrifuged peripheral venous blood recollected in 10 ml silica-coated tubes (*BD Vacutainer, Plymouth*):

- Immunoglobulin quantification of IgG, IgA and IgM by nephelometry (*IMMAGE 800, Beckman Coulter*)
- IgE quantification by fluoroenzimImmunoassay (*Phadia ImmunoCAP 250, ThermoScientific)*
- Complement functionality by CH50 test by turbidimetry (*CH50 Optilite reagent NK095.OPT, Binding Site)*
- C3 and C4 quantification by nephelometry (*IMMAGE 800, Beckman Coulter*)
- Cytokine analysis performed by Cytometric Bead Array (CBA) *(Human Th1/Th2/Th17 CBA Kit, Becton Dickinson*). It was run in a *FACSLyric cytometer* (*Becton Dickinson*) and analyzed with *FCAP Array Software v3.0* (*Becton Dickinson)*. The kit included IL-2, IL-4, IL-6, IL-10, IL-17A, TNF and IFNγ.

3.1.3. Flow cytometry analysis

Phenotypic analyses of the lymphocytic populations were performed by flow cytometry from peripheral venous blood recollected in 7 ml EDTA-coated tubes (*BD Vacutainer, Plymouth*). For these analyses, different mixtures of antibodies at optimal concentrations were prepared in four different tubes and mixed with 100 µL of whole blood. All the samples were acquired in a *Navios (Beckman Coulter)* cytometer and analyzed with the software *Kaluza (Beckman Coulter)*. The analyzed populations were defined as described in Table 2.

For the lymphocytic subpopulations study, pre-made commercial mixtures were used in two tubes:

- First tube: CD45-FITC, CD3-PC5, CD4-RD1 and CD8-ECD (*Beckman Coulter*, 4 µL)
- Second tube: CD45-FITC, CD56-RD1, CD19-ECD, CD3-PC5 (*Beckman Coulter*, 4 µL)

These mixtures were incubated for 10 min, lysed and fixed automatically with *TQPrep (Beckman Coulter)* and run through the cytometer.

For the differentiated T cell and T-helper populations study, the blood was incubated for 15 min with their respective antibodies's mixture as indicated below. Then, samples were lysed by incubation for 20 min with 2 ml of *Red blood cell lysis solution* (Miltenyi Biotec) before being centrifuged at 1800 rpm for 10 min. The supernatants were discarded by decantation and 2 ml of PBS were added. Then, the centrifugation and the decantation were repeated. Finally, the samples were resuspended in 500 µL of PBS before being run through the cytometer.

For the differentiated T cell populations study the sample was stained with:

- CD3-PC5 (*Beckman Coulter*, 2 µL): clone UCHT1
- CD4-PC7 (*Beckman Coulter*, 2 µL): clone SFCI12T4D11
- CD28-FITC (*Sysmex*, 7 µL), clone CD28.2
- CD27-PE (*BD Pharmigen*, 4 µL): clone M-T271

And for the T Helper populations study the sample was stained with:

- CD4-FITC (*Miltenyi*, 2.5 µL): clone REA623
- CCR4-APC (*Miltenyi*, 2.5 µL): clone REA279

- CCR6-PEVio615 (*Miltenyi*, 2.5 µL): clone REA190
- CCR10-PE (*Miltenyi*, 2.5 µL): clone REA326
- CxCR3-PEVio770 (*Miltenyi*, 2.5 µL): clone REA232

		Cell populations	Immunophenotype
Lymphocytic populations	**First tube**	T cells	$CD45^{+}$ $CD3^{+}$
		T $CD4^{+}$cells	$CD45^{+}$ $CD3^{+}$ $CD4^{+}$
		T $CD8^{+}$cells	$CD45^{+}$ $CD3^{+}$ $CD8^{+}$
	Second tube	B cells	$CD45^{+}$ $CD3^{neg}$ $CD19^{+}$
		NK cells	$CD45^{+}$ $CD3^{neg}$ $CD56^{+}$
T-helper		Th1 cells	$CD4^{+}$ $CCR4^{neg}$ $CXCR3^{+}$ $CCR10^{neg}$ $CCR6^{neg}$
		Th1/Th2 cells	$CD4^{+}$ $CCR4^{+}$ $CXCR3^{high}$
		Th2 cells	$CD4^{+}$ $CCR4^{+}$ $CXCR3^{neg}$ $CCR10^{neg}$ $CCR6^{neg}$
		Th1/Th17 cells	$CD4^{+}$ $CCR4^{neg}$ $CXCR3^{+}$ $CCR10^{neg}$ $CCR6^{+}$
		Th17 cells	$CD4^{+}$ $CCR4^{+}$ $CXCR3^{neg}$ $CCR10^{neg}$ $CCR6^{+}$
		Th9 cells	$CD4^{+}$ $CCR4^{neg}$ $CCR6^{+}$
		Th22 cells	$CD4^{+}$ $CCR4^{+}$ $CXCR3^{neg}$ $CCR10^{+}$ $CCR6^{+}$
		Th0 cells	$CD4^{+}$ $CCR4^{neg}$ $CXCR3^{neg}$
Differentiated T cells		Early diff. T cells	$CD3^{+}$ $CD27^{+}$ $CD28^{+}$
		Intermediate diff. T cells	$CD3^{+}$ $CD27^{+}$ $CD28^{neg}$
		Late diff. T cells	$CD3^{+}$ $CD27^{neg}$ $CD28^{neg}$
		Early diff. T $CD4^{+}$cells	$CD3^{+}$ $CD4^{+}$ $CD27^{+}$ $CD28^{+}$
		Intermediate diff. T $CD4^{+}$cells	$CD3^{+}$ $CD4^{+}$ $CD27^{+}$ $CD28^{neg}$
		Late diff. T $CD4^{+}$cells	$CD3^{+}$ $CD4^{+}$ $CD27^{neg}$ $CD28^{neg}$
		Early diff. T $CD8^{+}$cells	$CD3^{+}$ $CD4^{neg}$ $CD27^{+}$ $CD28^{+}$
		Intermediate diff. T $CD8^{+}$cells	$CD3^{+}$ $CD4^{neg}$ $CD27^{+}$ $CD28^{neg}$
		Late diff. T $CD8^{+}$cells	$CD3^{+}$ $CD4^{neg}$ $CD27^{neg}$ $CD28^{neg}$

Table 2. Analyzed populations in the flow-cytometry assays. Lymphocytic subpopulations, T-helper and T differentiated studies "Diff."=differentiated

A representative model of the gating strategy by Kaluza for differentiated T cells and T-helper populations are shown in Figure 6 and in Figure 7, respectively.

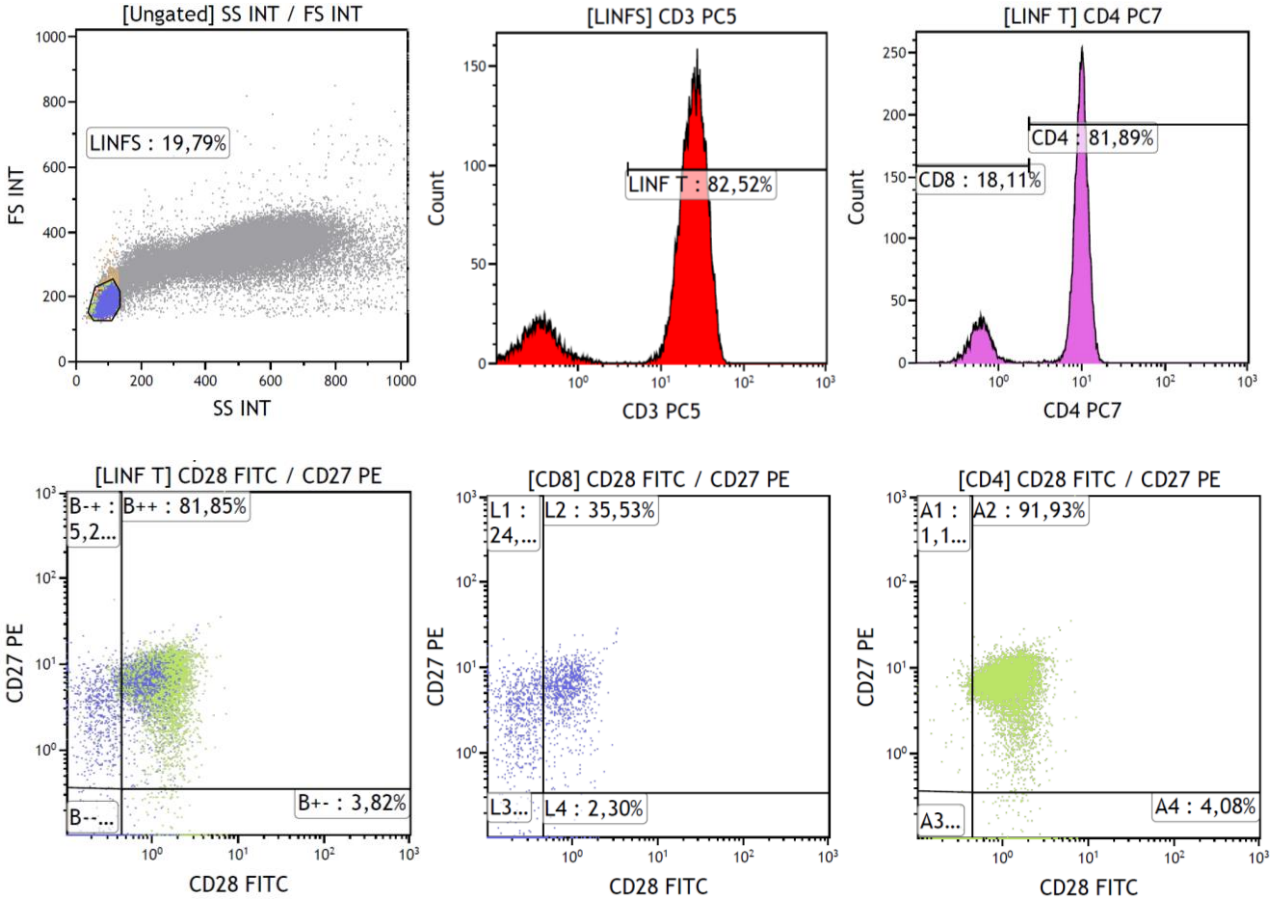


Figure 6. Gating strategy for the stages of differentiation of T lymphocyte populations. Lymphocytes were gated using forward scatter versus side scatter based on size and granularity. Afterwards, T cells were selected using CD3 positivity. Extended lymphocyte differentiated phenotype subpopulations were assessed with different panels according to CD28 and CD27 expression as described Table 2.

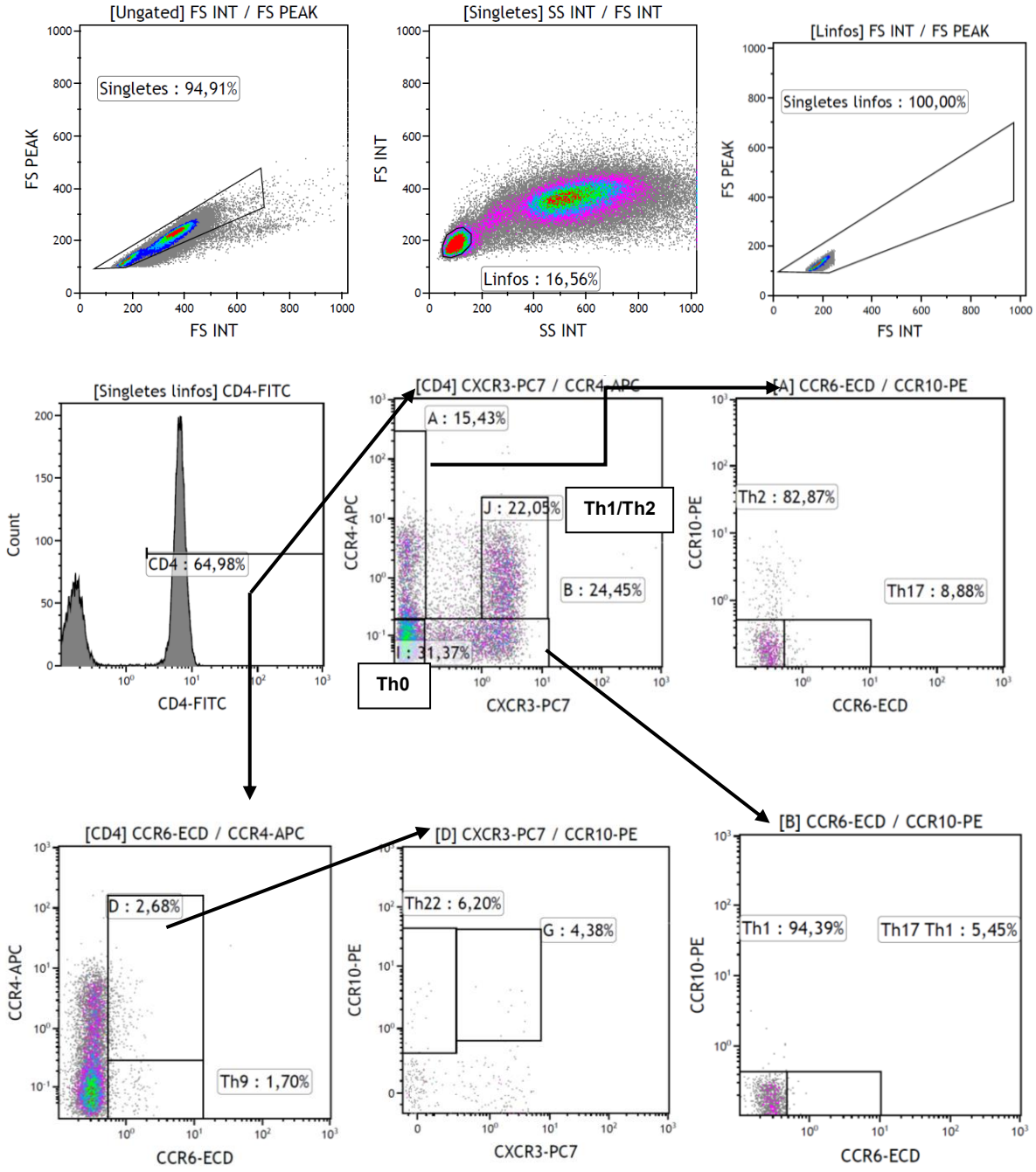


Figure 7. Designed gating protocol for the T-helper analysis. Lymphocytes were gated using forward scatter versus side scatter based on size and granularity. Afterwards, T-helper cells were selected using CD4 positivity. Extended lymphocyte subpopulations were assessed with different panels as described in Table 2.

3.1.4. Immune Risk Phenotype (IRP)

The immune risk phenotype analyzed included the following markers: positive serology for CMV, CD4/CD8 ratio <1, $CD8^{+}$ >600/µL and $CD28^{neg}$ >300/µL.

3.1.5. Data analysis and statistics

The software used to carry out statistical analysis were RStudio for Windows, version 2026.01.2+418 and GraphPad Prism version 5.03.

Parametric continuous variables included immunoglobulin, complement values and age. They were expressed as means and standard deviation (SD). Comparisons between two independent groups, stratified by survival status or sex, were performed using t-test. Group analysis for the combined sex-survival stratified analysis was analyzed by ANOVA test followed by a Bonferroni post hoc multiple comparisons correction.

Non-parametric continuous variables included hemogram, lymphocyte subpopulations and cytokine values. They were expressed as median and interquartile range (IQR). Comparisons between two independent groups, stratified by survival status or sex, were performed using the Mann–Whitney U test. Group comparisons for the combined sex-survival stratified analysis was performed by Kruskal-Wallis test followed by Dunn's post hoc multiple comparisons correction. Variable comparisons within the same group were compared with Friedman test. Differences between paired T0 and T1 samples from the described 46 patients were assessed using the Wilcoxon signed-rank test.

Categorical variables included sex, survival status, IRP and presence of neutrophilia, monocytopenia and/or lymphopenia. They were expressed as percentages relative to the pertinent sample and were compared with chi-square tests and Fisher's exact test when necessary. Paired analysis of IRP was analyzed with McNemar test.

Survival curves were estimated and represented with the Kaplan-Meier method and compared with log-rank test.

Univariate Cox proportional hazards models were adjusted for T-cell subpopulations by comparing 2-year (730 days) survival. Discrimination ability was estimated using the concordance index. Receiver operating characteristic (ROC) univariate curves were performed to explore potential predictors of survival and to obtain cut-off values to categorize the continuous variables. Areas under the curve (AUC) were calculated with 95% confidence intervals (CI).

Unsupervised clustering analysis of T-helper subpopulations was performed using the K-means algorithm. To determine the optimal number of clusters, models with k ranging from 2 to 9 were evaluated using both the elbow method (based on within-cluster inertia) and the silhouette coefficient. The final number of clusters was selected according to the best balance between intra-cluster cohesion and inter-cluster separation. Cluster visualization was subsequently performed using principal component analysis (PCA) by projecting the data into two dimensions.

Throughout all tests, $P<0.05$ values were considered significant.

3.2. PART II - CVID

3.2.1. Study design

In the first phase, between the years 2021–2022, 13 patients with an established or suspected diagnosis of Common Variable Immunodeficiency (CVID) who were already under regular follow-up at the Immunology Department at Hospital de la Santa Creu i Sant Pau, comprised the derivation cohort. CVID was defined as IgG hypogammaglobulinemia in an adult patient with recurrent infections in which other possible causes of hypogammaglobulinemia had been excluded. In the second phase (2022–2025), a validation cohort was prospectively recruited, consisting of 10 patients newly referred to the clinic and diagnosed with CVID during this period. The same studies and criteria were applied to the confirmation cohort. Clinical and laboratory parameters were systematically collected as part of routine clinical care. The systematic follow-up of these patients included:

- referral to Pneumology Department with a High-resolution thoracic CT-scan and spirometry
- referral to Digestive Pathology Department with an abdominal sonogram and hepatic elastography
- genetic testing with a virtual panel for inborn errors of immunity (IEI) over in-house clinical exome to rule-out other possibly existing IEI.

For the analysis of both cohorts, demographic data and age at diagnosis were recorded. Clinical variables included the presence or absence of the following common complications described in CVID patients: bronchiectasis, rare infections, cytopenia, lymphadenopathy, splenomegaly, hepatopathy and/or portal hypertension, inflammatory bowel disease, interstitial lung disease, hematological malignancy or solid organ malignancy.

Laboratory variables included: complete cell blood count and lymphocyte phenotyping. Specifically:

- Hemogram: hemoglobinemia, erythrocytes, platelets, leukocytes, neutrophils, monocytes and lymphocytes count,
- Lymphocytic subpopulations: T, B and NK cells,
- Differentiated T cell profile with early, intermediate and late differentiated T cells,
- T-helper subpopulations (Th1, Th2, Th17, Th1-2, Th1-17),
- T cell memory subpopulations with naive, central memory, effector-memory and TEMRA T cells,
- Treg cells,
- Activated HLA-DR$^+$ CD38$^+$ T cells,
- B cell subpopulations that included: naive, non-switched, and switched memory B cells, CD21low B cell and transitional B cells.

3.2.2. Flow cytometry analysis

Phenotypic analyses of the lymphocytic populations were performed by flow cytometry from peripheral venous blood recollected in 7 ml EDTA-coated tubes (BD Vacutainer, Plymouth). For these analyses, different mixtures of antibodies at optimal concentrations were prepared and mixed with whole blood,

except for the B cell subpopulations where pre-washed whole blood was stained. All the samples were acquired in a BD FACSLyric (Becton Dickinson) cytometer.

Lymphocytic subpopulations, differentiated T cell and T-helper populations were defined as described previously in Table 2. The rest of the analyzed subpopulations were defined as described in Table 3.

For the T, B, NK lymphocytic subpopulations study, samples were prepared automatically in a BD FACSDuet™ Sample Preparation System (Beckton Dickinson). In it, 50 µL of whole blood was stained with 20 µL of the pre-made commercial mixture BD Multitest 6-Color TBNK (Ref. 644611, Beckton Dickinson), which is comprised of the following antibodies: CD45-PerCP-Cy5.5/CD3-FITC/CD4-PE-Cy7/CD8-APC-Cy7/CD19-APC/CD16 and CD56 -PE. Then samples were incubated for 15 min and lysed by incubation for 20 min with 450 µL of BD FACS™ Lysing Solution lysis solution (Beckton Dickinson) before being run by the cytometer. These samples were analyzed with the software BD FACSuit Clinical (Becton Dickinson).

For the other T cell phenotype studies, 100 µL of whole blood were manually stained with the according antibody mixture. Then, samples were incubated for 15-20 min and automatically lysed and washed in a Lyse Wash Assistant (LWA) (Becton Dickinson) before being run through the cytometer. The solutions used by the LWA were: BD FACS™ Lysing Solution (Ref. 349202, BD) and BD® CellWASH (Ref. 349524, BD). Samples were analyzed with the software BD FACSuite (Becton Dickinson).

The differentiated and memory T cell populations were stained and analyzed in the same tube. The following mixture of antibodies was used:

- CD3-PerCP-Cy5.5 (Ref. 560835, BD,1 µL): clone UCHT
- CD4-V500-C (Ref. 647455, BD, 2 µL): clone SK3
- CD8-APC-H7 (Ref 561423, BD, 2 µL): clone SK1
- CCR7-BV605 (Ref 563711, BD, 1.5 µL): clone 3D12
- CD45 RA-PE (Ref 555489, BD, 3 µL): clone HI100
- CD28-BV421 (Ref 562613, BD, 2 µL): clone CD28.2
- CD27-APC (Ref. 561400, BD, 2 µL): clone M-T271

For the T-helper populations study, the sample was stained with:

- CD4-V500-C (Ref. 647455, BD, 1.5 µL): clone SK3
- CCR4-Alexa Fluor647 (Ref. 557863, BD, 1.5 µL): clone 1G1
- CXCR3-PE-Cy7.7 (Ref. 560831, BD, 1.5 µL): clone 1C6
- CCR6-BV421 (Ref. 562515 BD, 1.5 µL): clone 11A9
- CCR10-BB515 (Ref. 564769 BD, 1.5 µL): clone 1B5

For the Treg cells, the sample was stained with:

- CD4-V500-C (Ref. 647455, BD, 2 µL): clone SK3
- CD127-PE-Cy7 (Ref. 560822, BD, 2 µL): clone HIL-7R-M21
- CD45RO- FITC (Ref. PN IM1247U, Beckman Coulter, 5 µL): clone UCHL1

- CD25-PE (Ref. A 07774, Beckman Coulter, 5 µL): clone B1.49.9

And for the activated T cell analysis, the sample was stained with:

- CD3-PerCP-Cy5.5 (Ref. 560835, BD,1 µL): clone UCHT
- CD4- APC (Ref. 551980, BD, 0.5 µL): clone L200
- CD38-PE (Ref. 567131, BD, 2 µL): clone HB7
- HLA-DR-FITC (Ref. 347401, BD 2 µL): clone L243

For the B cell subpopulations, 200 µL of whole blood was pre-washed with the automated system LWA. Then, 200 µL of washed blood was stained manually, incubated for 15-20 min and lysed and washed with LWA before running it through the cytometer. The sample was stained with the following mixture of antibodies

- CD45-APC H7 (Ref. 560178, BD, 1 µL): clone 2D1
- CD19-BV510 (Ref. 562947, BD, 2 µL): clone SJ25C1
- CD27-APC (Ref. 561400, BD, 2 µL): clone M-T271
- IgD-PE (Ref. 555779, BD Pharmigen, 5 µL): clone IA6-2
- IgM-V450 (Ref. 561286, BD,1 µL): clone G20-127
- CD21-FITC (Ref. 11-0219-42, eBioscience, 2 µL): clone HB5
- CD24-PC5 (Ref. 561647, BD,2 µL): clone ML5
- CD38-PE-Cy7 (Ref. 560677, BD 1.5 µL): clone HIT2

A representative model of the gating strategy by BD FACSuite for differentiated and memory T cell populations, T-helper populations study, Treg cells, activated T cell analysis and B cell subpopulations are shown in Figure 8, Figure 9, Figure 10, Figure 11 and Figure 12, respectively.

	Cell populations	**Immunophenotype**
Memory T cells	Naive T cell	$CD3^+$ $CCR7^+$ $CD45RA^+$
	Central Memory T cell	$CD3^+$ $CCR7^+$ $CD45RA^{neg}$
	Effector Memory T cell	$CD3^+$ $CCR7^{neg}$ $CD45RA^{neg}$
	TEMRA	$CD3^+$ $CCR7^{neg}$ $CD45RA^+$
	$CD4^+$ Naive T cell	$CD3^+$ $CD4^+$ $CCR7^+$ $CD45RA^+$
	$CD4^+$ Central Memory T cell	$CD3^+$ $CD4^+$ $CCR7^+$ $CD45RA^{neg}$
	$CD4^+$ Effector Memory T cell	$CD3^+$ $CD4^+$ $CCR7^{neg}$ $CD45RA^{neg}$
	$CD4^+$ TEMRA	$CD3^+$ $CD4^+$ $CCR7^{neg}$ $CD45RA^+$
	$CD8^+$ Naive T cell	$CD3^+$ $CD8^+$ $CCR7^+$ $CD45RA^+$
	$CD8^+$ Central Memory T cell	$CD3^+$ $CD8^+$ $CCR7^+$ $CD45RA^{neg}$
	$CD8^+$ Effector Memory T cell	$CD3^+$ $CD8^+$ $CCR7^{neg}$ $CD45RA^{neg}$
	$CD8^+$ TEMRA	$CD3^+$ $CD8^+$ $CCR7^{neg}$ $CD45RA^+$
T reg/Teff cells	Regulatory T cell (Treg)	$CD4^+$ $CD45R0^+$ $CD25^+$ $CD127^{neg}$
	Effector T cell (Teff)	$CD4^+$ $CD45R0^+$ $CD25^{neg}$ $CD127^+$

Activated T cells	Activated CD4⁺ T cell	CD3⁺ CD4⁺ CD38⁺ HLA-DR⁺
	Activated CD8⁺ T cell	CD3⁺ CD8⁺ CD38⁺ HLA-DR⁺
B cell subpopulations	Naive B cell	CD45⁺ CD19⁺ IgD⁺ CD27^{neg}
	Marginal zone B cell	CD45⁺ CD19⁺ IgD⁺ CD27⁺
	Non-switched memory B cell	CD45⁺ CD19⁺ IgD⁺ IgM$^{+/low}$ CD27⁺
	Switched memory B cell	CD45⁺ CD19⁺ IgD^{neg} IgM^{neg} CD27⁺
	Transitional B cells	CD45⁺ CD19⁺ IgD⁺ IgM$^{+/low}$ CD24^{high} CD27^{neg} CD38^{high}
	Plasmablasts	CD45⁺ CD19⁺ IgD^{neg} IgM^{neg} CD27^{high} CD38^{high}
	CD19^{low} B cell	CD45⁺ CD19^{low} CD27⁺
	CD21 ^{low} B cell	CD45⁺ CD19⁺ CD21^{low} CD38^{neg}

Table 3. Analyzed populations in the extended phenotype flow-cytometry assays.

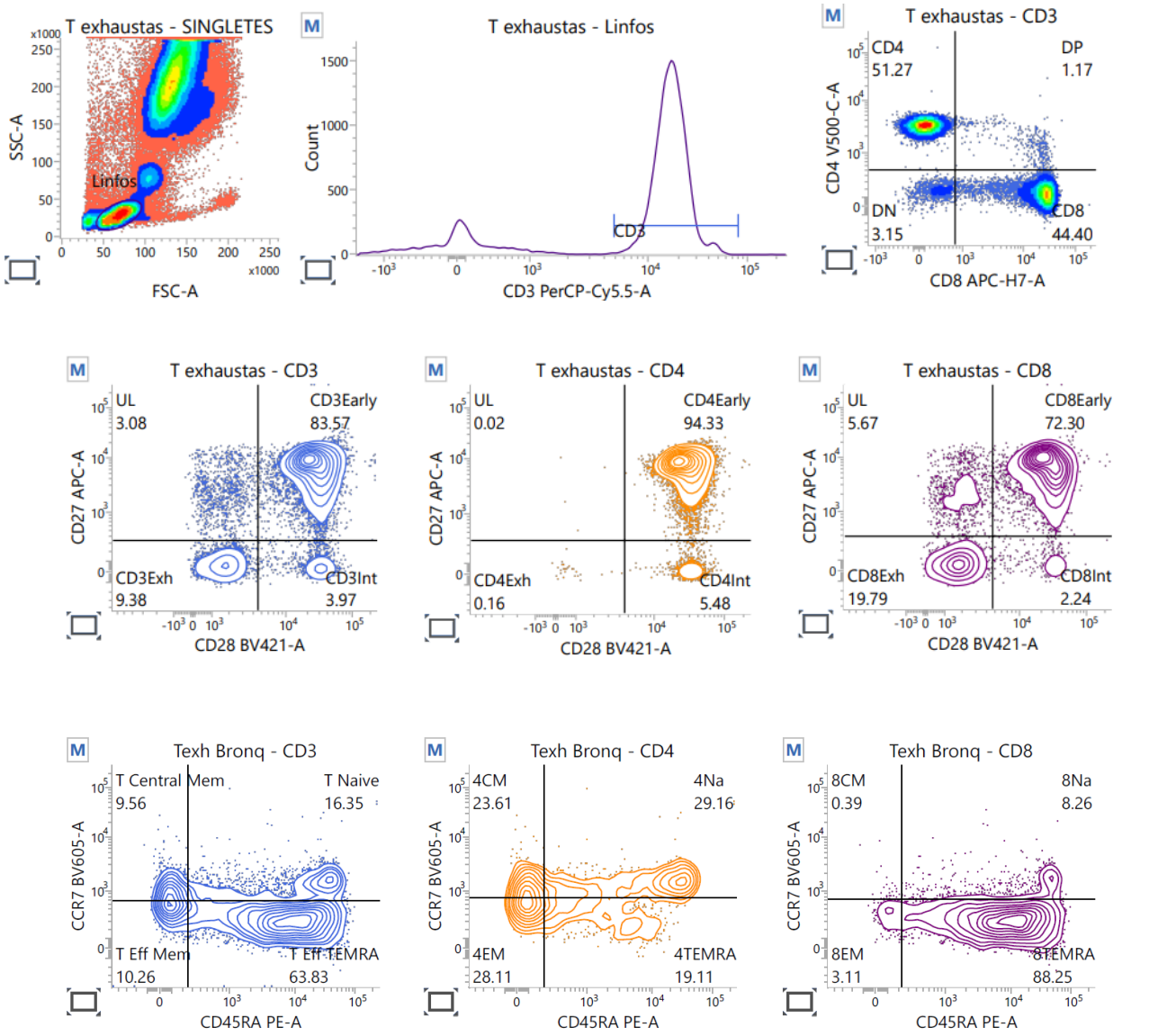


Figure 8. Designed gating protocol for the differentiated and memory T cell analysis. Lymphocytes were gated using forward scatter versus side scatter based on size and granularity after singlet gating over all events. Afterwards, T cells were selected using CD3 positivity. Extended lymphocyte subpopulations were assessed as described in Table 3.

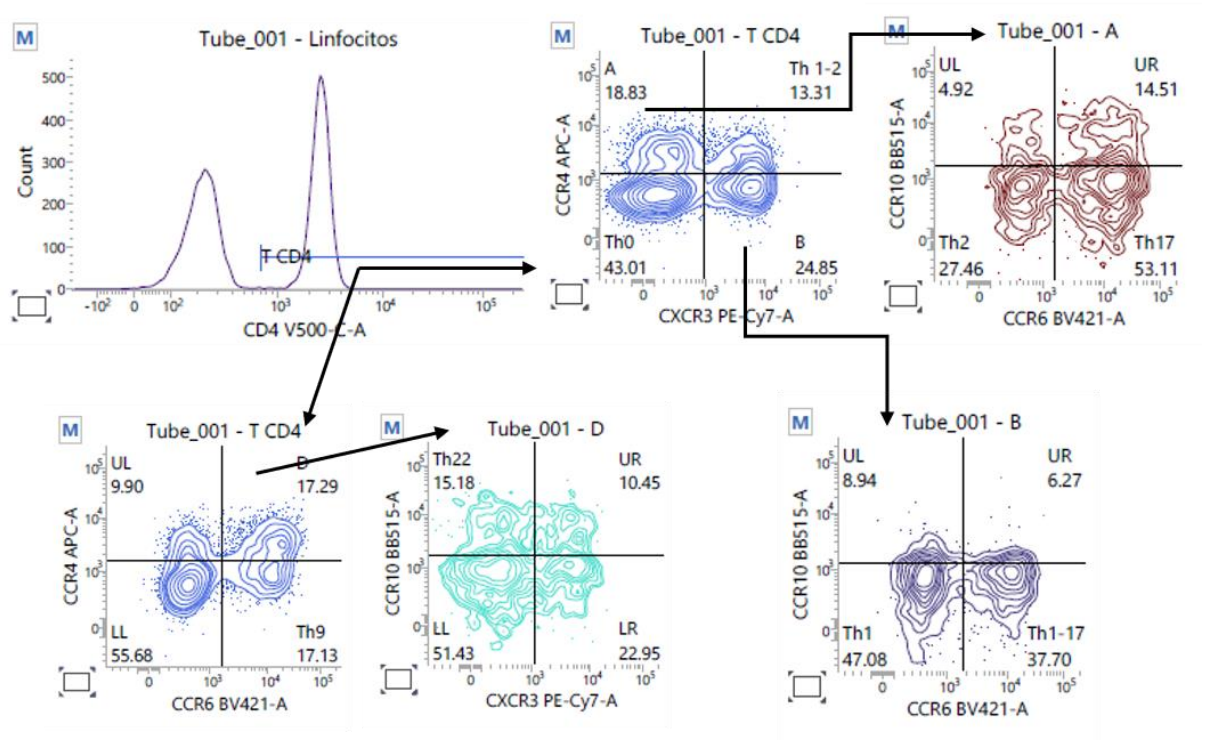


Figure 9. Designed gating protocol for the T-helper analysis. Lymphocytes were gated using forward scatter versus side scatter based on size and granularity. Afterwards, T-helper cells were selected using CD4 positivity. Extended lymphocyte subpopulations were assessed as described in Table 2.

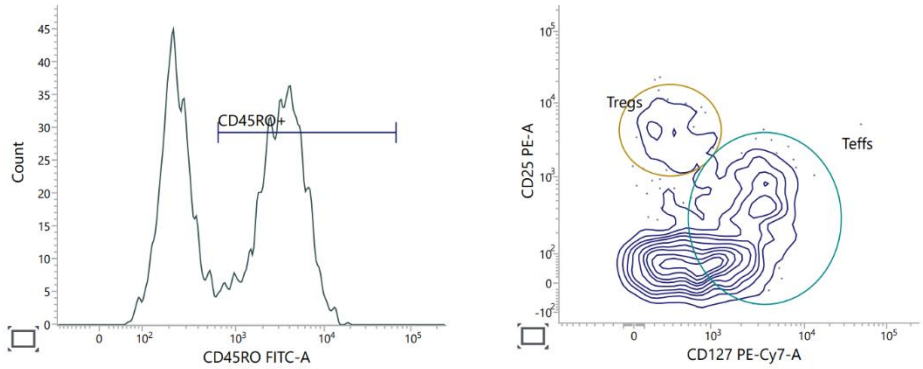


Figure 10. Designed gating protocol for the Tregs and Teffs cells analysis. Lymphocytes were gated using forward scatter versus side scatter based on size and granularity. Afterwards, CD4⁺ T cells were selected using CD4 positivity. Treg and Teff were assessed as described in Table 3. Tregs=regulator T cells, Teffs=effector T cells.

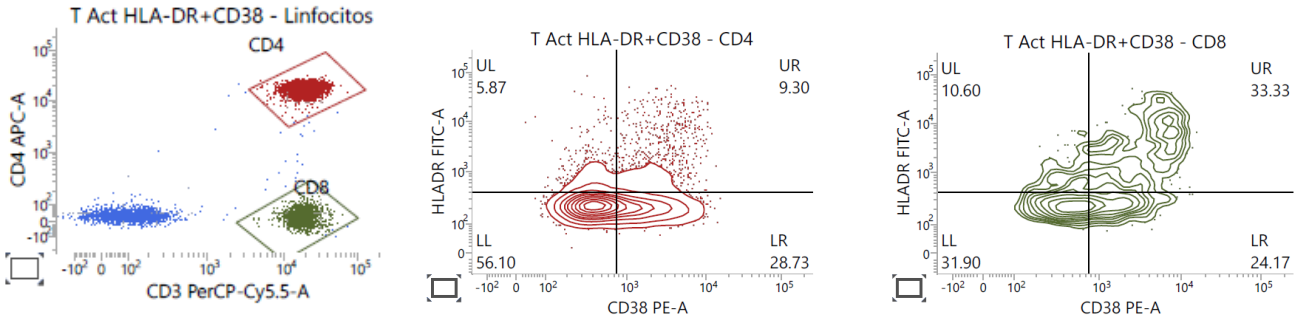


Figure 11. Designed gating protocol for the activated T cell analysis. Lymphocytes were gated using forward scatter versus side scatter based on size and granularity after singlet gating over all events. Extended lymphocyte subpopulations were assessed as described in Table 3.

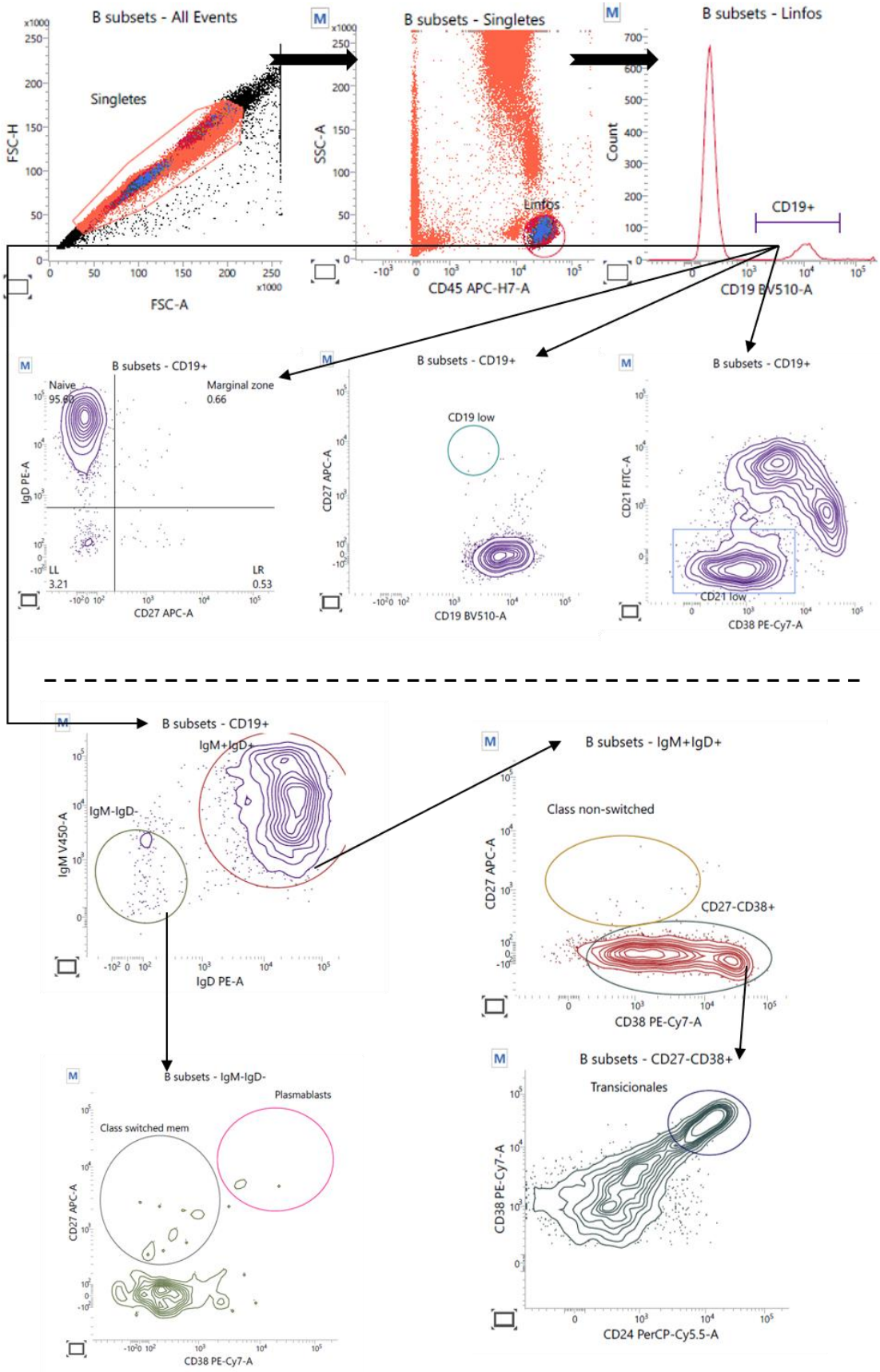


Figure 12. Designed gating protocol for the B cell subpopulations analysis. Lymphocytes were gated using CD45 versus side scatter after singlet gating over all events. Afterwards, B cells were selected using CD19 positivity. Extended lymphocyte subpopulations were assessed as described in Table 3.

3.2.3. Data analysis and statistics

The software used to carry out statistical analysis were also RStudio for Windows, version 2026.01.2+418 and GraphPad Prism version 5.03.

Parametric continuous variables were expressed as means and standard deviation (SD) and compared using t-test for 2-group comparisons such as the cohorts comparison, severe vs non-severe CVID or the two-cluster comparison.

Non-parametric continuous variables included most of the lymphocytic phenotype variables. They were expressed as median and interquartile range (IQR). Comparison between groups was performed with U-Mann Whitney test. Variable comparisons within the same group were compared with Friedman test. Distribution comparisons were performed with Lavene test.

Lymphocytic phenotype variables and clinical score were correlated using Spearman's rank correlation.

Receiver operating characteristic (ROC) univariate curves were performed to obtain cut-off values to the clinical score. Areas under the curve (AUC) were calculated with 95% confidence intervals (CI).

Unsupervised clustering analysis of the lymphocyte phenotype was performed using the K-means algorithm. To determine the optimal number of clusters, models with k ranging from 2 to 10 were evaluated using both the elbow method (based on within-cluster inertia) and the silhouette coefficient. As neither approach identified a clear optimal value of k, a two-cluster solution was selected to facilitate comparison with the binary clinical severity classification. Cluster visualization was subsequently performed using principal component analysis (PCA) by projecting the data into two dimensions.

Categorical variables included sex, severity status based on our clinical score and phenotypic cluster. They were expressed as percentages relative to the pertinent sample and compared with chi-square tests and Fisher’s exact test when necessary.

Throughout all tests, $P<0.05$ values were considered significant.

4. RESULTS

4.1.PART I - CAP in aged people

4.1.1. Demographics

During CAP (T0), 114 patients were included: 42 (36.8%) women and 72 (63.2%) men. Of those, 55 (48.2%) died during the 2-year follow-up, of which 16 (29.1%) were women and 39 (70.9%) were men. Although there was a tendency, no statistically significant differences were found between the 2-year mortality among men (54.2%) vs women (38.1%) (Log-rang test 0.09, Fisher's exact test p=0.12) (Figure 13A,B). Of note, 20 (17.6%) people died before 60 days, of whom 15 (75.0%) were men and 5 (25.0%) were women, finding no differences in mortality between the sexes. Mean age was 80.9 ±8.1 years-old for the overall cohort; 80.1 ±7.9 y.o. for men and 82.2 ±8.4 y.o. for women.

At follow-up (T1), 94 patients were included: 41 (43.6%) women and 53 (56.4%) men. Of those, 29 (30.9%) died during the 2-year follow-up, of which 8 (27.6%) were women and 21 (72.4%) were men. This time-point reached statistical significance difference between the mortality among men (39.6%) vs women (19.5%) (Log-rang test p<0.05, Fisher's exact test p<0.05) (Figure 5.1C,D). Mean age was 78.9 ± 8.2 years-old for the overall cohort; 77.5 ± 8.0 y.o. for men and 80.7 ± 8.2 y.o. for women.

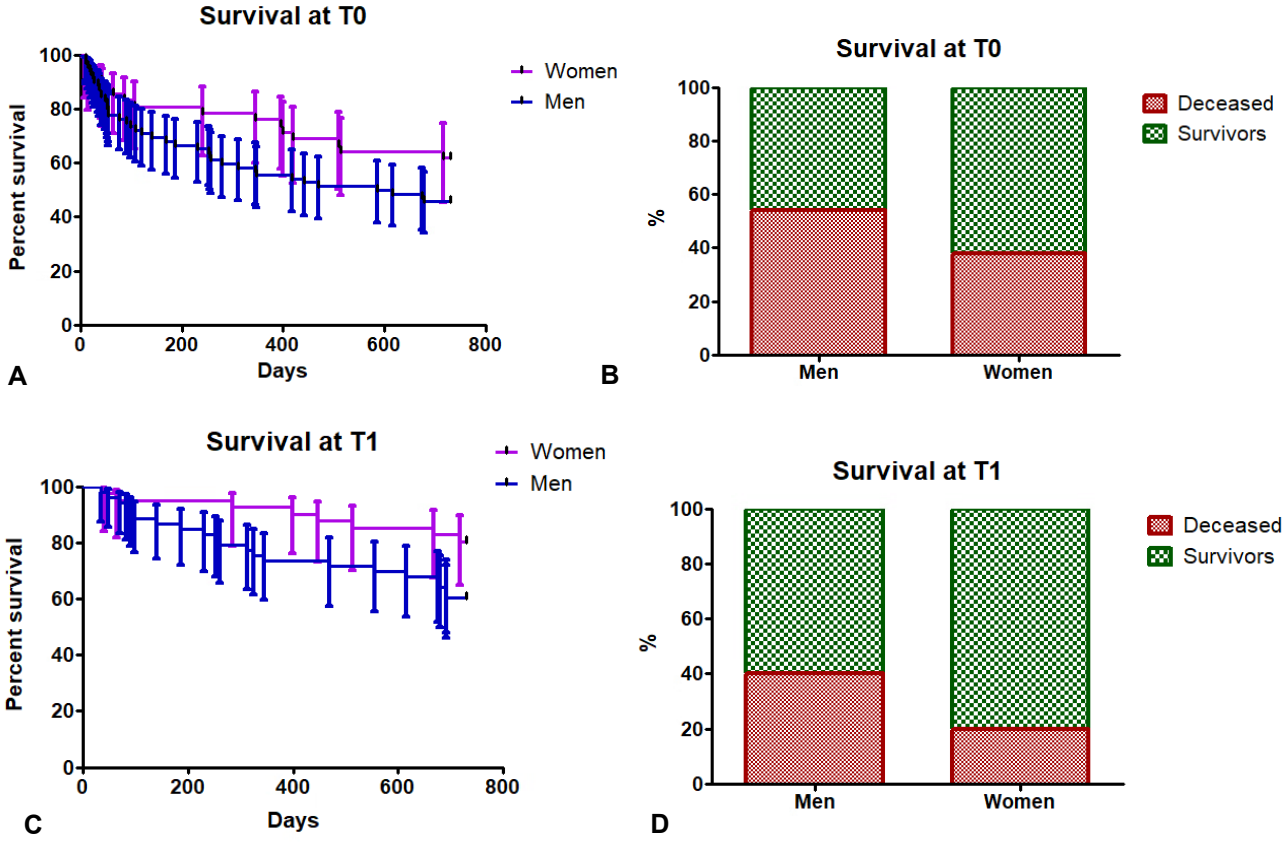


Figure 13. Sex stratified analysis of survival. T0: men (54%) vs women (38%). Log-rang test p=0.09 ***(A)****; Fisher's exact test p=0.12* ***(B)****. T1: men (39.6%) and women (19.5%). Log-rang test p<0.05* ***(C)****; Fisher's exact test p<0.05* ***(D)***

The 46 paired samples were representative of the overall cohort at both time points, as they showed no significant differences to the full T0 and T1 cohorts.

4.1.2. Immunoglobulin and complement

A T0, IgG and IgE were the only immunoglobulin isotypes that showed differences between 2-year survivors and non-survivors. Survivors showed lower levels of IgG (1030 mg/dL ±372) and higher levels of IgE (85.7 UI/mL [32.4 - 227.0]) than non-survivors (IgG: 1194 mg/dL ±376; IgE: 37.3 UI/mL [12.0 - 185.0]) ($p<0.05$). IgA and IgM showed no differences between survivors and non survivors. No differences were found in any of the immunoglobulin levels between sexes either. There were no significant differences in the functionality of the complement cascade as shown by the CH50 activity ($p=0.1844$) nor the complement factor C4. However, survivors had significantly more C3 than non-survivors (120.3 mg/dL ±32.4 vs 97.3 mg/dL ±33.7, $p<0.001$). The sex-stratified analysis showed that, specifically, survivor women had more C3 than non-survivor men (128.6 mg/dL ±41.0 vs 94.6 mg/dL ±34.8, ANOVA $p<0.001$) (Supplementary Table 1).

However, no differences were observed at T1 between survivors and nor survivors, nor between sexes. The paired cohort revealed that both survivors and non-survivors showed an increase of IgG (survivors $p<0.01$, non-survivors $p<0.05$) and decrease of IgE (survivors $p<0.01$, non-survivors $p<0.05$) between T0 and T1. Survivors also increased the number of IgM ($p<0.01$) but no other significant changes among the other immunoglobulins nor complement factors (Supplementary Table 1).

Overall, humoral immunity showed subtle differences between survivors and non-survivors at T0 and, notably, by T1 these differences had resolved. Furthermore, the paired analysis showed that both groups exhibited a convergent dynamic characterized by rising IgG and falling IgE levels, possibly reflecting a resolved consumption of IgG.

4.1.3. Leukocyte subpopulations

4.1.3.1. During CAP (T0)

No differences were found between survivors and non-survivors in the total number of leukocytes. However, significant differences emerged when individual leukocyte subpopulations were examined.

There were no significant differences in the absolute count of neutrophils ($p=0.94$) nor monocytes ($p=0.31$) (Figure 14A), so the proportion of patients with values outside of the normal reference range values were analyzed. As expected during an infectious episode, neutrophilia (defined as >7000 neutrophils/µL) was found in 50.9% of patients, with no significant differences between survivors (45.8%) and non-survivors (56.4%, $p=0.27$). However, monocytopenia (defined as <300 monocytes/µL) was significantly more frequently observed among non-survivors (14.5% vs 1.7%, $p<0.05$). In fact, patients with monocytopenia had nearly 10-fold higher odds of dying within 2 years (OR 9.87, 95% CI [1.19 - 81.8], $p=0.014$). (Figure 14B).

Lymphocytes did show differences between the groups: survivors had higher absolute lymphocyte counts than non-survivors (1490 cells/µL [1020 - 2040] vs 970 cells/µL [540 - 1520] $p=0.0003$) (Figure 14A). As a result, there also were significant differences in the leukocyte distribution. Survivors had a

lower proportion of neutrophils (71.2% [61.3 - 82.6] vs 77.0 [69.2 - 85.7], p <0.05) in favor of a higher proportion of lymphocytes (16.7% [7.3 - 24.8] vs 11.4% [5.6 - 16.1], p<0.05) (Figure 14C). Similar to monocytopenia, lymphopenia (defined as <1000 lymphocytes/µL), was also significantly more frequently observed among non-survivors (50.9% vs 23.7%, p<0.01) (Figure 14D). So, patients with lymphopenia had higher odds of dying within 2 years (OR 3.33, 95% CI [1.50 - 7.42], p<0.01).

Despite these results, there were no differences in the neutrophil-to-lymphocyte ratio (NLR) between survivors (5.93 [3.01 - 13.73]) and non-survivors (5.66 [2.96 - 10.44], p=0.96).

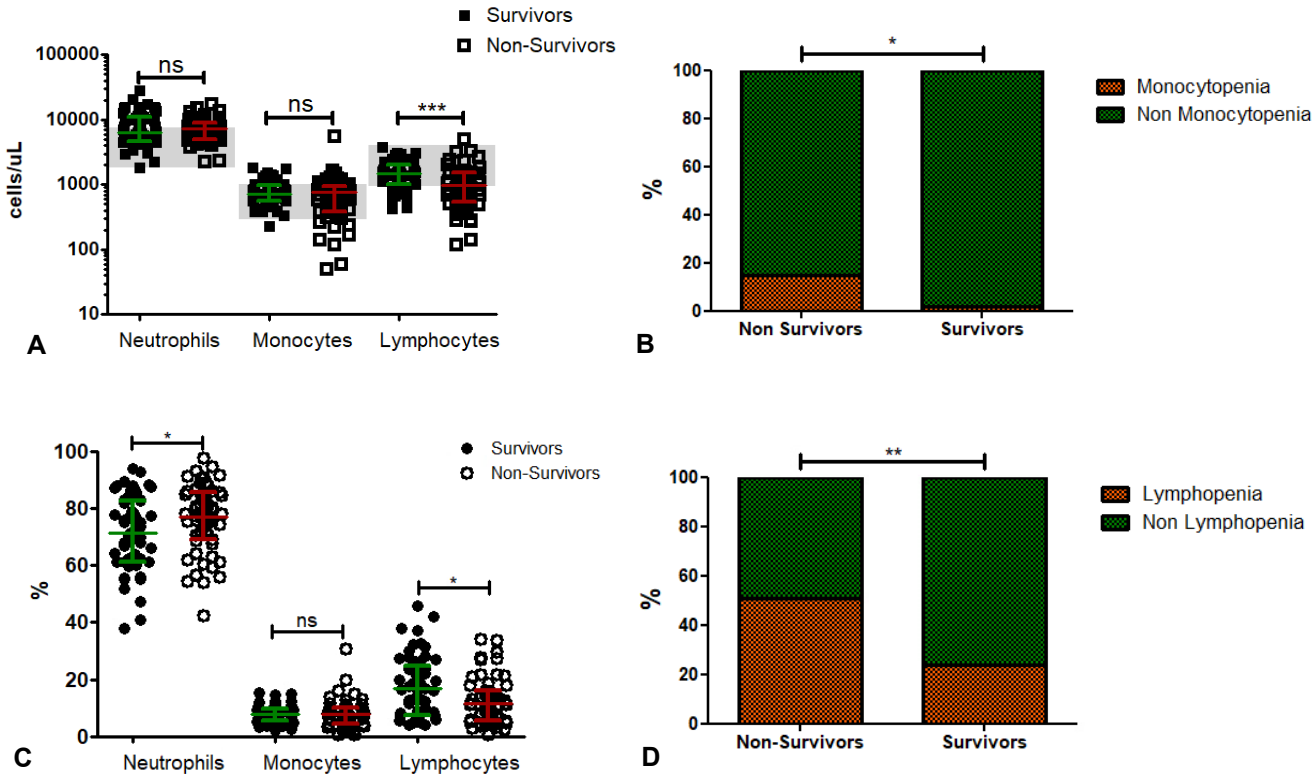


*Figure 14. Blood cell count in the T0 cohort **(A)** and leukocyte distribution **(C)**. Grey bands indicate reference ranges for healthy individuals. Proportion of monocytopenia (<300 cells/µL) **(B)** and lymphopenia **(D)**.*p<0.05, **p<0.01, ***p<0.001, ns=non-significant.*

Also, ROC curve analyses showed an area under the curve (AUC) of 0.67 for lymphocytes during CAP. We could also establish an optimal cut-off: <1150 lymphocytes/µL during CAP predicted 2-year mortality with 63.64% sensitivity and 72.88% specificity (Figure 15).

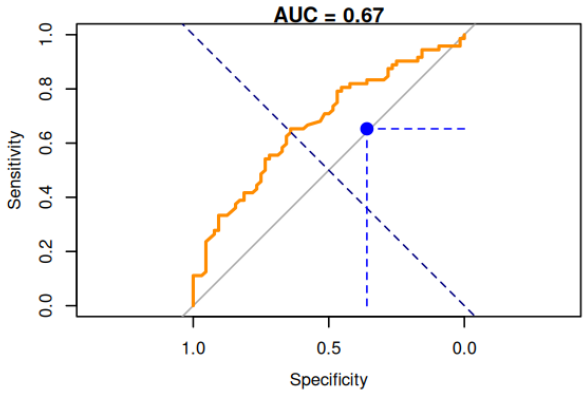


Figure 15 ROC curve for total lymphocytes for two-year survival. AUC = 0.67.

Sex-stratified analysis showed that men had significantly lower number of lymphocytes than women overall (1135 cells/µL [673 - 1603] vs 1430 cells/µL [920 - 2275], p<0.05). This difference was most pronounced when comparing non-survivor men with survivor women (940 [505 – 1435] vs 1530 [1295 – 2398], p<0.001) (Figure 16A). No more differences were found in other leukocytes when both gender and survival were considered (Supplementary Table 2). These differences translated into a significantly NLR in men compared to women (7.04 [4.60 - 14.71] vs 3.53 [2.26 - 10.12], p<0.01), and particularly in non-survivor men over surviving women (7.81 [4.93 - 15.92] vs 3.06 [2.02 - 7.06], p<0.01), despite the absence of differences between survivors vs non-survivors as a whole. Taken together, these findings suggest that biological sex was a significant modulating factor in the leukocyte response in our cohort.

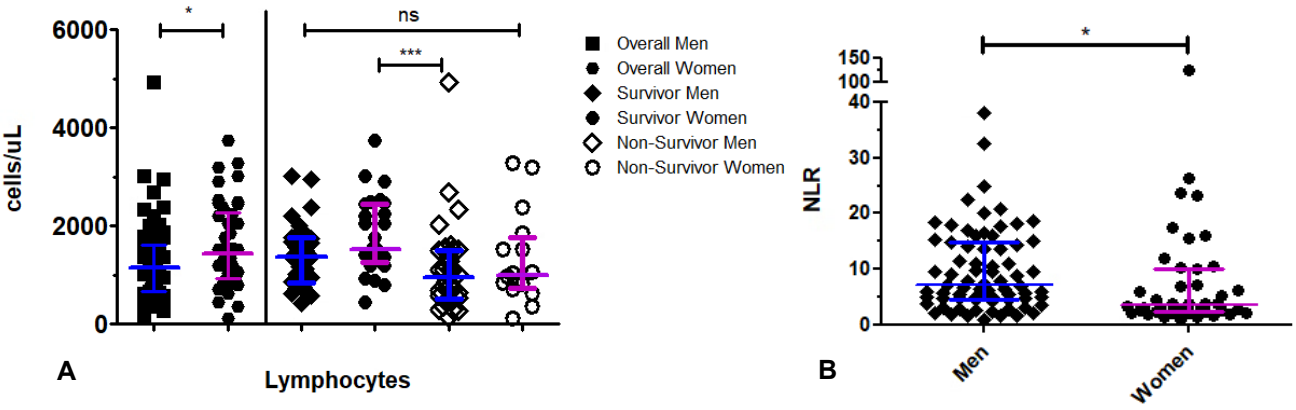


*Figure 16. Sex-stratified analysis from T0 cohort of lymphocytes **(A)** and neutrophil-to-lymphocyte ratio (NLR) **(B)**. *p<0.05, ***p<0.001, ns=non-significant.*

4.1.3.2. At 1-2 months follow-up (T1)

At T1 the leukocyte profile differed from that at T0. Survivors showed lower total leukocytes than non-survivors (6850 cells/µL [5835 - 8510] vs 7990 cells/µL [6220 - 10800], p<0.05), mainly driven by neutrophils (4160 [3095 - 5610] vs 5550 [4510 - 8190], p<0.01) (Figure 13A). In fact, neutrophilia was still present in 31.0% of non-survivors compared to 9.2% of survivors (p<0.05). So, neutrophilia at T1 caused a 4.35 OR for 2-year death. Monocytes showed no significant differences at this time-point.

On the contrary, survivors maintained higher lymphocytes than non-survivors at T1 (1690 cells/µL [1350 - 2125] vs 1340 cells/µL [880 - 1595], p<0.001), consistent with the results observed at the T0 cohort (Figure 13A). Lymphopenia was present in 34.5% of non-survivors vs 4.6% of survivors (p<0.001), showing a 10.88 OR for 2-year death.

These differences also reflected on the leukocyte distribution, where survivors showed much lower proportion of neutrophils (61.2% [54.5 – 68.8] vs 72.5% [65.9 – 79.1] vs p<0.0001) and higher proportion of lymphocytes (25.7% [20.8 - 31.6] vs 16.31% [12.3 – 20.6], p<0.0001) compared to survivors (Figure 17B). This resulted on a significantly lower NLR (survivors: 2.48 [1.81 - 3.37], non-survivors: 4.69 [3.14 -

6.54], p<0.0001). These results are consistent with the existing literature, in which NLR has been explored as an non-specific prognostic factor across many settings, including sepsis and cancer[73,134,135].

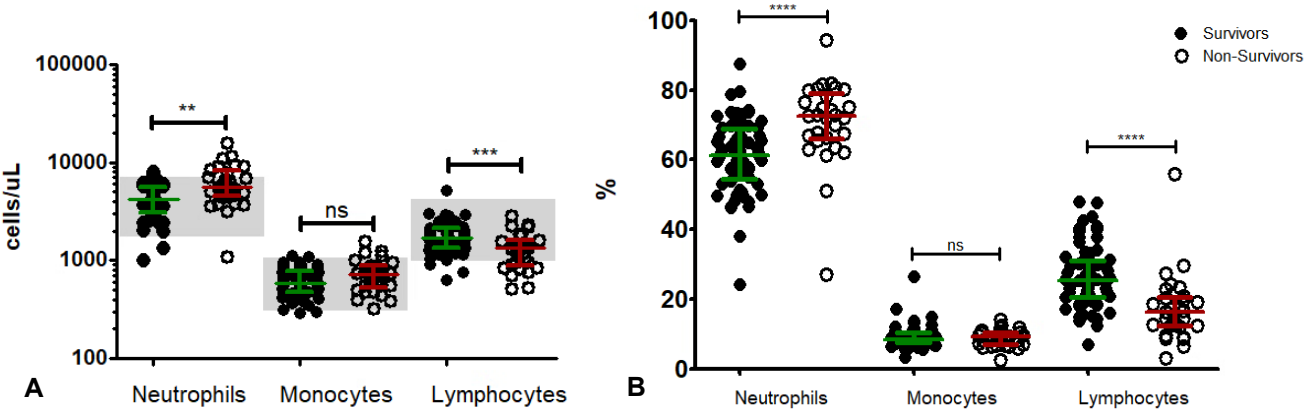


*Figure 17. Blood cell counts from T1 cohort **(A)** and percentage of leukocytes **(B)**. The grey bands indicate reference ranges for healthy individuals. *p<0.05, **p<0.01, ***p<0.001, ****p<0.0001, ns=non-significant.*

Isolated sex stratification showed that men continued to have less lymphocytes than women by absolute counts (men: 1480 cells/μL [1050 - 1880] vs women: 1670 cells/μL [1350 - 2170], p<0.05) (Figure 18A). When survival was incorporated into the stratification, non-survivor men emerged as the subgroup driving most of the observed differences in both neutrophil and lymphocyte counts and proportion compared to all survivors (Figure 18A,B, Supplementary Table 3).

So, sex remained a significant factor in neutrophils and lymphocytes dynamics, where non-survivor men were the most distinct group.

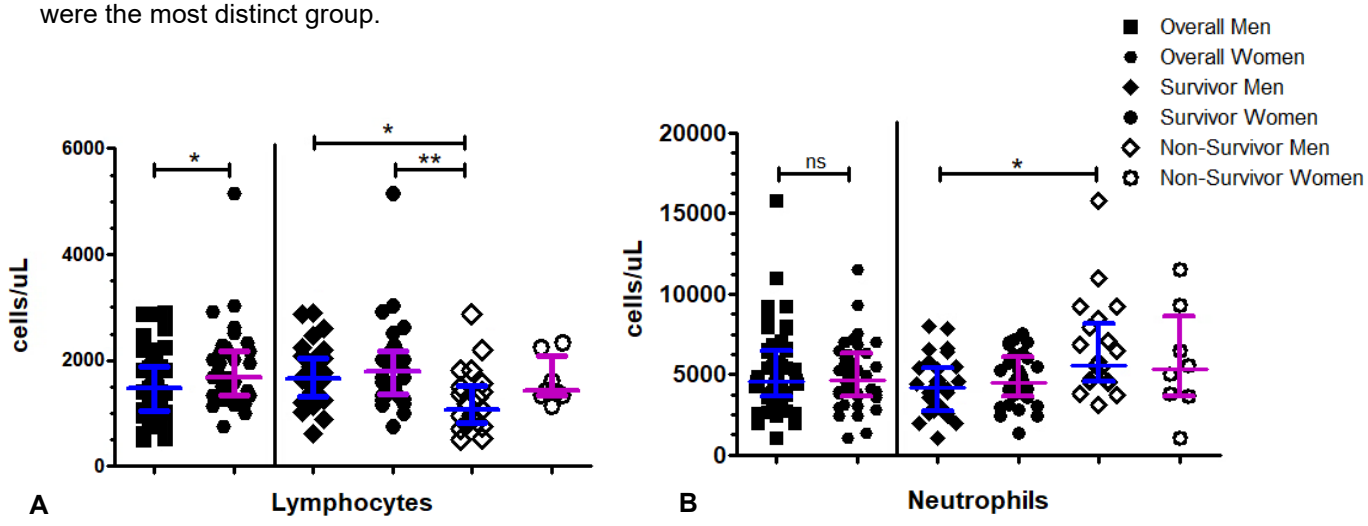


*Figure 18. Sex and sex-survival stratified analysis of total lymphocytes **(A)** and neutrophils **(B)** from T1 cohort. *p<0.05, **p<0.01, ns=non-significant.*

4.1.3.3. *Paired analysis*

Paired analysis showed that, as expected, patients' neutrophils descended overall (T0: 7320 cells/μL [5020 – 9448] vs T1: 4860 cells/μL [4123 – 6868], p<0.05). That was consistent in the survival-stratified analysis, with survivors going from 5875 cells/μL [4635 – 8853] at T0 to 4450 cells/μL [4008 – 6370] at T1 (p<0.05) and non-survivors from 7890 cells/μL [7108 – 9478] to 6025 cells/μL [4558 – 8335] (p<0.05) (Supplementary Table 4). Sex-stratified-analysis showed that men's dynamics were also consistent with these results as they went from 8065 cells/μL [6460 – 10333] at T0 to 5200 cells/μL [4253 - 7180] at T1 (p<0.01). However, women overall did not show such neutrophil descent: they went from 5465 cells/μL [4635 – 7600] at T0, to 4585 cells/μL [3963 - 6743] at T1 (p=0.12) (Figure 19). However, neither lymphocytes nor monocytes showed significant changes in absolute counts between T0 and T1 (Supplementary Table 4). Thus, neutrophils dynamics seemed to be faster between time-points in men.

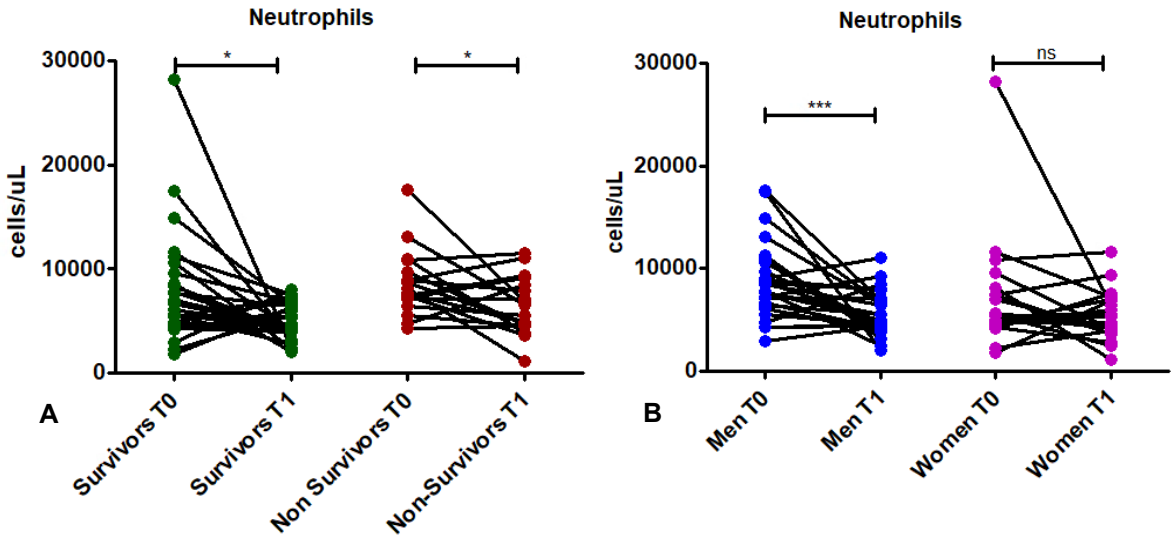


*Figure 19. Paired neutrophil absolute counts of survivors and non-survivors **(A)** and men and women **(B)**.*

4.1.4. Lymphocytic subpopulations

Although neutrophils had faster dynamics, survivors had more total lymphocytes than non-survivors at both time points so we explored lymphocytic subpopulations.

At T0, survivors had more T cells (p<0.001), $CD4^+$ T cells (p<0.001), $CD8^+$ T cells (p<0.05), and B cells (p<0.001), but there were no differences in the number of NK cells. In contrast, no differences were found in the percentage of either T, $CD4^+$, $CD8^+$, nor B cells, but survivors had a lower proportion of NK cells within their lymphocytes (8.6% [6.1 - 13.9] vs 14.0% [8.9 - 21.5], p<0.01) (Figure 20,Table 4).

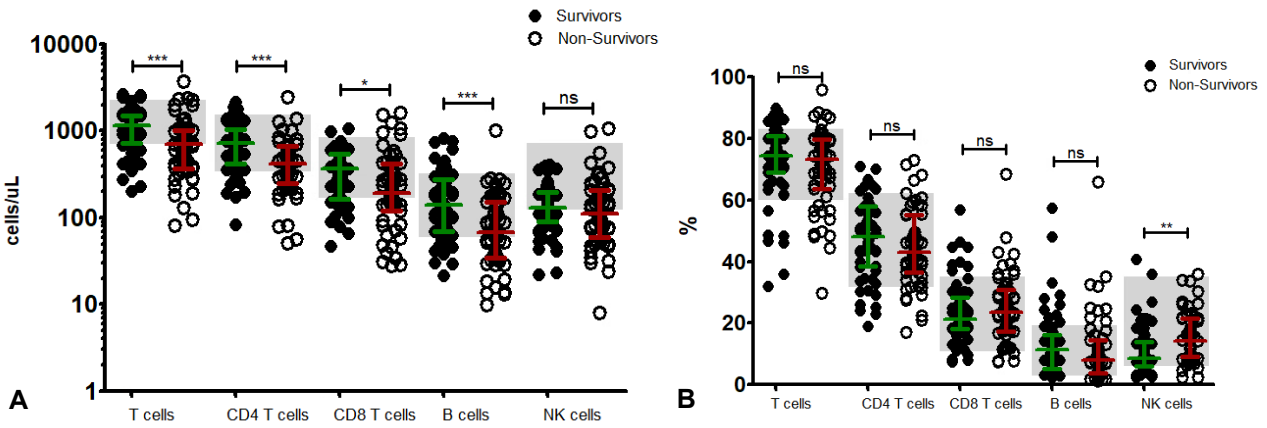


*Figure 20. Lymphocyte subsets in the T0 cohort, by cell counts **(A)**, and by percentage **(B)**. Grey bands indicate reference ranges for healthy individuals. *p<0.05, ***p<0.001, ns=non-significant.*

Sex-stratified analysis showed that men had significantly lower absolute counts of T cells (p<0.05), $CD4^+$ T cells (p<0.05) and $CD8^+$ T cells (p<0.01). They also showed a tendency towards lower B cells (p=0.07), while NK cells were comparable between sexes (p=0.98). When considering survival stratification, the main differences were found between survivor women and non-survivor men; the former had more T cells (p<0.001), $CD4^+$ T cells (p<0.001), $CD8^+$ T cells (p<0.01), and B cells (p<0.001). Regarding lymphocyte distribution, differences were restricted to the percentage of $CD8^+$ T cells and NK cells: non-survivor men had higher percentage of NK cells than survivor women (p<0.05), as well as they had lower percentage of $CD8^+$ T cells than, in this case, non-survivor women (p<0.05) (Figure 21, Table 4).

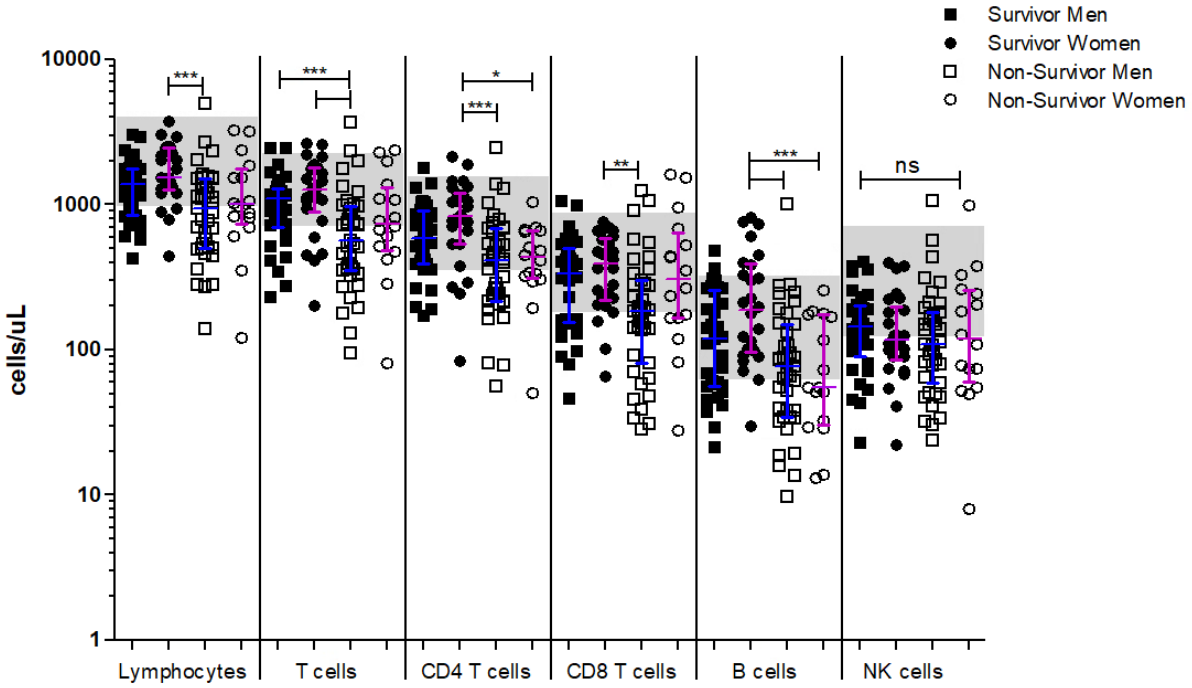


*Figure 21. Sex and survival stratified subanalysis of the lymphocyte subsets in the T0 cohort. Grey bands indicate reference ranges for healthy individuals. *p<0.05, **<0.01, ***p<0.001, ns=non-significant.*

	Men	Women	p	Surv			Non surv			p
				Men	Women	Total	Men	Women	Total	
	n = 72	n = 42		n = 33	n = 26	n = 59	n = 39	n = 16	n = 55	
T cells %	73,8 [64,4 - 80,4]	74,4 [67,7 - 80,1]	ns	74,1 [68,3 - 81,9]	75,7 [68,0 - 80,7]	74 [69 - 81]	73,2 [56,6 - 79,9]	74,2 [68,5 - 79,6]	73,3 [63,5 - 79,9]	ns
T cells (/µL)	774 [420 - 1182]	1104 [599 - 1772]	*	1104 [697 - 1284]	1269 [892 - 1791]	1142 [727 - 1512]	560 [351 - 972]	739 [486 - 1299]	711 [347 - 1003]	***
$CD4^+$ T cells %	45,1 [37,0 - 57,7]	47,0 [36,6 - 55,6]	ns	45,2 [35,7 - 57,3]	50,3 [43,4 - 58,1]	48,1 [38,5 -58,0]	45,1 [37,3 - 58,2]	38,9 [31,7 - 48,5]	42,9 [36,4 - 55,1]	ns
$CD4^+$ T cells (/µL)	469 [261 - 777]	666 [340 - 1047]	*	583 [389 - 898]	824 [539 - 1208]	723 [414 - 1049]	415 [216 - 681]	431 [311 - 660]	415 [245 - 664]	***
$CD8^+$ T cells %	21,6 [16,3 - 28,8]	23,3 [18,8 - 30,2]	ns	21,9 [18,1 - 30,8]	20,9 [17,7 - 26,6]	21,3 [18,0 - 28,2]	20,9 [12,4 - 23,8]	28,6 [23,4 - 36,4]	23,5 [17,4 - 30,7]	*
$CD8^+$ T cells (/µL)	208 [134 - 417]	362 [196 - 585]	**	336 [155 - 496]	392 [221 - 585]	362 [164 - 535]	183 [82 - 301]	307 [167 - 643]	189 [120 - 421]	**
B cells %	8,3 [4,7 - 14,8]	10,8 [4,1 - 17,6]	ns	8,6 [5,0 - 14,5]	13,8 [5,9 - 20,7]	11,2 [5,0 - 16,2]	7,8 [4,1 - 15,0]	8,3 [3,6 - 11,5]	7,9 [3,7 - 14,3]	ns
B cells (/µL)	87 [46 - 187]	119 [61 - 269]	0,074	119 [56 - 259]	187,8 [97 - 388]	140 [69 -273]	77 [34 - 148]	55 [30-173]	68 [34 - 151]	***
NK cells %	11,7 [8,4 - 18,4]	8,0 [5,6 - 15,7]	*	11,1 [7,2 - 17,3]	7,0 [5,0 - 10,5]	5,6 [6,0 - 13,9]	14,0 [9,0 - 21,5]	13,0 [7,5 - 21,4]	14,0 [8,9 - 21,5]	**
NK cells (/µL)	138 [74 - 193]	118 [74 - 226]	ns	145 [90 - 200]	118 [86 - 197]	129 [90 - 194]	109 [59 - 182]	118 [60 - 257]	110 [59 - 204]	ns

*Table 4. Lymphocytic subpopulations of men, women, survivors and non-survivors at T0. *p<0.05, **<0.01, ***p<0.001, ns=non-significant.*

Consistently, at T1 survivors had more total T cells (p<0.001), particularly more $CD4^+$ T cells (p<0.001) but $CD8^+$ T cells (p=0.06) as well as B cells (p=0.05) failed to reach statistical significance. The sex-stratified analysis showed that specifically women had more $CD4^+$ T cells (p<0.05) than men, and even more B cells (p<0.001), but there were no differences in the number of $CD8^+$ T cells (p=0.39) nor NK cells (p=0.25). When both sex and survival were considered, non-survivor men drove most of the differences, with less T cells than both survivor men (p<0.01) and women (p<0.01), specifically less $CD4^+$ T cells (survivor men p<0.05, survivor women p<0.001), and also less B cells than survivor women (p<0.01).

Thus, at T1 the dynamics were similar to those at T0 but $CD4^+$ T cells and B cells were the most relevant subpopulations at this time-point, while $CD8^+$ T cells lost the strength of the differences among groups found at T0 and NK cells became also comparable by percentage.

Paired analysis showed that, overall, both in absolute counts and by percentages, $CD4^+$ T cells did not change between time-points (p=0.89), while $CD8^+$ T cells increased (p<0.05), as well as NK cells (p<0.01) but B cells decreased (p<0.01) (Figure 22A). Survival stratification showed that these dynamics were driven by survivors, while non-survivors showed comparable numbers of all lymphocytic subpopulations except a decrease in the percentage of B cells (p<0.05) (Figure 22B). Interestingly, sex stratification showed that men drive the differences in T and NK cells but they did not show significant B cell decrease (178 [96 – 344] vs 140 [90 – 199], p=0.12), while it was women who showed a significant B cell decrease between T0 and T1 (106 [53 – 150] vs 74 [40 – 136], p<0.01) (Figure 22C).

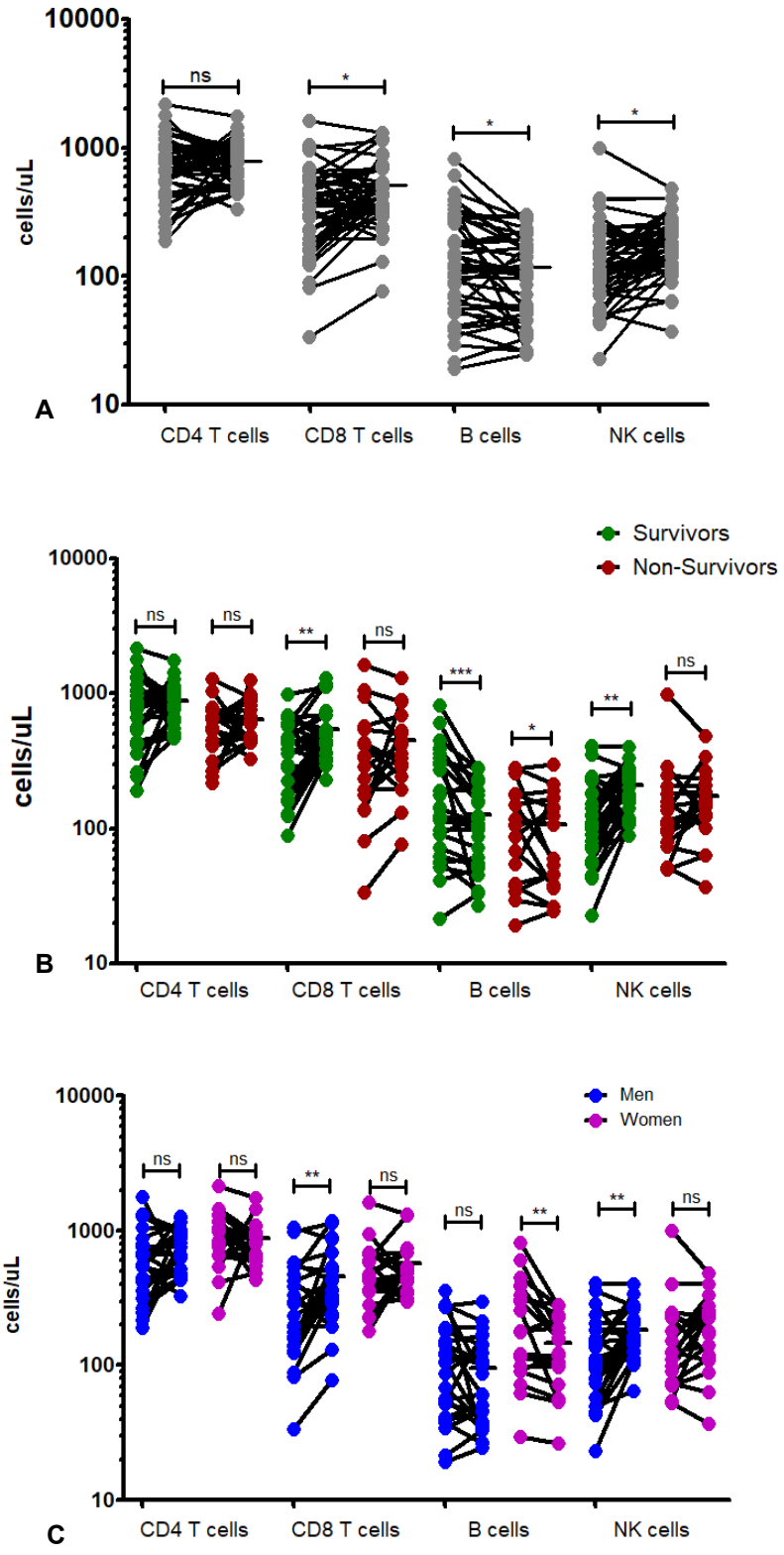


*Figure 22. Paired analysis of lymphocytic subpopulations in total **(A)**, by survival **(B)** and by sex stratification **(C)**.*

4.1.5. Differentiated T cell subpopulations

We analyzed the 3 populations relating to CD28 and CD27 expression as described in the bibliography [36,48]: Early differentiated $CD27^{+}$ $CD28^{+}$ (early), intermediate differentiated $CD27^{+}$ $CD28^{neg}$ (intermediate) and Late differentiated $CD27^{neg}$ $CD28^{neg}$ (late). We aimed to describe the differentiated T cell phenotype of aging patients during CAP (T0) and at follow-up (T1) and we found significant differences in the absolute counts of the subpopulations between the groups.

Initial analysis showed that total early were higher than intermediate and late both at T0 ($p<0.0001$) and T1 ($p<0.0001$). Likewise, late were higher than intermediate also at both time-points ($p<0.0001$). No significant differences were observed in any subpopulation between the T0 and the T1 cohorts (Figure 23). Paired analysis confirmed the absence of significant dynamics between time-points; however, a trend towards an increase in late ($p=0.06$) and intermediate ($p=0.05$) was noted. Still, wide ranges and considerable heterogeneity within subpopulations were shown, which granted further examination.

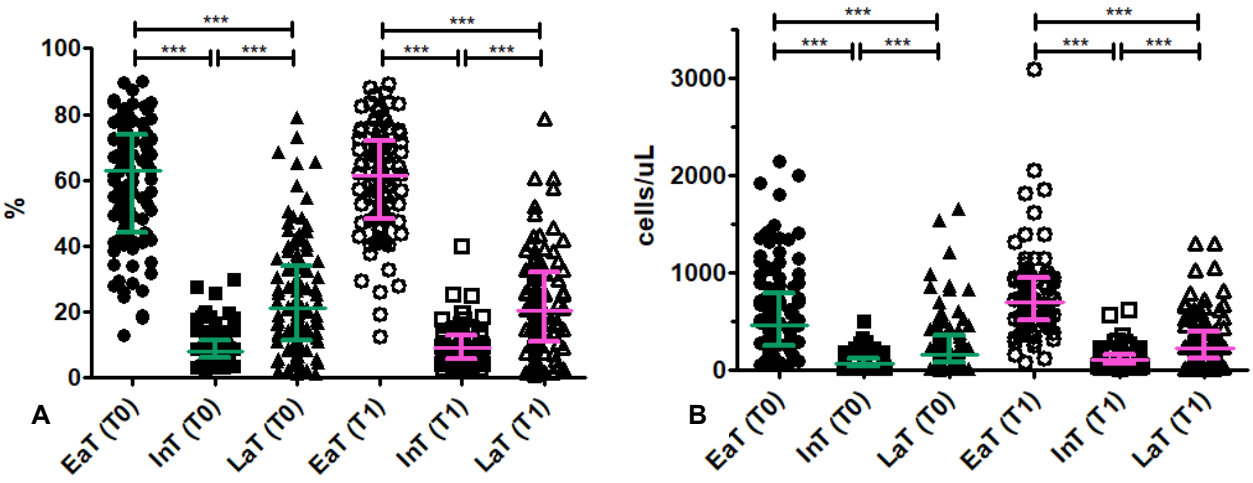


*Figure 23. Early differentiated (EaT) ($CD27^{+}$ $CD28^{+}$), intermediate (InT) ($CD28^{+}$ $CD27^{neg}$), and late T cells (LaT) ($CD28^{neg}$ $CD27^{neg}$) at T0 (green) and at T1 (pink) in percentage over total T cells **(A)** and by cells/μL **(B)**. *** <0.0001.*

4.1.5.1. $CD4^{+}$ vs $CD8^{+}$ T cells

First, we decided to analyze $CD4^{+}$ and $CD8^{+}$ T cells separately. $CD4^{+}$ and $CD8^{+}$ T cells showed distinct distributions across their respective differentiated subpopulations, which remained comparable between time points. On the one hand, $CD4^{+}$ T cells were mostly early (T0: 79.2% [66.0 - 85.6]; T1: 9.8% [7.3 - 15.2]) with lower intermediate (T0: 9.8% [2.6-15.2]; T1: 11.4% [7.6 - 15.7]) and late (T0: 6.8% [1.9 - 14.2]; T1: 5.5% [0.8 - 15.0]). On the other hand, $CD8^{+}$ T cells had a similar proportion of early (T0: 34.2% [19.2 - 47.4]; T1: 35.7% [23.1 - 48.1]) and late (T0: 47.3% [31.3 - 61.9]; T1: 42.8% [24.0 - 59.0]) (Figure 24A). This also resulted in higher absolute counts of $CD4^{+}$ early than $CD8^{+}$ early ($p<0.0001$ at T0 and T1), higher $CD4^{+}$ intermediate than $CD8^{+}$ intermediate ($p<0.0001$ at T0 and T1) and lower $CD4^{+}$ late than $CD8^{+}$ late ($p<0.0001$ at T0 and T1) (Figure 24B). Comparison of T0 and T1 cohorts only revealed higher absolute counts of early $CD4^{+}$ T cells at T1 compared to T0 (Figure 24B). No other differences were found of each subpopulation between time-points.

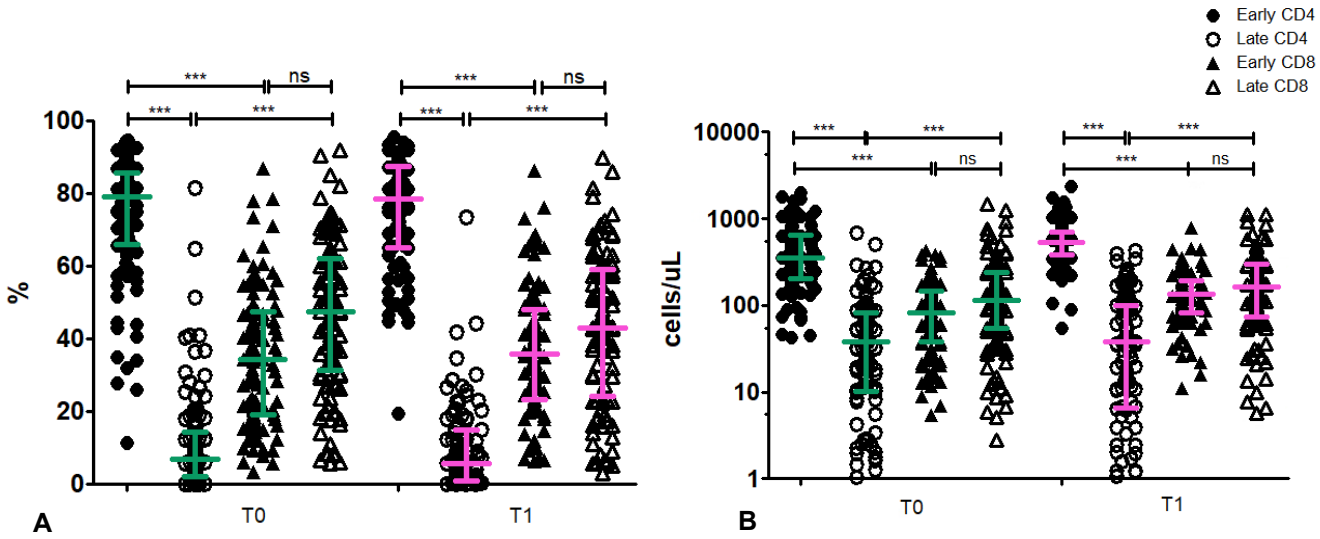


*Figure 24. CD4⁺ and CD8⁺ early (CD27⁺ CD28⁺) and late T cells (CD28^{neg} CD27^{neg}) at T0 (green) and at T1 (pink) in percentage over total CD4⁺ or CD8⁺ T cells **(A)** and in cells/µL **(B)**.*

Contrary to what was expected after comparing T0 and T1, paired analysis failed to show a significant increase in early CD4⁺ T cells in absolute counts (p>1.0). However, it showed a significant increase in intermediate (11 cells/µL [8 – 19] vs 19 cells/µL [12 – 33], p<0.05) and late (140 cells/µL [71 – 283] vs 205 cells/µL [123 – 334], p<0.01) CD8⁺ T cells that was not apparent comparing the T0 and T1 cohorts. These results may reflect the fact that T0 and T1 cohorts were fundamentally different due to the loss of the patients that died before 60 days (Figure 25).

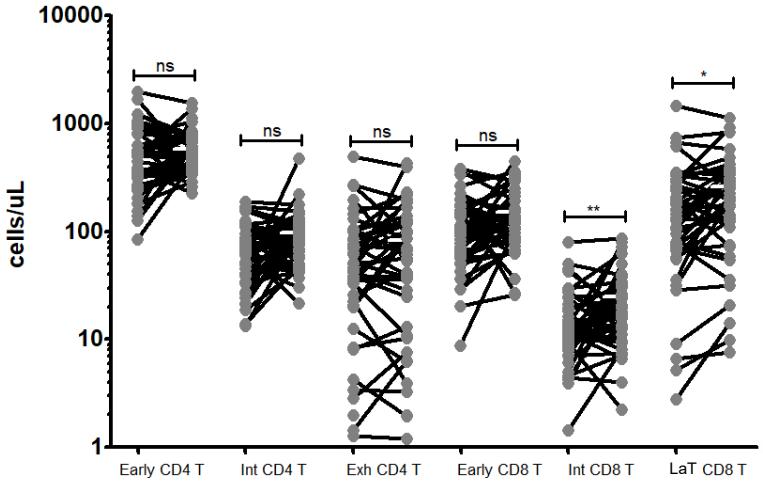


*Figure 25. Paired analysis of absolute counts of early, intermediate and late CD4⁺ T cells and CD8⁺ T cells. Int=Intermediate, LaT=Late. *p<0.05, **p<0.01.*

4.1.5.2. Gendered subanalysis

Since life expectancy is significantly different between men and women, a further gendered subanalysis was performed to describe men's and women's phenotypes independently[136]. At T0, the only percentage

difference was in the intermediate CD8⁺ T cells, of which men had more than women (

T1 (Median [IQR])	Men	Women	p	Surv			Non surv			p
				Men	Women	Total	Men	Women	Total	
	n = 53	n = 41		n = 32	n = 33	n = 65	n = 21	n = 8	n = 29	
Early T cells %	62.6 [48.7 – 72.9]	60.0 [48.4 – 71.4]	0.6750	64.4 [47.4 – 73.9]	61.3 [48.4 – 71.4]	62.2 [48.0 – 73.4]	62.3 [52.6 – 69.2]	57.9 [48.0 – 63.2]	60.0 [50.5 – 68.1]	0.7020
Int T cells %	9.9 [7.5 – 13.9]	8.3 [5.6 – 10.1]	0.0597	9.1 [7.3 – 12.5]	8.3 [5.8 – 10.1]	8.8 [6.6 – 12.0]	10.4 [7.7 – 15.0]	7.7 [5.3 – 10.1]	10.2 [5.7 – 14.9]	0.1280
Late T cells %	19.1 [9.8 – 32.3]	22.7 [14.7 – 30.4]	0.5752	16.9 [9.7 – 32.4]	21.5 [14.0 – 28.7]	19.6 [11.3 – 31.8]	21.0 [9.8 – 30.5]	26.1 [16.3 – 33.4]	22.2 [14.8 – 31.0]	0.8050
CD4+ Early T cells %	78.9 [65.3 – 88.4]	76.5 [60.8 – 87.0]	0.5023	82.4 [68.0 – 89.6]	78.3 [60.8 – 87.7]	81.2 [65.0 – 89.3]	78.4 [65.3 – 83.0]	75.2 [70.4 – 80.8]	77.8 [65.3 – 81.0]	0.4510
CD4+ Int T cells %	12.5 [8.1 – 17.4]	10.3 [7.5 – 13.7]	0.1145	9.6 [7.9 – 15.0]	10.0 [7.3 – 13.5]	9.8 [7.5 – 14.3]	14.2 [11.5 – 18.7]	12.4 [8.3 – 13.9]	13.7 [8.7 – 17.7]	0.1220
CD4+ Late T cells %	2.7 [0.4 – 12.2]	6.4 [3.2 – 17.5]	0.1036	1.9 [0.6 – 13.2]	6.4 [3.2 – 17.5]	5.5 [0.8 – 16.4]	3.1 [0.4 – 12.2]	6.4 [4.1 – 11.9]	5.1 [1.0 – 12.2]	0.3980
CD8+ Early T cells %	35.1 [25.8 – 50.3]	36.2 [21.2 – 41.6]	0.3683	33.8 [24.2 – 58.3]	36.2 [22.2 – 42.8]	34.8 [22.2 – 51.8]	36.3 [30.4 – 44.1]	30.0 [20.6 – 40.2]	36.3 [23.5 – 41.2]	0.7150
CD8+ Int T cells %	5.8 [3.1 – 9.2]	3.4 [2.6 – 5.8]	0.0163	6.0 [4.0 – 9.2]	3.9 [2.6 – 5.8]	5.0 [2.8 – 7.4]	4.0 [3.0 – 8.2]	3.1 [2.3 – 5.8]	3.9 [2.7 – 7.2]	0.0934
CD8+ Late T cells %	40.6 [19.1 – 59.1]	44.9 [32.9 – 58.1]	0.2196	41.9 [18.4 – 60.8]	44.1 [31.8 – 57.4]	43.4 [23.1 – 58.1]	39.3 [30.2 – 46.3]	53.7 [39.6 – 62.1]	40.6 [34.9 – 59.0]	0.5460
Early T cells/uL	712 [466 – 928]	691 [566 – 943]	0.2998	759 [604 – 975]	748 [587 – 957]	755 [592 – 967]	466 [318 – 712]	602 [565 – 681]	565 [381 – 712]	0.0027
Int T cells /uL	114 [66 – 150]	106 [68 – 155]	0.7488	117 [86 – 174]	106 [68 – 156]	114 [71 – 160]	101 [53 – 131]	103 [82 – 112]	101 [53 – 129]	0.3920
Late T cells /uL	189 [109 – 372]	273 [152 – 393]	0.0877	205 [135 – 415]	274 [161 – 393]	239 [142 – 407]	135 [96 – 303]	259 [149 – 417]	182 [108 – 303]	0.2430
CD4+ Early T cells /uL	494 [366 – 689]	559 [434 – 768]	0.1028	572 [426 – 721]	585 [448 – 790]	582 [436 – 785]	366 [255 – 575]	478 [379 – 550]	390 [270 – 575]	0.0022
CD4+ Int T cells /uL	81 [47 – 113]	81 [56 – 117]	0.6583	86 [55 – 114]	85 [56 – 124]	85 [55 – 118]	75 [43 – 109]	75 [61 – 81]	75 [45 – 95]	0.4440
CD4+ Late T cells /uL	13 [3 – 87]	54 [22 – 119]	0.0109	13 [5 – 90]	57 [22 – 124]	38 [8 – 119]	13 [2 – 58]	41 [21 – 84]	29 [3 – 80]	0.0766
CD8+ Early T cells/uL	139 [67 – 215]	122 [87 – 192]	0.9271	146 [106 – 252]	137 [86 – 192]	144 [97 – 248]	105 [62 – 159]	119 [89 – 135]	106 [63 – 155]	0.1400
CD8+ Int T cells /uL	22 [11 – 33]	15 [10 – 25]	0.1273	25 [15 – 45]	15 [10 – 25]	20 [11 – 34]	16 [9 – 24]	16 [12 – 22]	16 [9 – 24]	0.0569
CD8+ Late T cells /uL	133 [60 – 252]	188 [95 – 294]	0.1518	148 [62 – 271]	188 [88 – 294]	173 [86 – 294]	129 [54 – 211]	202 [129 – 359]	133 [72 – 256]	0.3970

Supplementary Table 9). However, in total cell-counts, women had more late T cells than men, either total (women: 202 cells/µL [111 – 388], men: 122 cells/µL [56 – 351], p<0.05), CD4⁺(women: 49 cells/µL [16 – 93], men: 32 cells/µL [5 – 70], p<0.05) or CD8⁺(women: 139 cells/µL [78 – 259, men: 90 cells/µL [37 – 214], p<0.05) (Figure 26A-F).

Similarly, at T1, the only percentage difference found was also on intermediate CD8⁺ T cells, of which men had more than women (Supplementary Table 9). However, in cell-count values, at this time-point women only had more late CD4⁺ T cells compared to men (women: 54 cells/µL [22 – 119], men: 13 cells/µL [3 – 87], p<0.05). Contrary to what we found at T0, late CD8⁺ T cells were not different (Figure 26A-F).

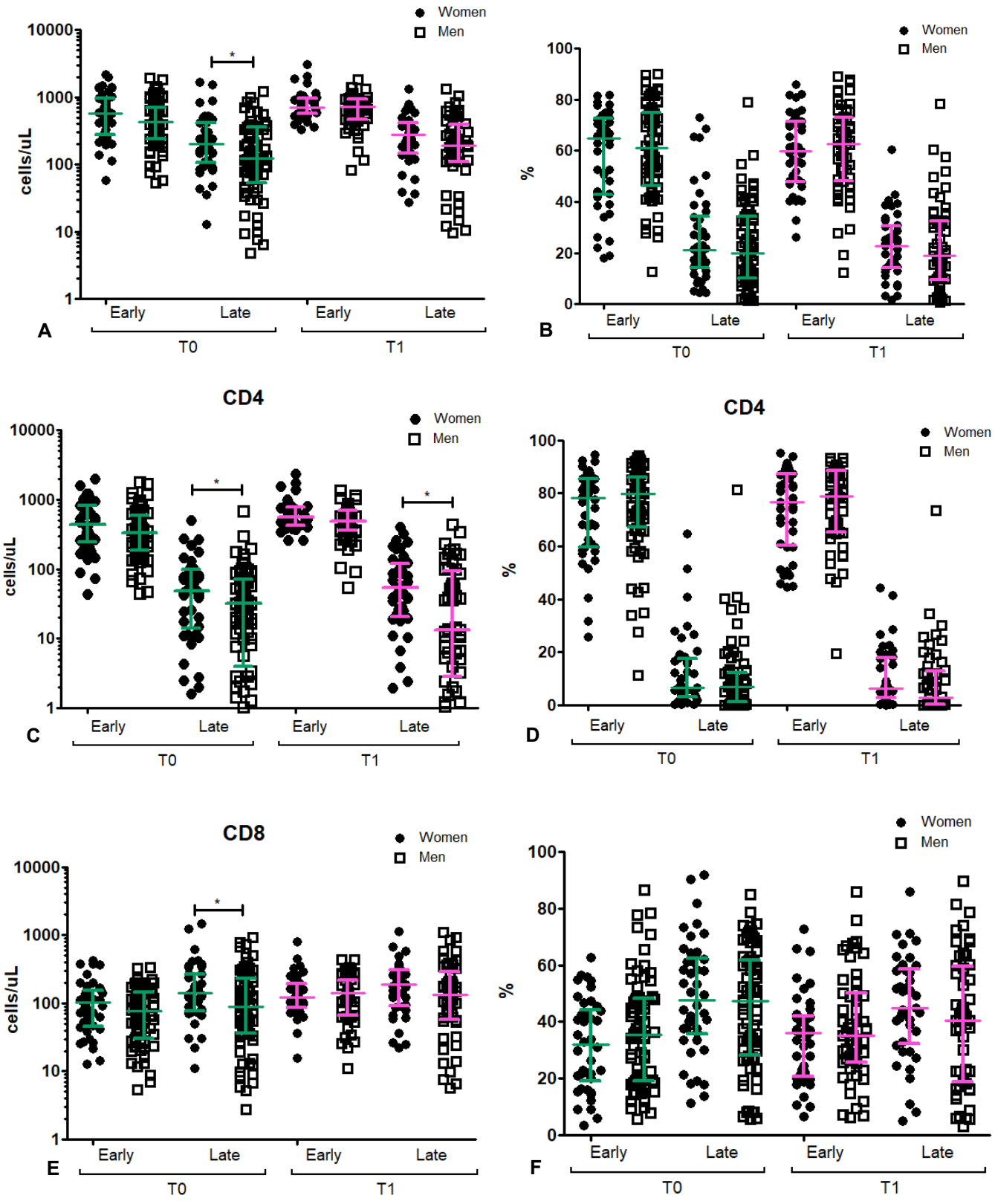


*Figure 26. Sex-stratified analysis of early (CD27⁺ CD28⁺) and late T cells (CD28^{neg} CD27^{neg}) at T0 and T1, in cells/µL for total CD3⁺ T cells **(A)**, CD4⁺ T cells **(C)**, CD8⁺ T cells **(E)** and percentage over total CD3⁺ T cells **(B)**, CD4⁺ T cells **(D)** and CD8⁺ T cells **(F)**.*

Paired analysis showed that men increased significantly the number and percentage of intermediate T cells between time-points (T0: 66 cells/µL [45 – 97] (8.3% [6.2 – 11.4]); T1: 126 cells/µL [96 – 151]

(10.3% [7.7 – 13.8]), p<0.05), driven by the increase of intermediate $CD4^+$ T cells (T0: 55 cells/μL [29 – 83] (9.8% [6.8 – 14.4]); T1: 93 cells/μL [61 – 119] (13.5% [9.5 – 17.6]), p<0.05). There were no differences in the percentage of $CD8^+$ subsets. However, the described increase in $CD8^+$ T cell count was reflected in an increase in all the differentiated subsets (p<0.05), although this increase was more pronounced in the intermediate subset (T0: 10 cells/μL [8 – 15], T1: 24 cells/μL [12 – 33], p<0.01). Women showed no differences between time-points, similarly to the absent differences in overall $CD4^+$ and $CD8^+$ T cells.

4.1.5.3. Survival stratification

At T0, survival stratification showed no differences in the percentage of any of the different subsets but there were significant differences in the cell-count subsets. We described above how survivors had more T cells in general but, interestingly, this difference was driven specifically early T cells, in total T cells (survivors: 616 cells/μL [390 – 1026], non-survivors: 333 cells/μL [208 – 555], p<0.001), but also by early $CD4^+$ T cells (survivors: 541 cells/μL [274 – 829], non-survivors: 260 cells/μL [170 – 431], p<0.001), and $CD8^+$ T cells (survivors: 111 cells/μL [56 – 171], non-survivors: 58 cells/μL [25 – 117], p<0.01). Furthermore, survivors also had more intermediate $CD4^+$ T cells (survivors: 64 cells/μL [36 – 103], non-survivors: 50 cells/μL [22 – 86], p<0.05) but there were no differences in the number of late T cells (

Figure 27).

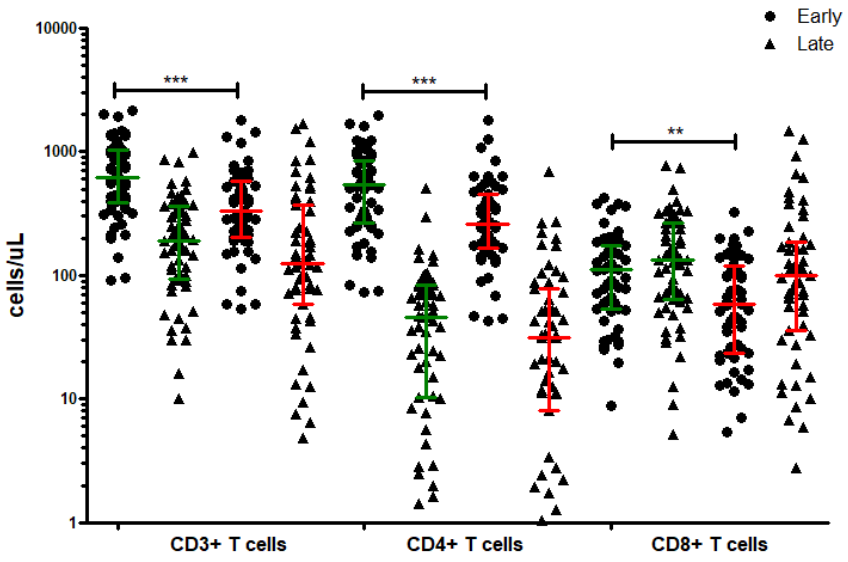


*Figure 27. Survival-stratified analysis of early and late T cell counts at T0. Green=survivors; Red=non-survivors. **<0.01, ***p<0.001*

At T1, non-survivors showed a higher percentage of intermediate $CD4^+$ T cells (survivors: 8.9% [6.9 – 14.2], non-survivors: 11.0% [8.2 – 15.7], p<0.05), similar to what we found in men. Moreover, survivors still showed higher cell-counts of total (survivors: 755 cells/μL [592 – 967], non-survivors: 565 cells/μL [381 – 712], p<0.001), $CD4^+$ (survivors: 582 cells/μL [436 – 785], non-survivors: 390 cells/μL [270 – 575], p<0.001) and $CD8^+$ (survivors: 144 cells/μL [97 – 249], non-survivors: 106 cells/μL [63 – 156], p<0.05) early T cells (Figure 28).

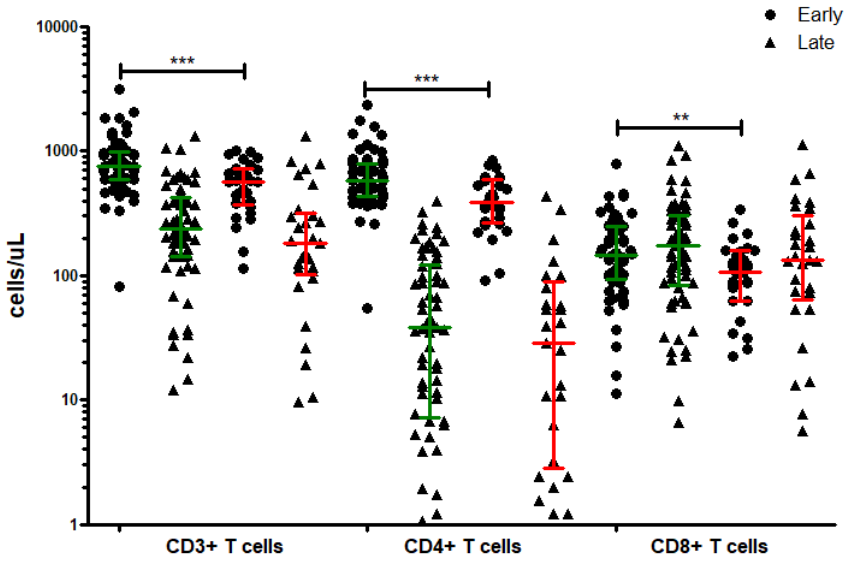


*Figure 28. Survival-stratified analysis of early and late T cell counts at T1. Green=survivors; Red=non-survivors. **<0.01, ***p<0.001*

Contrary to expected, paired analysis showed that it was survivors who increased the percentage of intermediate $CD4^+$ T cells (T0: 7.8% [5.0 – 11.5], T1: 9.8% [7.5 – 13.9], p<0.05), while non-survivors showed no difference here (T0: 12.8% [9.5 – 18.1], T1: 14.0% [11.8 – 17.6], p=0.64). This contradictory result to what was found at the previous cohorts highlights again that the T0 and T1 cohorts could be fundamentally different due to the deceased patients between time-points. There were no other

differences in the percentage distribution of the differentiated populations (

T1 (Median [IQR])	Men	Women	p	Surv			Non surv			p
				Men	Women	Total	Men	Women	Total	
	n = 53	n = 41		n = 32	n = 33	n = 65	n = 21	n = 8	n = 29	
Early T cells %	62.6 [48.7 – 72.9]	60.0 [48.4 – 71.4]	0.6750	64.4 [47.4 – 73.9]	61.3 [48.4 – 71.4]	62.2 [48.0 – 73.4]	62.3 [52.6 – 69.2]	57.9 [48.0 – 63.2]	60.0 [50.5 – 68.1]	0.7020
Int T cells %	9.9 [7.5 – 13.9]	8.3 [5.6 – 10.1]	0.0597	9.1 [7.3 – 12.5]	8.3 [5.8 – 10.1]	8.8 [6.6 – 12.0]	10.4 [7.7 – 15.0]	7.7 [5.3 – 10.1]	10.2 [5.7 – 14.9]	0.1280
Late T cells %	19.1 [9.8 – 32.3]	22.7 [14.7 – 30.4]	0.5752	16.9 [9.7 – 32.4]	21.5 [14.0 – 28.7]	19.6 [11.3 – 31.8]	21.0 [9.8 – 30.5]	26.1 [16.3 – 33.4]	22.2 [14.8 – 31.0]	0.8050
CD4+ Early T cells %	78.9 [65.3 – 88.4]	76.5 [60.8 – 87.0]	0.5023	82.4 [68.0 – 89.6]	78.3 [60.8 – 87.7]	81.2 [65.0 – 89.3]	78.4 [65.3 – 83.0]	75.2 [70.4 – 80.8]	77.8 [65.3 – 81.0]	0.4510
CD4+ Int T cells %	12.5 [8.1 – 17.4]	10.3 [7.5 – 13.7]	0.1145	9.6 [7.9 – 15.0]	10.0 [7.3 – 13.5]	9.8 [7.5 – 14.3]	14.2 [11.5 – 18.7]	12.4 [8.3 – 13.9]	13.7 [8.7 – 17.7]	0.1220
CD4+ Late T cells %	2.7 [0.4 – 12.2]	6.4 [3.2 – 17.5]	0.1036	1.9 [0.6 – 13.2]	6.4 [3.2 – 17.5]	5.5 [0.8 – 16.4]	3.1 [0.4 – 12.2]	6.4 [4.1 – 11.9]	5.1 [1.0 – 12.2]	0.3980
CD8+ Early T cells %	35.1 [25.8 – 50.3]	36.2 [21.2 – 41.6]	0.3683	33.8 [24.2 – 58.3]	36.2 [22.2 – 42.8]	34.8 [22.2 – 51.8]	36.3 [30.4 – 44.1]	30.0 [20.6 – 40.2]	36.3 [23.5 – 41.2]	0.7150
CD8+ Int T cells %	5.8 [3.1 – 9.2]	3.4 [2.6 – 5.8]	0.0163	6.0 [4.0 – 9.2]	3.9 [2.6 – 5.8]	5.0 [2.8 – 7.4]	4.0 [3.0 – 8.2]	3.1 [2.3 – 5.8]	3.9 [2.7 – 7.2]	0.0934
CD8+ Late T cells %	40.6 [19.1 – 59.1]	44.9 [32.9 – 58.1]	0.2196	41.9 [18.4 – 60.8]	44.1 [31.8 – 57.4]	43.4 [23.1 – 58.1]	39.3 [30.2 – 46.3]	53.7 [39.6 – 62.1]	40.6 [34.9 – 59.0]	0.5460
Early T cells/uL	712 [466 – 928]	691 [566 – 943]	0.2998	759 [604 – 975]	748 [587 – 957]	755 [592 – 967]	466 [318 – 712]	602 [565 – 681]	565 [381 – 712]	0.0027
Int T cells /uL	114 [66 – 150]	106 [68 – 155]	0.7488	117 [86 – 174]	106 [68 – 156]	114 [71 – 160]	101 [53 – 131]	103 [82 – 112]	101 [53 – 129]	0.3920
Late T cells /uL	189 [109 – 372]	273 [152 – 393]	0.0877	205 [135 – 415]	274 [161 – 393]	239 [142 – 407]	135 [96 – 303]	259 [149 – 417]	182 [108 – 303]	0.2430
CD4+ Early T cells /uL	494 [366 – 689]	559 [434 – 768]	0.1028	572 [426 – 721]	585 [448 – 790]	582 [436 – 785]	366 [255 – 575]	478 [379 – 550]	390 [270 – 575]	0.0022
CD4+ Int T cells /uL	81 [47 – 113]	81 [56 – 117]	0.6583	86 [55 – 114]	85 [56 – 124]	85 [55 – 118]	75 [43 – 109]	75 [61 – 81]	75 [45 – 95]	0.4440
CD4+ Late T cells /uL	13 [3 – 87]	54 [22 – 119]	0.0109	13 [5 – 90]	57 [22 – 124]	38 [8 – 119]	13 [2 – 58]	41 [21 – 84]	29 [3 – 80]	0.0766
CD8+ Early T cells/uL	139 [67 – 215]	122 [87 – 192]	0.9271	146 [106 – 252]	137 [86 – 192]	144 [97 – 248]	105 [62 – 159]	119 [89 – 135]	106 [63 – 155]	0.1400
CD8+ Int T cells /uL	22 [11 – 33]	15 [10 – 25]	0.1273	25 [15 – 45]	15 [10 – 25]	20 [11 – 34]	16 [9 – 24]	16 [12 – 22]	16 [9 – 24]	0.0569
CD8+ Late T cells /uL	133 [60 – 252]	188 [95 – 294]	0.1518	148 [62 – 271]	188 [88 – 294]	173 [86 – 294]	129 [54 – 211]	202 [129 – 359]	133 [72 – 256]	0.3970

Supplementary Table 9 and Supplementary Table 9).

In the cell-count values, survivors showed an increase in the number of total late populations (T0: 206 cells/µL [106 – 357], T1: 371 cells/µL [187 – 468], p<0.05). It was mainly driven by CD8⁺ T cells (T0: 140 cells/µL [77 – 271], T1: 239 cells/µL [136 – 321], p<0.01), while CD4⁺ T cells barely reached significance (T0: 44 cells/µL [17 – 87], T1: 68 cells/µL [10 – 128], p=0.05). However, non-survivors didn't show any significant difference between time-points (Figure 29).

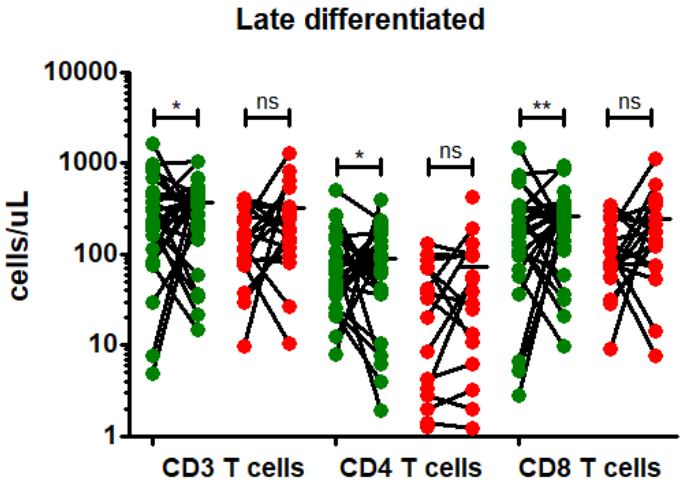


*Figure 29. Survival-stratified analysis of paired data of late T cell subpopulations. Green=survivors; red=non-survivors. *p<0.05 **<0.01, ns=non-significant.*

4.1.5.4. Sex-survival stratification

Consistent with the previous results, when we stratified the data by both sex and survival we observed that survivor women showed the most significant differences, mostly when compared to non-survivor men. By percentages, at T0 they had less late T cells (18.1% [9.6 – 25.7]) than non-survivor women (32.3% [20.4 – 52.7], p<0.05), but specifically less $CD8^+$ late T cells (38.9% [29.5 – 56.1]) than both non-survivor women (61.1% [45.4 – 72.1]) and non-survivor men (40.9% [31.0 – 61.5]) (p<0.05 for all mentioned comparisons). Of note, >50% of the $CD8^+$ T cells of non-survivor women showed an late phenotype.

By cell-count values, survivor women had more early than non-survivor men, in total T cell counts (survivor women: (756 cells/μL [466 – 1313]), non-survivor men: 304 cells/μL [196 – 577], p<0.01) but also in $CD4^+$ T cells (survivor women: 634 cells/μL [318 – 1026], non-survivor men: 241 cells/μL [160 – 473], p<0.01) and $CD8^+$ T cells (survivor women: 113 cells/μL [68 – 167], non-survivor men: 58 cells/μL [24 – 110], p<0.05). They also had more intermediate T cells than non-survivor men (survivor women: 103 cells/μL [55 – 171], non-survivor men: 60 cells/μL [26 – 110]), driven by $CD4^+$ T cells (survivor women: 83 cells/μL [45 – 131], non-survivor men: 50 cells/μL [18 – 86]) (p<0.05 for both). Interestingly, they also had more $CD8^+$ late T cells than no-survivor men (survivor women: 130 cells/μL [78 – 189], non-survivor men: 76 cells/μL [30 – 127], p<0.05). Thus, the lymphopenia found in non-survivor men described before was affecting almost all subsets.

At T1, non-survivor men showed all the significant differences, as they had less early (466 [318 – 712]) and specifically less $CD4^+$ early T cells (366 cells/μL [255 – 575]) than both men (early T: 759 cells/μL [604 – 975], p<0.01; early $CD4^+$ T: 572 cells/μL [426 – 721], p<0.05) and women survivors (early T: 748 cells/μL [587 – 957], early $CD4^+$ T: 585 cells/μL [448 – 790], p<0.01 for both).

Therefore, non-survivor men were the most different group at both times. But, while at T0 the differences were found compared to survivor women and were driven by their profound lymphopenia, at T1 the difference was specifically limited to the number early T cells and was found compared to all survivors. Furthermore, the only difference between survivor and non-survivor women was the percentage of late T cells at T0.

4.1.5.5. Differentiated T cell subpopulations' predictive value

We tested the predictive value of the differentiated T-cell phenotype by evaluating the association between these subpopulations and 2-year survival using univariate Cox proportional hazards models. Predictive performance was compared using the concordance index (CI). It showed that absolute number of early, either total, $CD4^+$ or $CD8^+$ T cells, had a protective effect with a CI of 0.65 for all three populations at T0, and 0.70 for total and $CD4^+$ early T cells at T1 (Figure 30).

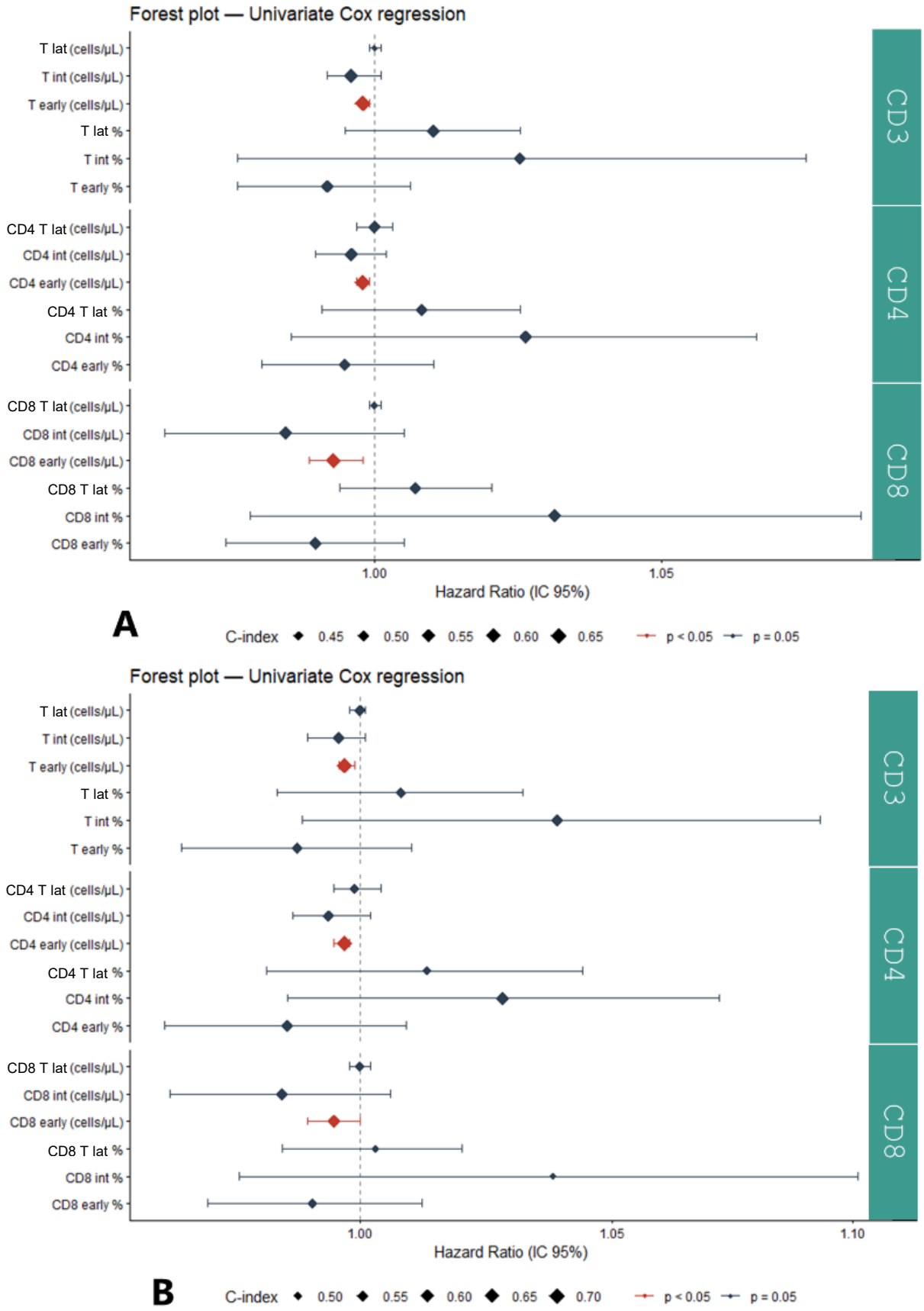


*Figure 30. Univariate Cox regression and concordance index (C-index) for early differentiated (early) ($CD27^{+}$ $CD28^{+}$) and late (lat) T cells ($CD28^{neg}$ $CD27^{neg}$) at T0 **(A)** and T1 **(B)**.*

So, we performed ROC and AUC analysis for these 3 populations, which showed that the number for total early and CD4⁺ early had the best AUC for overall two-year survival both at T0 (0.71 AUC for CD4⁺ and total early) and at T1 (0.73 AUC for CD4⁺ and total early).

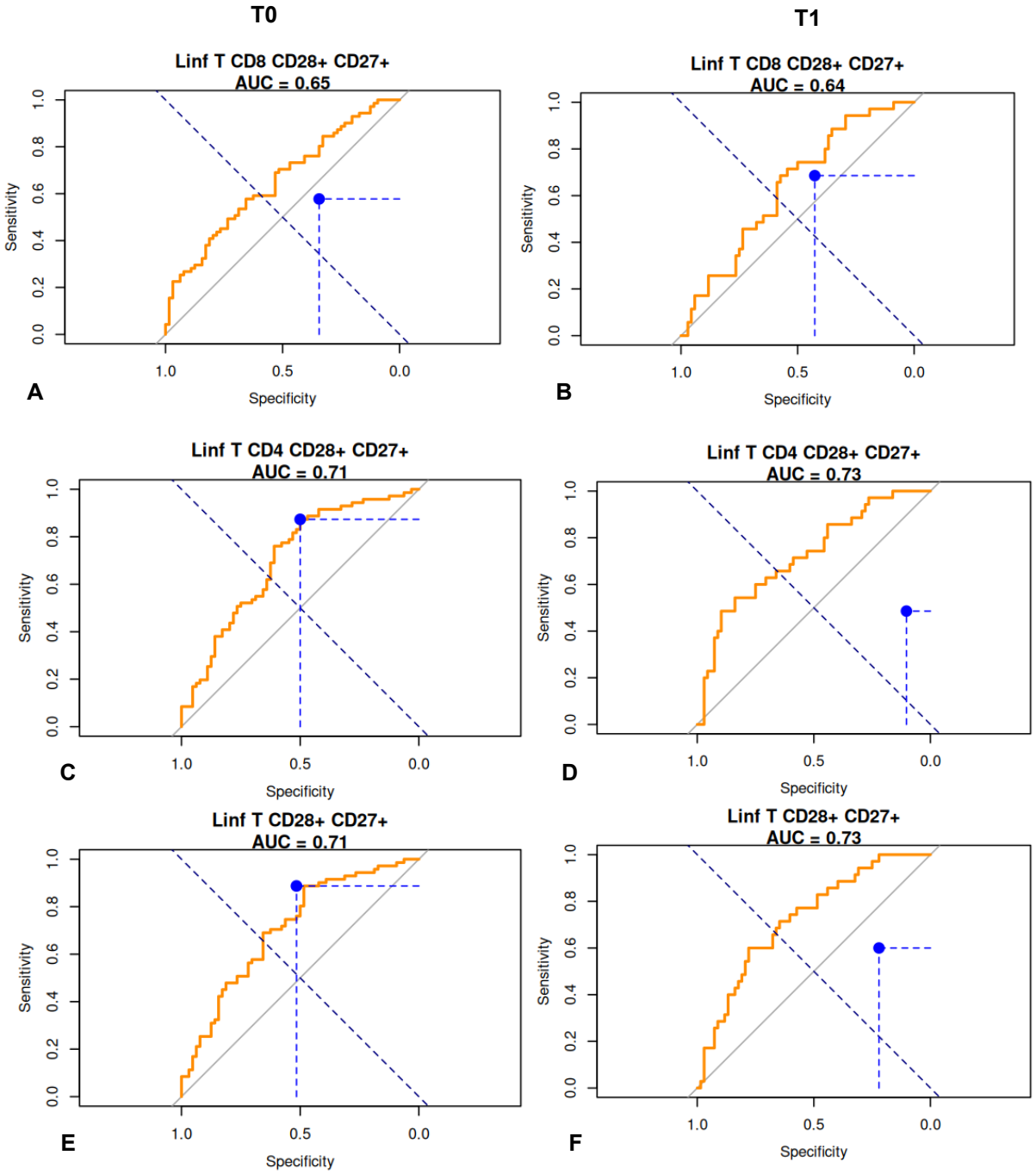


Figure 31. ROC curves for predicting 2-year mortality by early T subpopulations. CD8⁺ T cells at T0 ***(A)*** *and T1* ***(B)****, CD4⁺ T cells at T0* ***(C)*** *and at T1* ***(D)****, and total early T cells at T0* ***(E)*** *and T1* ***(F)****.*

Optimal cut-off points were also established. At T0, a high-sensitivity cut-off of 532 cells/μL for total yielded 74.6% sensitivity and 62.7% specificity (likelihood ratio: 2.00), while a high-specificity cut-off point of 338 cells/μL yielded 50.9% sensitivity and 79.7% specificity (likelihood ratio: 2.50). For CD4⁺ early, the high-sensitivity cut-off was established at 416, yielding 74.6% sensitivity and 59.3% specificity (likelihood

ratio: 1.83), while the high-specificity cut-off was established at 262, yielding 50.9% sensitivity and 76.3% specificity (likelihood ratio: 2.15).

At T1, a high-sensitivity cut-off for total early was established at 666 cells/µL yielding 72.4% sensitivity and 64.63% specificity (likelihood ratio: 2.05). For $CD4^+$ early a high-sensitivity cut-off of 523/µL yielded 72.4% sensitivity and 58.5% specificity (likelihood ratio: 1.74), while a high-specificity cut-off point of 435 cells/µL yielded 58.6% sensitivity and 75.4% specificity (likelihood ratio: 2.38).

4.1.6. Immune Risk Phenotype Markers

The IRP marker is defined in the bibliography as CMV seropositivity plus one of the following cell-count criteria: CD4/CD8 ratio <1, $CD8^+$ T cells >600 cells/µL or $CD28^{neg}$ T cells >300 cells/µL [46,51]. Thus, it integrates some of the populations analyzed previously and we wanted to explore its predictive capacity in our cohort.

At T0, 40 (35.1%) of the patients met the IRP criteria, while 74 (64.9%) didn't. Of those, 22 (29.3%) patients didn't meet it due to CMV seronegativity. Of interest, 9 (40.9%) out of these patients still would have met the cell-count criteria for IRP. On the contrary, out of the 92 (80.7%) seropositive patients, 52 (56.5%) did not meet the cell-count criteria. Neither survival nor sex-stratification showed significant differences in the percentage of patients with IRP (Figure 32A). Out of the 40 patients with IRP, 39 (97.5%) met the $CD28^{neg}$ T cells criterion, and only 1 depended on the inverted CD4/CD8 ratio to have IRP. The inversed CD4/CD8 ratio was found in 9 (22.5%) of patients, and the $CD8^+$ T cells criterion was found in 14 (35.0%) of patients. Furthermore, 21 (52.5%) patients met only 1 cell-count criterion, 16 (40.0%) met 2 cell-count criteria and 3 (7.5%) patients met the 3 cell-count criteria. Thus, the $CD28^{neg}$ T cells criterion, which is the only one that could correlate to the differentiated phenotype of our patients, was the most sensitive out of all the three IRP cell-count criteria.

At T1, 49 (52.1%) patients met the IRP criteria, while 45 (47.9%) didn't. Of those, 16 (35.6%) patients didn't meet it due to CMV seronegativity. Notably, in this case, no seronegative patients would have met the cell-count criteria for IRP. On the contrary, out of the 77 (81.9%) seropositive patients, 29 (37.7%) did not meet the cell-count criteria. Again, neither survival nor sex-stratification showed significant differences in the percentage of patients with IRP (Figure 32B). Out of the 49 patients with IRP, 47 (95.9%) met the $CD28^{neg}$ T cells criterion, while the remaining 2 patients met the IRP based on the other two criteria individually. The inversed CD4/CD8 ratio was found in 12 (24.5%) of patients, and the $CD8^+$ T cells criterion was found in 20 (40.8%) of patients. Furthermore, 27 (55.1%) patients met only 1 cell-count criterion, 14 (28.6%) met 2 cell-count criteria and 8 (16.3%) patients met the 3 cell-count criteria. Thus, again the $CD28^{neg}$ T cells criterion was the most sensitive out of all the IRP cell-count criteria.

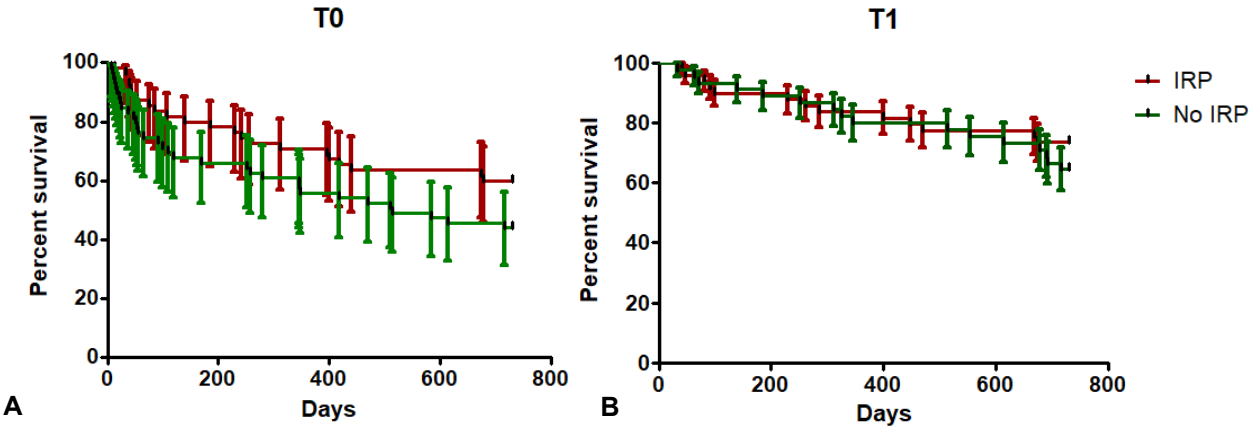


*Figure 32. Kaplan-Meier survival curves by immune-risk phenotype (IRP) positivity at T0 **(A)** and T1 **(B)**. No differences were found between patients with or without IRP at neither time-point.*

4.1.6.1. Paired IRP

Paired analysis of IRP showed that 14 (30.4%) patients changed their IRP status from T0 to T1: 10 (21.7%) patients acquired the IRP while 4 (8.7%) patients lost the IRP. However, 32 (69.6%) patients remained with the same IRP status: 15 (32.6%) patients kept the IRP while 17 (37.0%) patients still did not meet the IRP criteria. The proportion of patients with each scenario was not significantly different (p=0.18). All the patients that acquired the IRP at T1 was because they met the $CD28^{neg}$ T cells criterion, and inversely, all the patients that lost the IRP at T1 was because they stopped meeting the $CD28^{neg}$ T cells criterion.

Out of the cell-count criteria and regardless of CMV seropositivity status, 22 (47.8%) patients initially met at least 1 IRP cell-count criteria and 24 (52.2%) patients did not meet any criteria at T0. Out of the latter 24, at T1, 14 (58.3%) patients stayed without reaching any criteria, 9 (37.5%) patients acquired 1 criteria and 1 (4.2%) patient acquired 2 criteria. Out of the 22 patients who reached at least 1 criteria at T0, 8 (36.4%) patients met less criteria, 6 (27.3%) patients stayed the same, and 8 (36.4%) patients acquired one more criteria. All the changes are described in Table 5. So, overall, 20 (43.5%) patients kept meeting the same number of IRP criteria, 8 (17.4%) got better and 18 (39.1%) got worse.

T0 \ T1	0	1	2	3
0	14 (30.4%)	9 (19.6%)	1 (2.2%)	0
1	6 (13.0%)	2 (4.3%)	5 (10.9%)	0
2	1 (2.2%)	1 (2.2%)	3 (6.5%)	3 (6.5%)
3	0	0	0	1 (2.2%)

Table 5. IRP cell-count criteria on the paired cohort. Patients met 0, 1, 2 or 3 criteria at T0 (column) or T1 (row). Expressed as n(%), percentage relative to the overall paired cohort (n=46).

4.1.7. T-helper phenotype

Analysis of the T-helper cell panel revealed no significant differences in the proportional distribution of any of the subpopulations examined. We therefore adopted an alternative approach. It is well reported that different pathogens elicit specific T-helper differentiation profiles. In other words, T-helper differentiation is defined in response to the specific pathogen and the cytokine environment that it may trigger. For example, viral or intracellular bacteria elicit Th1 differentiation driven by IFNγ, while parasites drive a Th2 differentiation through IL-4 or fungal infections need a Th17 profile [53,55]. Thus, the T-helper profile and cytokine levels in an immunocompetent individual should reflect the causative pathogen in an infection.

However, in everyday clinical practice, the etiology of community acquired pneumonia (CAP) remains unidentified in up to 70% of cases [137]. Among the cases with confirmed etiology, approximately 60% are attributable to *Streptococcus pneumoniae*, whereas the remaining cases are caused by other bacterial species, viruses, or, less frequently, fungal pathogens. In our sample, 77.2% of the cases were of unknown etiology, and among those with confirmed etiology, *Streptococcus pneumoniae* was the most frequent, consistent with the literature [21,137]. Interestingly, the second most common etiology among our confirmed cases was Gram-negative bacteria (Table 6).

Pathogen	n	%
Unknown	125	77.2
S. pneumoniae	16	9.88
GNB	15	9.26
Other	4	2.47
Viral	2	1.23

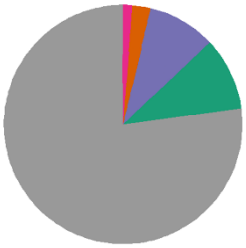
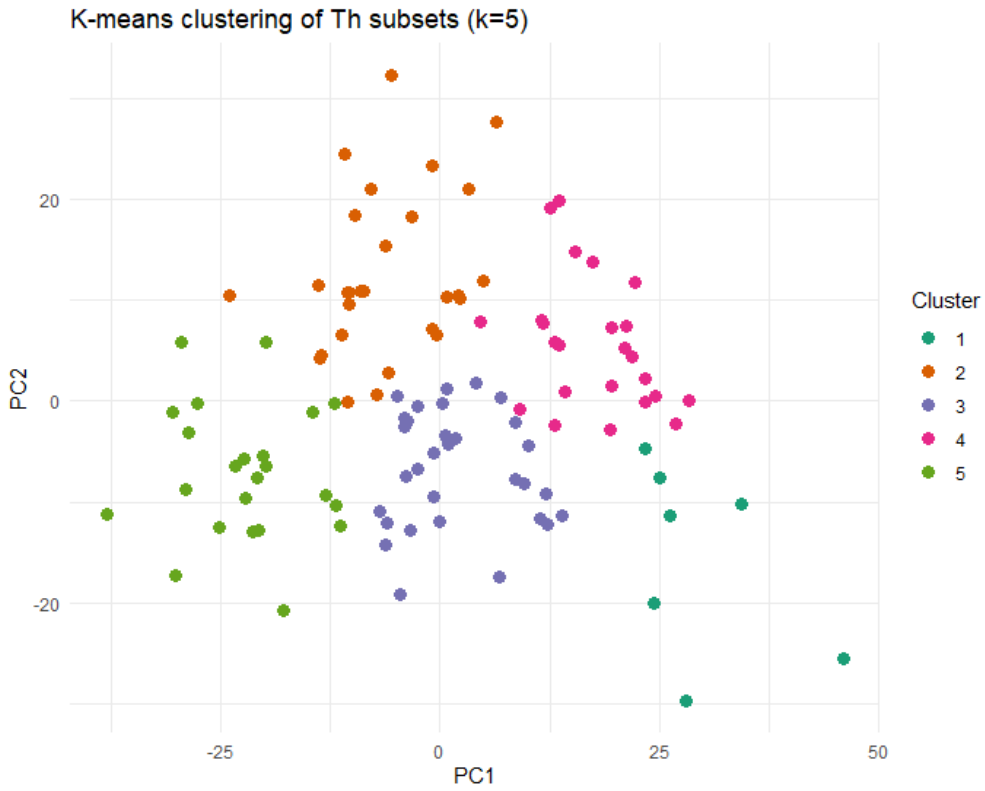


Table 6. Microbiological etiology of community acquired pneumonia in our cohort.

So, we aimed to discriminate different T-helper profiles to infer distinct microbiological etiology. Using k-means clustering, we distinguished 5 clusters of T-helper profiles among the patients suffering CAP, described in Table 7.



Cluster	n	Th 0% (x̄ ±SD)	Th1% (x̄ ±SD)	Th2% (x̄ ±SD)	ThTh1-17% (x̄ ±SD)	Th17% (x̄ ±SD)
1	7	15,22 (±6,4)	**50,93 (±10,41)**	7,69 (±4,98)	2,23 (±1,38)	1,53 (±1,31)
2	28	30,04 (±8,19)	13,1 (±4,06)	**28,9 (±7,38)**	1,87 (±2,43)	3,48 (±2,2)
3	32	**32,4 (±5,87)**	**26,23 (±5,79)**	12,59 (±4,41)	2 (±1,923)	2,76 (±1,79)
4	24	12,19 (±5)	24,57 (±7,62)	14,15 (±5,67)	**3,54 (±2,3)**	**4,74 (±3,66)**
5	23	**52,3 (±6,61)**	13,39 (±4,97)	15,87 (±6,28)	1,6 (±2,02)	2,54 (±1,66)

Table 7. K-means clustering of patients with CAP based on T-helper profiles (A) and their mean values for each variable (B).

Cluster 1 showed a strong proinflammatory Th1 profile, cluster 2 showed a Th2 skewed phenotype, cluster 3 had a more balanced profile between Th0 and Th1, cluster 4 had a higher representation of Th17 and the intermediate Th1-Th17 phenotype than the other clusters, while cluster 5 was mainly undifferentiated, with >50% of T-helper lymphocytes being Th0.

There were no significant differences in 2-year survival between the clusters, suggesting survival was not truly affected by microbiological agent (Figure 33). Not enough patients had a known etiology to correlate them with each cluster significantly.

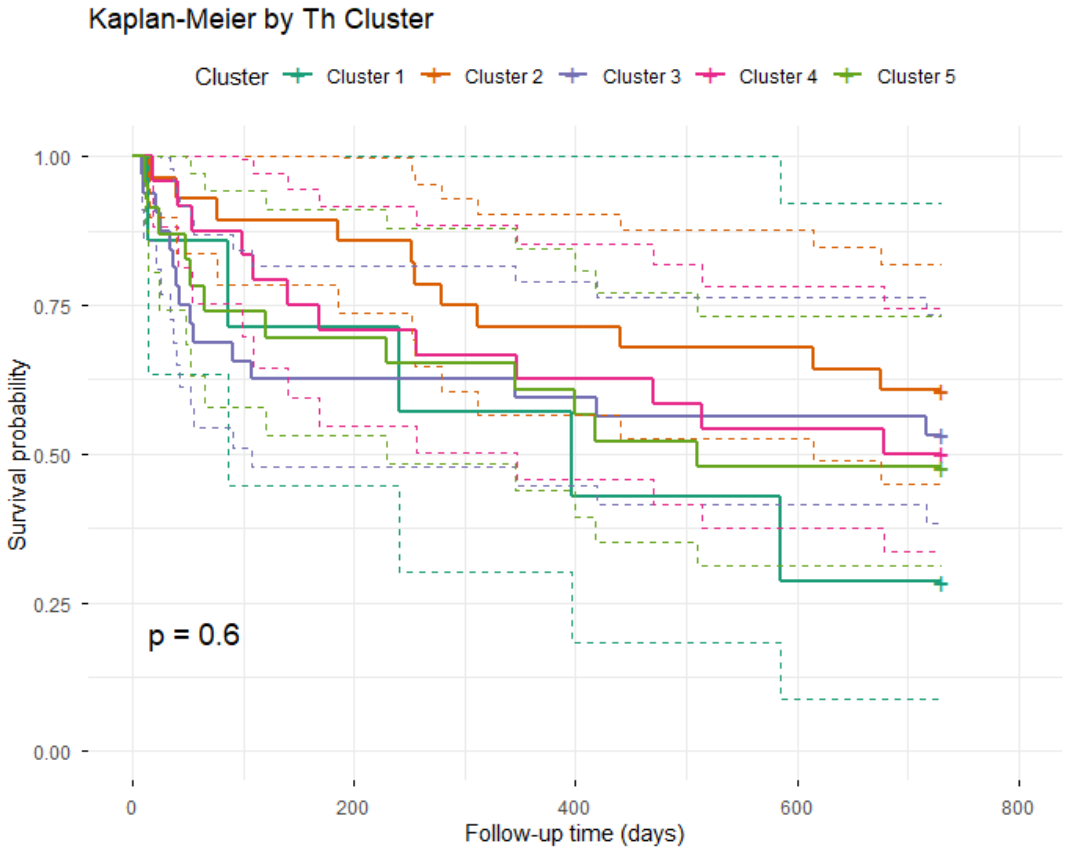


Figure 33. Kaplan-Meier survival curves for the 5 clusters of patients with CAP based on their T-helper profiles (95% CI shown as dotted line). No significant differences were found between the clusters' survival curves.

Even so, there were differences in the T cell differentiation profile showed between clusters (Supplementary Table 5). Cluster 1 was characterized by the lowest proportion of early differentiated T cells, both total and $CD4^+$, and the highest proportion of late T cells, consistent with its low Th0 and high Th1 proinflammatory profile. In contrast, clusters 2 and 5 showed the opposite pattern, with the highest frequencies of early differentiated total and $CD4^+$ T cells and the lowest proportions of late T cells. Clusters 3 and 4 showed intermediate profiles, with cluster 4 notable for higher intermediate T cells.

4.1.8. Serum cytokines

Serum cytokines representative of distinct T-helper function were measured by CBA assay in 95 patients from the T0 cohort. The assay included interleukin (IL-)2, IL-4, IL-6, IL-10, IL-17A, Tumor Necrosis Factor (TNF) and interferon-γ (IFNγ), Overall, cytokine levels were very low across the cohort. We compared the cytokine levels of each cluster defined previously by the T-helper profile and only IL-4 showed any significant difference. Specifically, cluster 1 showed significantly higher levels of IL-4 than cluster 4 ($p<0.05$) (Figure 34, Supplementary Table 6).

Given the little differences, and contrary to expected, the cytokine profile of each cluster did not match each cluster's T-helper composition. For example, cluster 1 and 3, with predominant Th1 composition, were expected to show a predominance of IFNγ and IL-2; while cluster 4, which had the highest Th17 and Th1-17 composition of all the clusters, was expected to have the highest presence of IL-17A. However, none of the expected differences were found (Table 7, Supplementary Table 6).

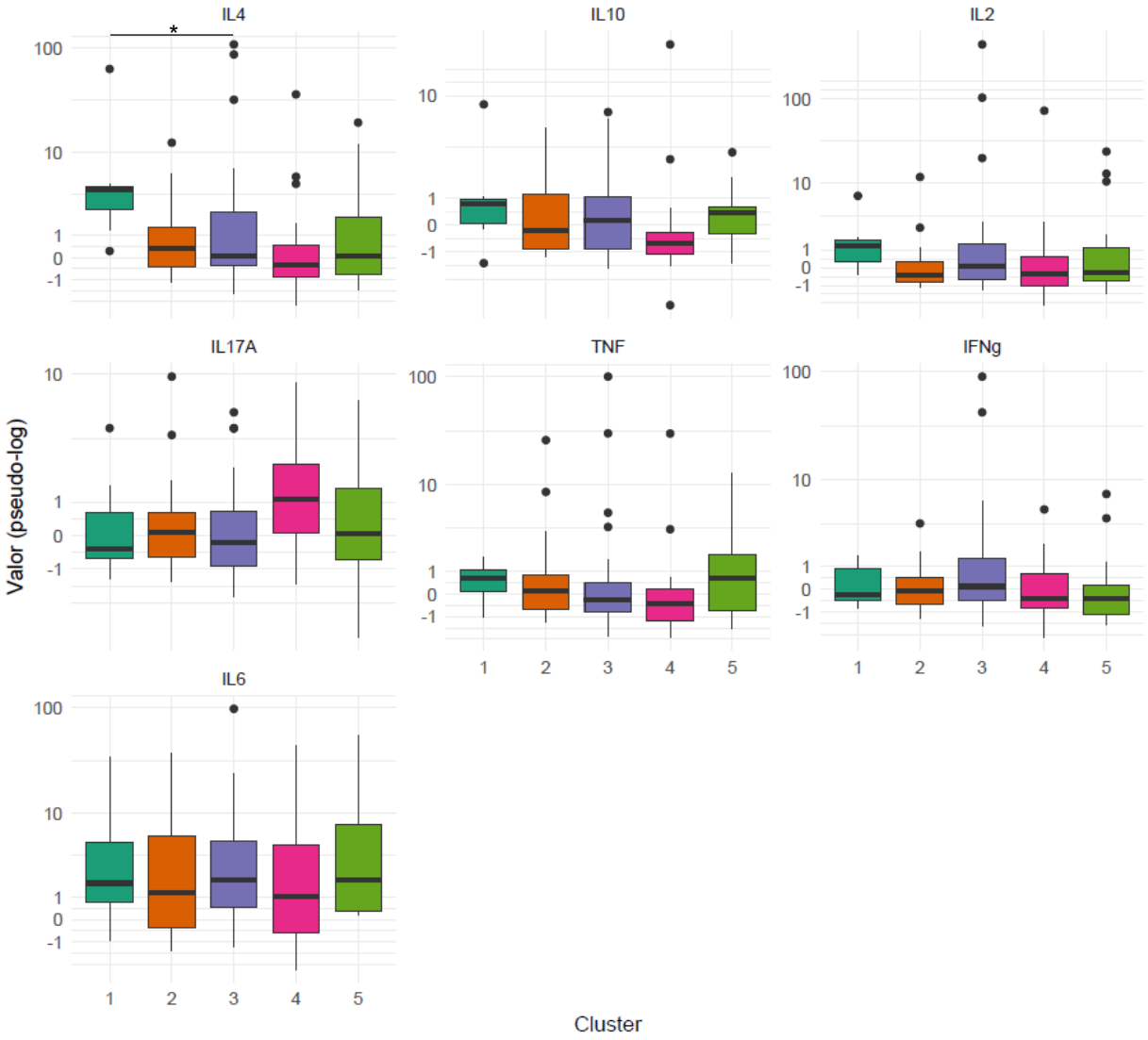


*Figure 34. Cytokines of each of the 5 clusters defined by T-helper profiles. Only significant finding was in IL-4 between cluster 1 and 4 (p<0.05). * = p<0.05.*

Accordingly, no differences were found in serum cytokine levels between survivors and non-survivors (Supplementary Table 7). However, sex-stratified analysis showed that women had higher IL-4 ($p<0.05$) and lower IL-17A ($p<0.01$) than men during CAP. Specifically, these differences were driven by non-survivor women, who exhibited higher IL-4 and lower IL-17A levels compared to both survivor and non-survivor men ($p<0.05$).

4.2.PART II – Common Variable Immunodeficiency

The clinical presentation of immunosenescence shares many clinical characteristics with common variable immunodeficiency (CVID). Therefore, we decided to study our patients with CVID as a potential model for patients at high risk of respiratory infections. We wanted to know if the immunodeficiency was comparable to immunosenescence. Thus, we studied 22 patients in two cohorts.

4.2.1. Demographics

The derivation cohort included 13 patients, of which 7 (53.8%) were women and 6 (46.2%) were men, with a mean age of 51.8 years, ranging from 30 to 82 years old. The confirmation cohort was comprised of 9 patients of which 7 (88.9%) were women and 2 (22.2%) were men, with a mean age of 55.1 years, ranging from 28 to 79 years old. There were no age differences between the cohorts nor the sex. Although, the confirmation cohort had a higher proportion of women than the derivation cohort, this difference did not reach statistical significance (p=0.38) due to the sample size (Figure 35).

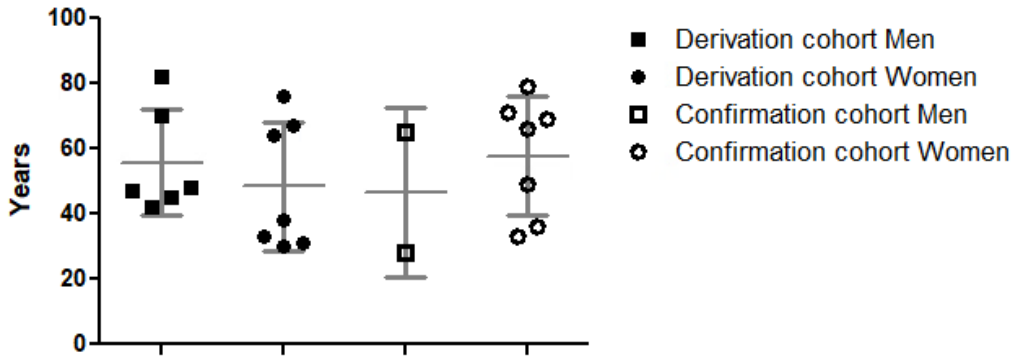


Figure 35. Ages of men and women from the derivation and the confirmation cohorts.

4.2.2. Clinical characteristics

CVID patients are clinically heterogeneous, and we hypothesized that patients with complicated CVID, defined as presenting with many non-infectious complications, were different from those who might present as immunosenescent patients. So, we needed to categorize the patients clinically.

The most prevalent clinical finding in the derivation cohort was bronchiectasis, present in 12 patients (92.3%), followed by lymphopenia (61.5%) and splenomegaly (38.5%). Liver disease, in the form of porto-sinusoidal vascular disease (PSVD), interstitial lung disease (ILD), lymphadenopathy, thrombocytopenia, and unusual infections were each found in approximately 30% of patients. Less frequent findings included anemia (15.4%), solid neoplasia (15.4%), inflammatory bowel disease (IBD) (15.4%), neutropenia (7.7%), monocytopenia (7.7%), and lymphoma (7.7%) (Table 8).

These findings were largely consistent in the second cohort. Bronchiectasis remained the most common manifestation (100%). Lymphopenia was present in 55,6% of patients, as well as splenomegaly and ILD, a higher proportion than in the derivation cohort. Notably, monocytopenia showed a higher

frequency in the confirmation cohort (44.4%) compared to the derivation cohort (7.7%), whereas unusual infections and neutropenia were absent in the confirmation cohort (Table 8). However, none of these differences were statistically significant.

Regarding sex distribution, no striking differences were observed between men and women within either cohort, although some findings such as lymphopenia and splenomegaly showed numerically higher frequencies in men in the derivation cohort (Table 8).

	Derivation cohort						Confirmation cohort					
	Total		Men		Women		Total		Men		Women	
Bronchiectasis	12	92.3 %	6	100.0%	6	85.7%	10	100.0%	2	100.0%	8	100.0%
Lymphopenia	8	61.5%	5	83.3%	3	42.9%	5	50.0%	1	50.0%	4	50.0%
Splenomegaly	5	38.5%	3	50.0%	2	28.6%	5	50.0%	2	100.0%	3	37.5%
PSVD	5	38.5%	2	33.3%	3	42.9%	3	30.0%	1	50.0%	2	25.0%
ILD	4	30.8%	2	33.3%	2	28.6%	5	50.0%	2	100.0%	3	37.5%
Lymphadenopathy	4	30.8%	2	33.3%	2	28.6%	3	30.0%	2	100.0%	1	12.5%
Trombocitopenia	4	30.8%	2	33.3%	2	28.6%	2	20.0%	1	50.0%	1	12.5%
Unusual infections	4	30.8%	2	33.3%	2	28.6%	0	0.0%	0	0.0%	0	0.0%
Solid neoplasia	2	15.4%	2	33.3%	0	0.0%	2	20.0%	1	50.0%	1	12.5%
IBD	2	15.4%	2	33.3%	0	0.0%	1	10.0%	1	50.0%	0	0.0%
Anemia	2	15.4%	1	16.7%	1	14.3%	2	20.0%	0	0.0%	2	25.0%
Monocytopenia	1	7.7%	0	0.0%	1	14.3%	3	30.0%	1	50.0%	2	25.0%
Lymphoma	1	7.7%	1	16.7%	0	0.0%	0	0.0%	0	0.0%	0	0.0%
Neutropenia	1	7.7%	0	0.0%	1	14.3%	0	0.0%	0	0.0%	0	0.0%

Table 8. Heatmap of the prevalence of the clinical characteristics of both derivation cohort and confirmation cohorts, and stratified by sex. PSVD: Porto-sinusoidal vascular disease. ILD: interstitial lung disease. IBD: inflammatory bowel disease.

A clinical scoring system was developed in which each evaluated item contributed 1 point, with an additional point assigned to features indicative of immune dysregulation: lymphadenopathy, splenomegaly, PSVD, IBD, ILD, lymphoma, and solid neoplasia; yielding a maximum possible score of 21 points. The mean score was 6 points in the derivation cohort and 6.89 for the confirmation cohort. The interquartilic range (IQR) of derivation cohort was 2-9 and IQR of confirmation cohort was 4-7 (Figure 36Figure 1).

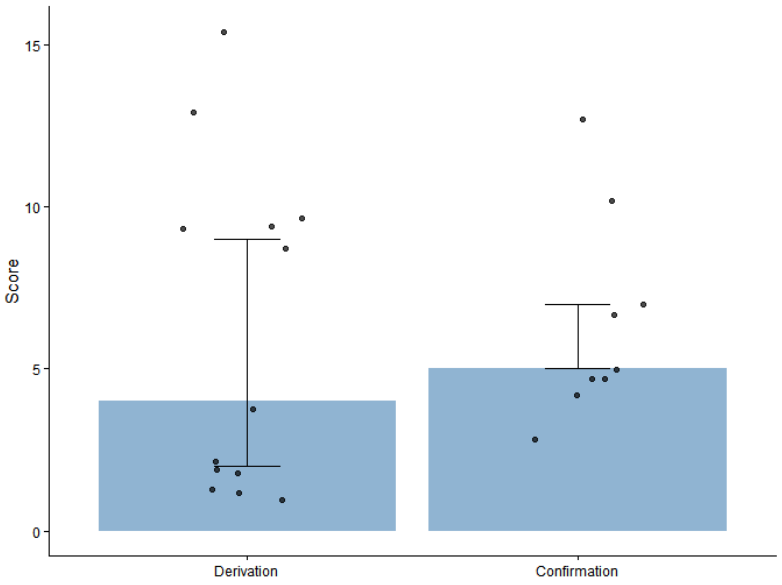


Figure 36. Clinical score in our derivation and confirmation cohorts. No differences were found between cohorts.

We used Q3 of the clinical score of the derivation cohort (9 points) to establish a preliminary severity cut-off point. Thus, initially patients with a score <9 points were classified as non-complicated CVID, while patients with ≥9 points were classified as complicated CVID. This cut-off was also clinically coherent. Therefore, in the derivation cohort, 6 (46.1%) patients were preliminarily classified as complicated CVID while in the confirmation cohort 2 (20.0%) patients were classified as such.

In the derivation cohort, the comparison between preliminary complicated CVID and non-complicated CVID showed some significant differences. The complicated CVID cohort had more splenomegaly (5 (83.3%) vs 0, p<0.01), more ILD (4 (66.7%) vs 0, p<0.05) and more lymphadenopathy (4 (66.7%) vs 0, p<0.05). Furthermore, the mean age of complicated CVID in this cohort was 40.8 ±7.6, while the non-complicated group had a mean age of 61.1 ±19.2. In the confirmation cohort, since there were only 2 patients initially classified as complicated no findings reached statistical significance. In this cohort the mean age of complicated CVID was 46.5 ±26.2 while the mean age of non-complicated CVID was 57.6 ±18.2. All the results are described in Table 9.

	Derivation cohort					Confirmation cohort				
	Non-complicated CVID		Complicated CVID		p	Non-complicated CVID		Complicated CVID		p
Bronchiectasis	6	85,7%	6	100,0%	ns	7	100,0%	2	100,0%	ns
Lymphopenia	3	42,9%	5	83,3%	ns	4	57,1%	1	50,0%	ns
Splenomegaly	0	0,0%	5	83,3%	**	3	42,9%	2	100,0%	ns
PSVD	1	14,3%	4	66,7%	ns	2	28,6%	1	50,0%	ns
ILD	0	0,0%	4	66,7%	*	3	42,9%	2	100,0%	ns
Lymphadenopathy	0	0,0%	4	66,7%	*	1	14,3%	2	100,0%	0,08
Trombocitopenia	1	14,3%	3	50,0%	ns	1	14,3%	1	50,0%	ns
Unusual infections	1	14,3%	3	50,0%	ns	0	0,0%	0	0,0%	ns
Solid neoplasia	0	0,0%	2	33,3%	ns	1	14,3%	1	50,0%	ns
IBD	0	0,0%	2	33,3%	ns	0	0,0%	1	50,0%	ns
Anemia	0	0,0%	2	33,3%	ns	2	28,6%	0	0,0%	ns
Monocytopenia	0	0,0%	1	16,7%	ns	2	28,6%	1	50,0%	ns
Lymphoma	0	0,0%	1	16,7%	ns	0	0,0%	0	0,0%	ns
Neutropenia	0	0,0%	1	16,7%	ns	0	0,0%	0	0,0%	ns

*Table 9. Heatmap of the prevalence of the clinical characteristics of complicated (≥9) and non-complicated (<9) CVID in the derivation and confirmation cohorts. PSVD: Porto-sinusoidal vascular disease. ILD: interstitial lung disease. IBD: inflammatory bowel disease. CVID: common variable immunodeficiency. *<0.05, **<0.01. ns=non-significant.*

4.2.3. Differentiated phenotype

We were interested in learning if the differentiated phenotype of CVID patients was similar to those general aged patients who also had respiratory infections but did not have an inborn error of immunity. As described in the CAP cohorts, in the CVID cohorts $CD4^+$ T cells were mostly early (derivation cohort: 80.45% [76.1 – 88.67]; confirmation cohort: 92.69% [73.84 – 93.49]) while $CD8^+$ T cells had comparable early and late T cells (Derivation cohort: early 44.35% [34.57 – 67.57], late 36.81% [22.08 – 40.68], p=0.82; Confirmation cohort: early 50.59 [42.41 – 71.5]. Late: 34.65 [19.09 – 47.66], p=0.75). There were no differences across the two cohorts, supporting the validity of the confirmation cohort as representative of the derivation cohort.

Contrary to expected, the severity stratification showed little differences between the non-complicated and the complicated patients. Interestingly, the only significant finding was that, in the derivation cohort,

complicated CVID had less number (0.11 cells/μL [0 – 3.1]) and percentage (0.03% [0 – 0.36]) of late $CD4^+$ T cells than non-complicated CVID (14.4 cells/μL [6.8 – 62.8], $p<0.05$; 1.6% [1.4 – 10.4], $p<0.05$).

In the confirmation cohort there were no differences between complicated and non-complicated patients in the differentiated phenotype. Notably, the dispersion of late $CD4^+$ T cells values seemed to be different between the groups. The patients classified as non-complicated CVID seemed to show a high dispersion (0.17% [0.05 – 5.1], 1.03 cells/μL [0.29 – 21.39]), while the 2 complicated CVID patients of the confirmation cohort were similar in their values (0.6% [0.31 – 0.88], 1.12 cells/μL [0.65 – 1.59]). However, the n was insufficient to show statistical significance (Lavene test: $p=0.52$ for percentage values, $p=0.70$ for absolute counts).

4.2.4. Immune Risk Phenotype

We also evaluated the IRP of our patients with CVID. In the derivation cohort, 10 (76,9%) patients had positive serology for CMV, and 4 (30,8%) met the criteria for IRP. Those 4 patients were:

- 30 years-old woman who met all the cell-count criteria and had a clinical score of 9.
- 82 years-old men who met only the $CD28^{neg}$>300 cells/uL criteria and had a clinical score of 1
- 2 men of 45 and 48 years-old that met the inversed CD4/CD8 ratio criteria and had a clinical score of 9 and 10, respectively.

In the derivation cohort 8 (88.8%) patients had positive serology for CMV and 2 (22.2%) met the IRP criteria. Here, we had:

- 66 years-old woman who met all the cell-count criteria and had a clinical score of 3.
- 79 years-old woman who met only the inversed ratio criteria and had a clinical score of 5.

Thus, contrary to what we found in the CAP cohort, the $CD28^{neg}$ criteria was not so predominant and instead the inversed CD4/CD8 ratio was more determinant to meet the IRP criteria.

4.2.5. T-helper phenotype

In the CVID patients, the T-helper phenotype was explored in a stable situation, not within an infectious episode. Thus, we expected the results to differ from those of the patients with CAP. No statistically significant differences were observed between the derivation and confirmation cohorts for any of the T-helper subset percentages analyzed, confirming the comparability of both groups. The median and IQR of the distribution of T-helper populations are described in Table 10.

Median [IQR]	**Derivation cohort**	**Confirmation cohort**	**p**
Th0%	20.87 [11.72 – 40.91]	37.73 [8.86 – 40.51]	0.84
Th1 %	21.02 [16.45 – 32.38]	21.06 [18.42 – 21.99]	0.65
Th1-2 %	14.11 [8.62 – 24.24]	12.36 [9.2 – 19.99]	0.90
Th2 %	2.54 [1.07 – 4.69]	5.21 [2.64 – 5.93]	0.14
Th17 %	3.61 [0.94 – 5.29]	5.82 [5.06 – 7.84]	0.19
Th1-17 %	11.74 [7.82 – 20.31]	12.03 [9.93 – 17.24]	0.83

Table 10. T-helper subpopulations distribution within the derivation and confirmation cohorts. No differences were found between the cohorts.

The severity stratification showed that in the derivation cohort, non-complicated CVID had significantly higher percentage of Th0 (40.91% [33.3 – 45.34]) compared to complicated CVID (10.71% [7.26 – 13.09], p<0.01), which evidenced a more differentiated phenotype within the complicated patients. Within the confirmation cohort there was a trend towards a replication of this pattern in Th0:, non-complicated CVID had 40.16% [32.39 – 42.06], while complicated CVID had 8.58% [8.44 – 8.72], p=0.07). However, it did not reach statistical significance, probably driven by the few complicated patients in this cohort.

With these results, we aimed to broaden the phenotypic analysis of these patients, including their B cell phenotype.

4.2.6. Individual variable correlation to clinical score

Preliminary observations already suggested potential associations between several immunological variables and the clinical score. So, a correlogram analysis was performed with the derivation cohort to systematically identify the variables that independently correlated with the score. This revealed significant correlations with a broad set of T and B cell subpopulations.

Within the T cell compartment, lymphopenia impacted most of the significant absolute-counts variable correlation (Figure 37A). By panel: we found no statistically significant correlation between any of the differentiated T cell phenotype subsets and the clinical score, but memory T cell differentiation subsets did show significant correlations. When analyzed based only on CD45RA expression, all of $CD4^+$ subpopulations showed significant correlations percentage-wise: memory $CD45RA^{neg}$ T cells had a positive correlation to the score (r=0.75 (p<0.001), while naive $CD45RA^+$ T cells had the inverse correlation (r= -0.76 (p<0.01)). For $CD8^+$ T cells, only memory $CD45RA^{neg}$ $CD8^+$ T cells showed significant correlation (r=0.58 (p<0.05)), while naive $CD45RA^+$ $CD8^+$ T cells showed a trend but didn't reach statistical significance (r= -0.51 (p=0.07)). However, in absolute counts, only the number of $CD4^+$ $CD45RA^+$ T cells retained a significant inverse correlation (r= -0.81, p<0.001).

Further subclassification by CCR7 and CD45RA expression was analyzed. This showed that the correlations were driven particularly by $CD4^+$ naive and effector memory (EM) T cells which were significantly correlated to the score (naive: r= -0.84, p<0.001; EM: r=0.69, p<0.001), but not central memory (CM) (r=0.13, p=0.66) nor TEMRA (r= -0.16, p=0.61). Surprisingly, no $CD8^+$ T cell memory subset reached statistical significance, although the percentage of EM had a slight trend (r=0.50, p=0.08).

T-helper subsets showed little independent correlations. By percentage, only Th0 showed a strong negative correlation (-0.72, p<0.01). This was consistent with the previous results, as Th0 which corresponds with the naive subset. By absolute counts, Th0 still showed a robust negative correlation (r= -0.78, p<0.01), but, so did the number of Th2 (r= -0.68, p<0.05) and Th17 (r= -0.56, p<0.05).

In the T cell activated panel by HLA-DR and CD38 expression, only $CD8^+$ T cell activation states showed strong but opposite correlations with the score: activated $CD8^+$ T cells correlated positively (Spearman's r=0.62, p<0.01), while non-activated $CD8^+$ T cells correlated inversely (r=−0.67, p<0.05). However, Treg also showed robust correlations. In this case, the absolute number of Treg showed a

negative correlation of -0.72 ($p<0.01$), while, surprisingly, the absolute number of effector T cells did not ($p=0.84$).

Therefore, the low naive T cells, particularly $CD4^+$ T cells, and Treg cells, as well as a differentiated T-helper phenotype and activated $CD8^+$ T cells were the T cell related variables that could independently correlate with the clinical score.

Within the B cell compartment, the percentage of naive B cells ($r=0.66$, $p<0.05$) and non-switched memory B cells ($r= -0.57$, $p<0.05$) correlated significantly, though inversely, with the clinical score. $CD21^{low}$ B cells showed a trend but did not reach statistical significance in our cohort ($r=0.48$, $p=0.09$). In absolute counts, non-switched memory and marginal-zone B cells showed significant negative correlation (non-switched memory $r= -0.73$, $p<0.01$; marginal-zone $r= -0.60$ $p<0.05$). These findings were consistent with the bibliography. Although it failed to confirm the strength of the correlation between expanded $CD21^{low}$ B cell populations and the score, this B cell subset has been specifically linked to autoimmunity and might need to be correlated specifically to those items of the score[13,123].

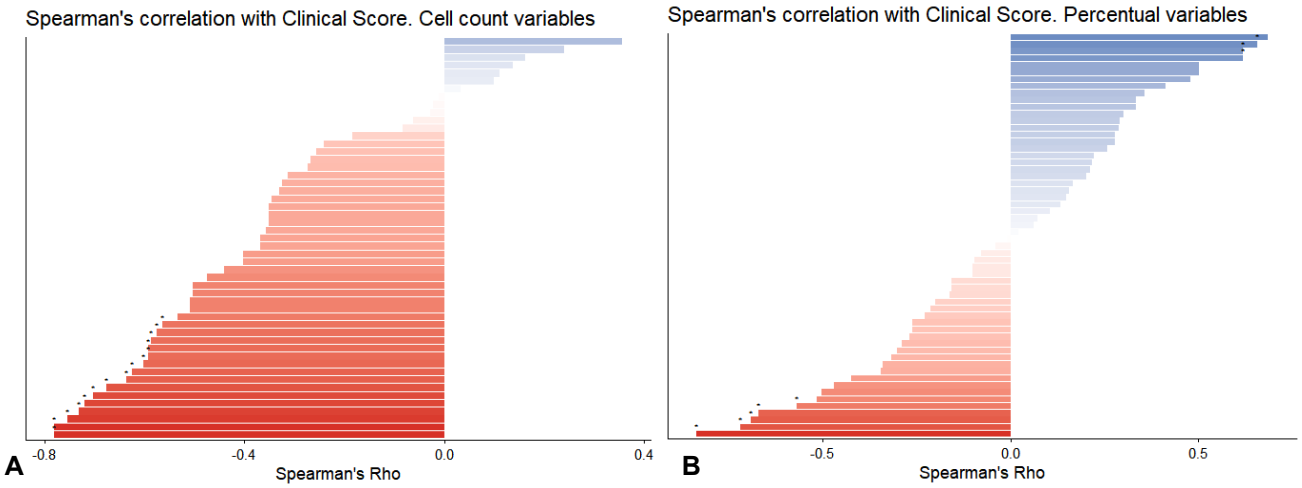


*Figure 37. Spearman's correlation of the cell phenotype cell count **(A)** and percentual **(B)** variables with the clinical score. *p<0.05.*

4.2.1. Phenotype clustering – Derivation cohort

Individual variable associations are highly informative but they offer a limited perspective. To explore the combined contribution of multiple variables without introducing prior bias, an unsupervised k-means clustering analysis was performed with the derivation cohort. The variables included the total number of lymphocytes and the percentage values of: T, $CD4^+$ T, $CD8^+$ T, B and NK cells, differentiated T cell phenotype, T-helper subsets, T cell memory subpopulations, Treg cells, effector T cells and the ratio Teff/Treg, HLA-DR CD38 T cell phenotype subpopulations and B cell subpopulations including naive, non-switched, and switched memory B cells, marginal zone, $CD21^{low}$ B cell $CD19^{low}$ and transitional B cells. As there was no clear optimal value of k with the elbow method, a two-cluster solution was selected to facilitate comparison with the binary clinical severity classification. Therefore, of the confirmation cohort, 4 (30,8%) patients were assigned to cluster 1, while 9 (69,2%) patients were assigned to cluster 2 (Figure 38). The mean of each variable included by cluster is described in Supplementary Table 10.

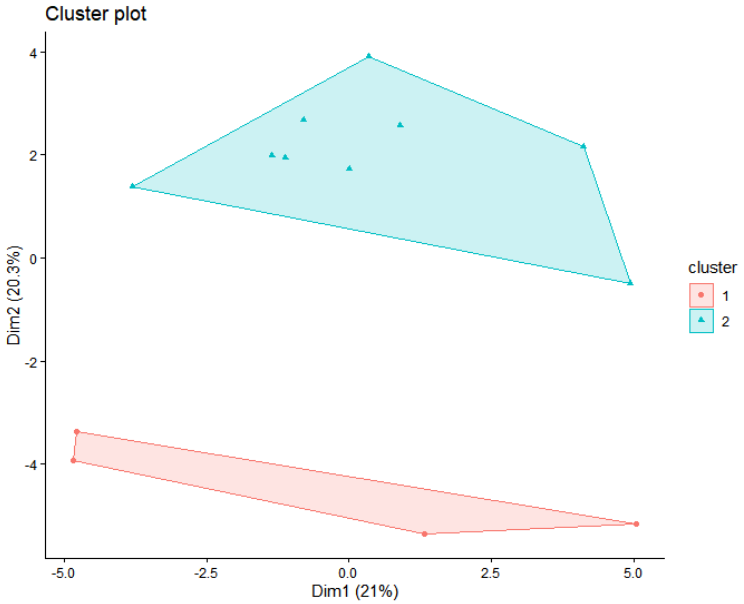


Figure 38. Principal component analysis (PCA) showing the distribution of patients according to the k-means clustering solution. Shaded ellipses represent the 95% confidence region for each cluster.

We found the following significant differences between the clusters. Cluster 1 had, compared to cluster 2: less NK cells ($p<0.05$); less $CD8^+$ $HLA\text{-}DR^{neg}$ $CD38^{neg}$ ($p<0.01$) and more $CD8^+$ $HLA\text{-}DR^+$ $CD38^+$ ($p<0.01$); less Th0 ($p<0.01$), Th2 ($p<0.01$) and Th17 ($p<0.05$) but more Th1/Th17 ($p<0.01$); less Treg ($p<0.05$) and higher Teff/Treg ratio ($p<0.05$); less total naive T cells ($p<0.05$) and $CD4^+$ naive T cells ($p<0.05$) but more $CD4^+$ intermediate T cells ($p<0.01$); more $CD21^{low}$ B cells ($p<0.01$) and more transitional B cells ($p<0.05$). As said above, all of these variables were percentage values. Therefore, cluster 1 showed an overall differentiated activated profile with populations associated with autoimmunity and proliferation such as $CD21^{low}$ B and transitional B cells. The means of all variables for each cluster are described in Supplementary Table 10.

Fisher test showed significant association between cluster phenotype and the severity assessment with the first cut-off point of 9 ($p<0.05$). Still, a ROC curve analysis was performed to accurately identify the optimal cut-off, using cluster membership as the binary outcome and the score as the continuous predictor. The AUC was 0.917 and the optimal cut-off value was 6.5 with a 100% sensitivity and 77.8% specificity (Figure 39). This cut-off was similar to the mean score value of both cohorts and was also clinically coherent.

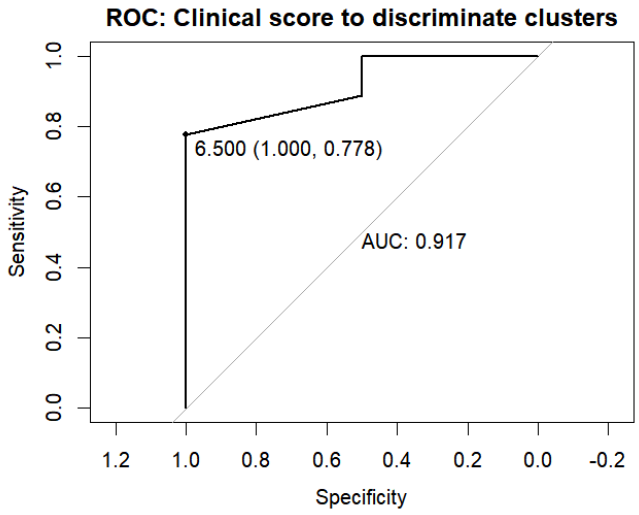


Figure 39. ROC curve for defining the clinical score that distinguished the 2 phenotypic clusters. Cut-off point was established at 6.5, with 100% sensitivity and 77.8% specificity. AUC = 0.917.

Thus, patients with a score ≤6 points were still classified as non-complicated CVID, while patients with ≥7 points were reclassified as complicated CVID. As a result, in the derivation cohort, 6 (46.1%) patients were classified as complicated CVID.

4.2.2. Confirmation cohort

With the new defined cut-off, in the confirmation cohort 4 (44.4%) patients were then classified as complicated CVID. So, the patients of the confirmation cohort were assigned to the predefined phenotypical clusters based on their Euclidean distance. In this cohort, 1 patient was assigned to cluster 1 while 8 patients were assigned to cluster 2 (Figure 40). The n was too low to obtain a significant Fisher's exact test (p=0.44), but the patient assigned to cluster 1 had a score of 10. However, as shown in Figure 40, 6 (66.6%) out of the 9 patients of this cohort were situated in an intermediate gray area space between the clusters. In fact, 2 patients with a score of 7 and one patient with a score of 13 were assigned to cluster 2. Thus, phenotypic classification showed 25% sensitivity and 100% specificity for distinguishing complicated from non-complicated CVID in the confirmation cohort when considering the 6 point cut-off, but 50% sensitivity and 100% specificity when considering the 9 point cut-off. Interestingly, the patient assigned to cluster 2 despite a high clinical score of 13, was the oldest within all patients with complicated-CVID phenotype, as he was 68 years-old while the mean age of patients with a clinical score >6.5 was 45.6 ±13.6. He was also one of the few with an identified molecular diagnosis that eventually reclassified him as an LRBA deficiency instead of a CVID. When further analyzing what variables pushed in his classification, the low percentage of intermediate $CD4^+$ T cells (5.24%) and activated HLA-DR^+ $CD38^+$ T cells (5.98%) but high non-activated HLA-DR^{neg} $CD38^{neg}$ T cells (78.39%) contributed positively to his pertaining to cluster 2. Inversely, his low percentage of Th0 (8.30%) was his most different variable compared to the cluster 2's centroid.

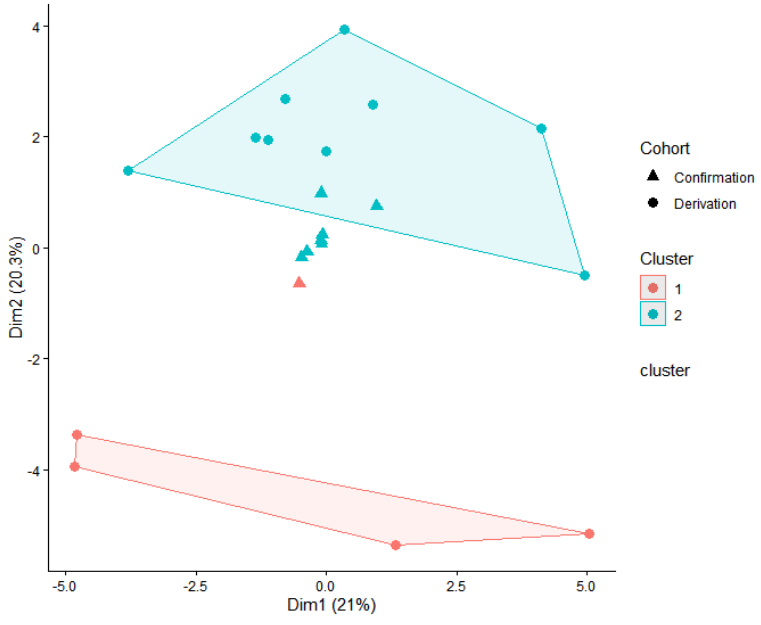


Figure 40. Principal component analysis (PCA) showing the distribution of patients according to the k-means clustering solution. Shaded ellipses represent the 95% confidence region for each cluster.

Thus, although the clustering generated with the derivation cohort was highly suggestive, the confirmation cohort showed shortcomings in the direct application of the initial phenotypic criteria.

4.2.3. Genetic background

All patients from both cohorts had genetic testing by Next Generation Sequencing with a virtual panel over in-house clinical exome. Moreover, 5 patients had genome sequencing due to a severe phenotype but inconclusive findings in the virtual panel. One patient from the confirmation cohort was transferred to our center already with a found mutation that could explain her phenotype. Consistent with the literature, in our cohort 7 (31.8%) of overall patients reached a definitive molecular diagnosis, 5 (38.5%) patients from the derivation cohort and 2 (22.2%) from the confirmation cohort, including the external finding.

Of those with found molecular diagnosis we identified:

Derivation cohort:

- *CTLA4* haploinsuficiency: NM_005214.5: c.308G>T, p.C103F, heterozygous. Missense non-reported mutation. It affected an aminoacid in which another pathogenic missense variant had been reported. Functional testing of CTLA4/CD80-GFP transendocytosis test by flow cytometry was performed by the Immunology laboratory at Hospital Clínic (Barcelona) and confirmed a >50% reduction of CTLA4-CD80 co-expression compared to healthy control. Patient received several treatment strategies with only partial response. This patient had a clinical score of 9 but was classified within the phenotypic cluster 2. Reclassified as dysregulation IDP.
- *CD3G* insufficiency: NM_000073.3: c.473A>G, p.Q158R, heterozygous. Missense non-reported mutation with compatible alterations shown by functional testing. The patient showed lower intracellular expression of CD3-γ compared to controls (functional testing in collaboration with the research group of “Inmunobiología linfocitaria”, Universidad Complutense de Madrid (Madrid)). This patient had a clinical score of 1 and was classified within the phenotypic cluster 2. Reclassified as combined IDP.
- *EZR* deficiency: NM_001111077.2: c.385G>A, p.A129T. Missense mutation in a gene not previously associated with pathology. Our group published this case in collaboration with the research group of the Laboratory of Immunogenetics of Human Diseases, IdiPAZ Institute for Health Research (Madrid), in 2023[138]. This patient had a clinical score of 2 and was classified within the phenotypic cluster 1. Reclassified as combined IDP.
- *IFIH1* dominant negative variant. NM_022168.4: c.855_874+1del, p.G285_S291del, heterozygous. Non-reported mutation with compatible functional testing (functional testing in collaboration with Universidad CEU San Pablo (Madrid)). This patient had a clinical score of 9 and was classified within the phenotypic cluster 1.
- *IKBKB:* NM_001556.3: c.194T>C , p.M65T, heterozygous. Missense mutation recently reported as pathogenic due to a gain-of-function mechanism[139]. This patient had a clinical score of 10 but was classified within the phenotypic cluster 2. Reclassified as combined IDP.

Confirmation cohort:

- *TACI (TNFRSF13B):* NM_012352.2: c.542C>A, p.A181E, heterozygous. Missense variant previously reported as CVID-causative. This case was evaluated and diagnosed in Turkey before the patient was transferred to our hospital. The pathogenic role of TACI remains controversial, and many authors interpret its variants as susceptibility factors rather than direct disease-causing defects[140,141]. This patient had a clinical score of 5 and was classified within the phenotypic cluster 2.
- *LRBA* deficiency: NM_001364905.1: c.8362dupA, p.R2789Kfs*22, homozygous. (manuscript in progress). Non-reported frameshift mutation with compatible functional testing. A CTLA4/CD80-GFP transendocytosis test by flow cytometry was performed by the Immunology laboratory at Hospital Clínic (Barcelona). It showed >50% of CTLA4-CD80 co-expression compared to healthy control. The patient was treated successfully with abatacept. This patient had a clinical score of 13 but was classified within the phenotypic cluster 2. Reclassified as dysregulation IDP.

5. DISCUSSION

Aging has proved to affect the immune system in many ways incurring into a state that has been called immunosenescence [19]. The longitudinal studies from Wikby *et al* with elderly people defined an Immune Risk Phenotype (IRP), which predicted mortality using immune characteristics as criteria [45–47]. In 2011, Plonquet *et al* related the IRP to a higher risk of developing infection[51]. However, the prediction value of IRP is limited and, to the best of our knowledge, it had not been used to predict outcome of an acute infection such as community acquired pneumonia.

Thus, this work aimed to study more thoroughly the immunological phenotype of patients that presented with respiratory infections, looking specifically at senescent phenotypes. We aimed to identify characteristics of their immune phenotype that would predict a better risk stratification of these patients and eventually result in a more individualized care.

5.1.PART 1 - CAP

To reach our goal, we first studied aged patients with CAP both during the pneumonia and 1-2 months after, and followed them clinically for two years.

5.1.1. Humoral immune system

Hypogammaglobulinemia is certainly a potential infectious risk, as is well known in humoral immunodeficiencies such as CVID. Méndez *et al* described that, particularly during CAP, low IgG2 levels predicted higher 30-day mortality[83]. However, in our cohort we found that non-survivors had significantly higher total IgG than 2-year survivors. Our finding is coherent with the study of Alagna *et al*, where they found that higher IgG levels in patients with sepsis predicted higher 90-day mortality[142]. In their study they interpreted this elevated IgG as a marker of higher immune dysregulation and hyperinflammation. This reasoning in our cohort, however, contradicts the lower level of C3 that we found in non-survivors compared to survivors, which could both indicate a higher inflammation or higher C3 consumption in survivors[143]. So, our findings keep contributing to the controversy of the predicting value of IgG levels measured during infection. The contradictions in the literature likely reflect the possibility that, in response to an infection, either immunoparesis or hyperinflammation may occur. The accurate identification of such scenarios is relevant and broadly discussed in the literature[144,145]. Chaturvedi *et al*, for example, proposed the analysis of T-cell activated phenotype to distinguish these two circumstances[146]. So, within these possible scenarios, IgG levels do not appear to be an independent variable to analyze on their own, but rather part of a more complex picture in which their distinction should be carefully evaluated.

5.1.2. Myeloid – lymphoid axis

It has been described that, with age, hematopoietic stem cells shift their output favoring myeloid lineage while declining in their lymphoid lineage[24,147]. This is one of the factors contributing to the known reduced TCR and BCR repertoire diversity, which contributes to overall immunosenescence[148–150]. In our CAP cohort, during infection, approximately 50% of the patients in both survivors and non-survivors had

neutrophilia, which was expected in an infectious event. However, at follow-up, non-survivors remained with higher neutrophil counts while survivors normalized their levels. This could be caused by two possible scenarios. On the one hand, it may indicate a persistence of infection. This could be caused either by failure to resolve the recent pneumonia or reinfection. These patients are at high risk of respiratory reinfection by bronchoaspiration due to dysphagia, which is common among fragile patients[151,152]. However, it could also indicate failure to recover immune homeostasis. The ability of recovery after an immune stressor is a phenomenon recognized as immune resilience, which also worsens with age[153].

Interestingly, monocytopenia, although infrequent, was almost exclusive to non-survivors, granting it almost x10 odds ratio for two-year mortality. This is consistent with the existing literature, where some studies have also identified monocytopenia as a risk factor in infections, such as Listeria or COVID-19, and sepsis[154–157].

However, the main difference between survivors and non-survivors was found in lymphocytes. Non-survivors showed lower levels of overall lymphocytes. This had been described as a risk factor specifically in CAP by Bermejo-Martin *et al* in 2017[84], denominating it as L-CAP. What was new is that this lower lymphocyte counts were still present at follow-up. This, together with the normalization of neutrophils in survivors, granted a higher neutrophil-to-lymphocyte ratio (NLR) in non-survivors compared to survivors. Elevated NLR has been described as a risk predictor in many circumstances including during sepsis, SARS-CoV2 infection, and cancer [72,73,134,158,159]. In our cohort, no differences in the NLR were observed during infection, but the elevated NLR was present at follow-up. NLR may be acting as an indirect biomarker for the myeloid-lymphoid imbalance associated with immunosenescence. However, during infection, it may lose its sensitivity due to the expected neutrophil increase in response to infection in immunocompetent patients.

Of note, gender stratification showed that most significant differences were found between survivor women and non-survivor men. This is coherent with the well-known fact that women overall have longer life-spans. However, non-survivor women had comparable counts to that of non-survivor men. Coherently, in 2023 Ahuja *et al* published a report on immune resilience and how it promoted favorable health outcomes including resistance to infection. In that article they showed that immune resilience was more common among women while non-optimal immune resilience was more common, albeit not exclusive, among men[153]. Our results consistently support their report and underscore the need to conduct studies stratified by sex, including in the context of the immune system.

5.1.3. Lymphocyte subpopulations

We also analyzed lymphocyte subpopulations and found that, during pneumonia, non-survivors had lower levels of T, $CD4^+$ and $CD8^+$ and B cells, while NK cells remained comparable between groups. By percentages, it led to higher NK cell percentage over total lymphocytes. This results are consistent with the fact that immunosenescence favors the innate immune system over the adaptive system[48,160]. Interestingly, at follow-up, $CD4^+$ T cells continued to be different for survivors and non-survivors but $CD8^+$ T cells lost the statistical difference that they had at follow-up. We initially thought that that could indicate that $CD8^+$ T cell counts may be more dynamic in response to an infection, rising during it but declining

fast after resolution. However, paired analysis showed that $CD8^+$ T cells as well as NK cells actually increase for both survivor and non-survivors, but the increase was specifically seen in men. Sex differences have been described in the immune response, particularly, testosterone seems to potentiate IFNγ response in NK cells[161]. Thus, we may speculate a hormonal mechanism driving these differences but further studies should be performed to specifically assess these variables. On the other hand, the literature reports stronger antibody responses in women[162]. Our findings support this, given that the gendered analysis showed the first difference between survivor and non-survivor women with the number of B cells. Survivor women had higher number of B cells that decreased after CAP, but non-survivor women had lower B cell counts that stayed equally low after CAP. B cell responses are responsible for antibody production, and humoral or vaccine responses are reportedly impaired in immunosenescence[49,68]. Therefore, our results may indicate that the one defining immunosenescence failure in women would specifically the B cell failure. However, this finding should be further studied for example with specific vaccination responses.

5.1.4. The differentiated phenotype and the IRP

We further studied the T cell senescent state further with their differentiation phenotype. It is relevant to notice the difference between exhaustion and true senescence. Exhaustion refers to a state where the cell needs a strong stimulus to replicate and, in the literature, it is usually identified in T cells with PD1 or $CD28^{neg}$ as markers of T cell exhaustion[36,37,163,164]. However, some studies already related $CD28^{neg}$ to true senescent cells by the correlation with another senescent marker $CD57^+$ [36,37,163,164]. Moreover, Plunkett *et al* defined a further state of exhaustion with the combined loss of CD27 and CD28. These cells were the later stage of differentiation and behaved effectively as senescent cells, and this has been also analyzed in HIV patients by Banica et al[36,40,165]. In our study, we identified these late-differentiated T cells as true exhausted and as markers of T cell senescence. Furthermore, we described the phenotype in $CD4^+$ and $CD8^+$ T cells during an acute infectious event. Our results support what has been reported in the literature, where there are few late $CD4^+$ T cells but $CD8^+$ T cells show comparable numbers of early and late T cells. Of note, at follow-up survivors were the ones that increased the number of late $CD8^+$ T cells, and the percentage of intermediate $CD4^+$ T cells, while non-survivors showed no differences. This suggested that, following an infectious event, a detectable immune alteration persisted for at least 1-2 months post-pneumonia, akin to an immunological "scar." This is consistent with the well-described phenomenon in which each cycle of proliferation in response to an antigenic stimulus leads to the accumulation of late cells[36]. Yet, it was the survivors who showed an increase in these cells, which suggested that the capacity to generate and retain this immunological memory may itself be a marker of immune resilience, and be a more favorable outcome than the inability to mount and sustain such a response in the first place.

In a similar line, the absolute number of early differentiated T cells emerged as the strongest predictor of mortality, outperforming the late T cell subset that we had initially hypothesized to be most informative and contrary to what has been reported. This predictive value was observed for total T cells, $CD4^+$, and $CD8^+$ subsets during CAP. However, at follow-up, only total T cells and $CD4^+$ early differentiated cells retained statistical significance, while the $CD8^+$ cells lost predictive power. This pattern suggests that what

best reflected immunocompetence in our cohort was not the burden of late cells during infection, but rather the proliferative capacity to generate new early differentiated T cells. In other words, it was the preserved ability to mount and renew an effective T cell response that best reflected a less senescent immune system, rather than the accumulation of late cells. We already observed that early differentiated T cells predicted 2-month and 1-year mortality and published our findings in 2022[166].

Still, the absence of significant differences in late T cell counts between survivors and non-survivors in our cohort contradicts existing literature like what was described in the studies of Wikby *et al* [167]. We propose two possible explanations. First, the previous studies were performed in stable patients and not during an acute episode. The measurement of this subset during an acute episode might vary and increase the numbers in peripheral blood, which, coupled with the non-survivors overall lymphopenia, might have distorted the potential differences between these two groups of patients. Second, all of our cohort may be relatively homogeneous with respect to baseline late T cells, as all patients had, by definition, developed CAP. A comparison with healthy age-matched controls would likely be needed to reveal differences in late T cell burden that might be masked within a population already selected for this degree of susceptibility to infection.

These same reasons might be causing the inability of the IRP to accurately discriminate the prognosis of our patients. The IRP relies in T cell counts and $CD28^{neg}$ T cells. In our cohort, 97.5% of the patients that met the IRP during CAP, met it due to, at least, the $CD28^{neg}$ T cells criterion. However, as we stablished, lymphopenia and specifically early T cell lymphopenia (that is, necessarily $CD28^{+}$ T cells) proved to be more decisive in our cohort. Thus, by definition, patients who were more at risk due to severe early T cell lymphopenia could not reach the necessary T cell count criteria to be classified as IRP. Specifically, non-survivor men showed the lowest numbers of overall T cells, which made them the least possible to reach the criteria despite being the group with the highest mortality risk. It is specially relevant since, all but one patient that met IRP criteria met at least the $CD28^{neg}$ >300/μL cell-count criterion. In the same line, at follow-up, we saw a higher proportion of IRP, and all of the patients that acquired IRP were due to the $CD28^{neg}$ criterion.

Interestingly, it was only when we stratified the data by both sex and survival that we observed differences in late T cells. Particularly, non-survivor women had higher percentage of total late T cells and particularly higher percentage and number of $CD8^{+}$ late T cells than both non-survivor men and survivor women. Thus, it seemed that, while in men the main risk marker was lymphopenia, in women, a combination of lymphopenia and higher late T cells might be a better indicator. Still, in all groups the number of early T cells was the better predictor. Our results show a complex picture where immunesenescence is sex-dependent and should be taken into account. A very recent paper showed sex-specific dynamics of immunosenescence that supports our finding that is women in particular who have an expansion of cytotoxic $CD8^{+}$ effector memory T cell subsets, which would coincide with the late $CD8^{+}$ T cell populations[168].

We need to keep in mind that technical limitations didn't allow us to stain for both $CD4^{+}$ and CD8. Instead, we assumed that all $CD4^{neg}$ T cells were $CD8^{+}$, when in reality other T cell subpopulations such as MAIT or γδT cells would be included. Still, these cells usually represent a minority of T cells, while

$CD8^+$ T cells constitute the largest subpopulation within the $CD4^{neg}$ subgroup; therefore, the results should be sufficiently representative of true $CD8^+$ T cells.

5.1.5. Etiology and specific immune response

A legitimate question would be whether these T cell differentiated phenotype changes were influenced by the etiology of CAP. The literature indicates that, among cases in which a causative organism is identified, *Streptococcus pneumoniae* accounts for the majority. However, in routine clinical practice an etiological diagnosis is reached in only a minority of cases[137]. In our cohort, no etiological diagnosis was achieved in >70% of patients, and among those with an identified pathogen, *Streptococcus pneumoniae* and gram-negative bacteria were equally represented.

To infer etiology indirectly, we used the T helper differentiation profile, since polarization toward Th1, Th2, or Th17 is broadly associated with intracellular pathogens, parasites, and extracellular bacteria or fungi, respectively. This approach allowed us to define five patient subgroups based on their T-helper phenotype. However, we were unable to relate these subgroups to etiology in the small number of patients with a confirmed microbiological diagnosis. Furthermore, since we did not observe differences in the proportion of early differentiated or late T cells across these subgroups, we may assume that the late phenotype is independent of CAP etiology.

This independence represents a practical strength of our findings, as it supports the direct applicability of the differentiated phenotype to real-world clinical practice, where etiology is frequently unknown at the time of assessment. Nonetheless, we acknowledge that etiology-stratified analysis would be the ideal approach to formally test this assumption. This is illustrated by a prior study comparing T, $CD4^+$, $CD8^+$, B, and NK cell populations between CAP and COVID-19, which did identify significant differences between these etiologically distinct groups[169].

On the other hand, it is noteworthy that we did not find a cytokine profile consistent with the T helper subgroup classification. This is likely explained, at least in part, by the limited sensitivity of the method used, given that most patients presented very low concentrations across all cytokines measured. Nonetheless, a subset of patients did present more notable cytokine levels, although not enough patients nor in a distribution that differentiated significantly between the T-helper clusters.

The only significant difference identified was higher IL-4 in cluster 1 compared to cluster 3. This finding is counterintuitive, as cluster 1, despite comprising only 7 patients, was characterized by the highest Th1 and lowest Th2 proportions, the opposite of what would be expected if elevated IL-4 reflected genuine Th2 polarization. One possible explanation is that the elevated Th1 phenotype blocked a potential Th2 polarization despite high IL-4. In fact, it has been described that the net functional effect of cytokines depends on their relative ratios rather than absolute concentrations, and since IL-4 is known to decline with age, it is possible that this group simply had comparatively higher IL-4 while other cytokines related to the Th1 were proportionally even more elevated, though still not significantly compared to the other clusters[170,171]. Given the very small sample size in this subgroup, this finding should be interpreted with caution.

5.1.6. Immune exhaustion vs immune resilience

So, we hypothesized that a more late differentiated immune phenotype would predict all-cause mortality, reflecting a broader frailty in which the immune system plays not merely a correlative but a causal role. Indeed, little after we started this study, it was established in the literature that an aged immune system contributed causally to the senescence of solid organs, extending the consequences of immunosenescence beyond the immune compartment itself[25].

However, the fact that our assessment was performed during and shortly after an acute infectious event appears to have revealed a different perspective. Rather than capturing the cumulative burden of immunosenescence, our analysis seems to have reflected the reserve of immunoresilience that patients still retained, or not, at the time of the challenge. This context-dependency is relevant in itself: it suggests that the late T cell phenotype during infection may better reflect functional immunocompetence under stress rather than reflect a static measure of biological aging, as had been previously used in literature. Therefore, both situations, while related, are not equivalent. In fact, a published paper in 2023 by Ahuja *et al* supports this approach, identifying immune resilience despite inflammatory stress, as one relevant factor to promote longevity and resistance to infection [153].

5.2.Part II – CVID

One limitation of the CAP study was that we could not have samples taken before CAP. This option would have been challenging to carry out in a hospital setting, which by definition does not typically have access to a healthy population. Then again, patients with CVID share many clinical characteristics with immunosenescence. First, they have an increased risk of infections, which most of them are respiratory infections[97,172]. Second, the defining characteristic of their humoral defect is impaired response to vaccines, which is well described in the elderly too[49,68]. Third, up to 70% have non-infectious complications which include autoimmunity and immune dysregulation accompanied with a proinflammatory Th1 phenotype, which could be akin to inflammaging[88,117]. Therefore, we decided to study them as a potential natural model for immunosenescence and assess whether they could serve as a model for patients with pneumonia.

5.2.1. Clinical phenotype

CVID patients are highly clinically heterogeneous so we also aimed to identify which patients had a phenotype that could model immunosenescence, and which patients might have a more complex primary immune defect. The high prevalence of bronchiectasis reflected the toll of recurrent respiratory infections in these patients. Next, the symptoms of splenomegaly, PSVD, lymphadenopathy and ILD, which was mostly GLILD, reflected phenotypes more associated with lymphoproliferation. These characteristics have been reported to relate to worse outcomes and would be distinctive to a senescent phenotype[88,89,99,173]. In our score, lymphoproliferative symptoms scored 2 points to reflect the severity of these clinical findings, thus, senescent-like patients had to have a lower score.

5.2.2. Differentiated T cells and IRP

The differentiated phenotype showed dynamics similar to those found in patients with CAP, in that the $CD4^+$ population consisted mainly of early T cells, while the $CD8^+$ population had comparable levels of early and late. It is noteworthy that the only significant difference observed in the severity stratification was that non-complicated CVID had a higher percentage of late $CD4^+$ T cells while, at the same time, the mean age of non-complicated CVID was also higher. This result supports the idea that, while complicated CVID might be a complex disease often characterized by lymphopenia and profound immune dysregulation, non-complicated CVID resembled our aged patients and might reflect a prematurely aged immune system.

In our CVID cohorts, the IRP did not discriminate between complicated and non-complicated CVID. Furthermore, contrary to what we found in the CAP cohorts, the $CD28^{neg}$ T cells criterion was not the most relevant among the patients that had the IRP. In the CVID cohort, the inversed CD4/CD8 ratio criterion defined as much positives as the $CD28^{neg}$ criterion. These results, highlight another limitation of the IRP. While it might be useful to screen general elderly population, younger patients with complex immune defects show different immune characteristics, including lymphopenia, that interfere with the capacity to meet the IRP criteria. At the same time, these patients may have false negative serologies to CMV due to their humoral defect, also interfering with the capacity to meet the IRP.

5.2.3. Expanded lymphocytic phenotype complicated CVID vs LOCID

Given the limitations in the IRP and the differentiated phenotype, we aimed to expand the lymphocytic phenotyping in these patients. We hypothesized that expanded phenotyping would allow us to distinguish between patients with complicated CVID from those with non-complicated CVID. Several phenotypic characteristics have been related to non-infectious complications in CVID patients. For example, higher $CD21^{low}$ B cells, as well as increased Th1 or Th17 have been associated to autoimmunity[117,123]. Similarly, the loss of naive T cells has been related to more dysregulated phenotypes[174]. Multiple groups have looked at multiple of the mentioned phenotypical characteristics independently or by T cell or B cell phenotype. But, to the best of our knowledge, few[121,123,175–177] groups had included both expanded B cell and T cell phenotype analysis, including activated T cell markers defined with HLA-DR and CD38 expression. Still, the existing evidence increasingly suggests that complicated CVID is characterized by a profound T cell defect, pointing to what may be better understood as a late-onset combined immunodeficiency (LOCID) rather than a purely humoral disorder[124].

In line with that, the phenotypical variables that correlated with the clinical score suggested that a more for naive, undifferentiated, non-activated $CD8^+$ T cells correlated with a milder clinical phenotype, while the loss of naive T cells, and a highly activated $CD8^+$ T cell phenotype correlated with a more sever clinical picture. $CD21^{low}$ B cells did not significantly correlate to the score. However, these subpopulations have been more related to autoimmune manifestations, while our clinical score is heavily influenced by proliferative phenomena, which may interfere with a clear correlation[13,123]. A specific correlation of $CD21^{low}$ B cells and autoimmune manifestations might have shown different results. However, the score did reveal that a higher percentage of naive B cells correlated to a higher score, while a higher percentage of non-

switched memory B cells correlated negatively to the score. These results suggest that, although all patients have a B cell maturation defect, and therefore have very low or no switched memory B cells, the more premature the B cell arrest, the worse the clinical phenotype.

To avoid introducing biases, an unsupervised clustering of the phenotypic variables was performed in our CVID derivation cohort and correlated it to the clinical stratification of complicated vs non-complicated CVID. The variables that mainly distinguished the clusters were NK cells, activated $CD8^+$ T cells, T-helper differentiation, higher Teff/Treg ratio, loss of naive T cells, mainly $CD4^+$, but more $CD4^+$ intermediate T cells ($p<0.01$); and $CD21^{low}$ B cells ($p<0.01$) and more transitional B cells ($p<0.05$). The clusters successfully distinguished complicated from non-complicated CVID in the derivation cohort, and ROC curves suggested that lowering the clinical score cut-off point was more optimal to distinguish both groups. However, when applying the same clusterisation criteria and lowering the cut-off, the correlation between cluster assignation and clinical classification was worse for the confirmation cohort than the original preliminary cut-off of 9 points. On the one hand, patients from the derivation cohort were quite polarized in their clinical score, with no patients with intermediate values, contrary to what we found in the confirmation cohort. Furthermore, clusterisation assigned the patients with 7 points to cluster 2, which we had previously associated to non-complicated CVID. Thus, suggesting that our original cut-off was better than the one defined by ROC curve.

5.2.4. The complexity of CVID phenotypes

It is also of interest to notice that, in the confirmation cohort, the most conflicting patient was the one with a clinical score of 13 but that was classified in cluster 2. We propose two possible explanations. First, this patient was also the oldest among the complicated-CVID and in him, one of the variables that most contributed to his assignation to cluster 2 was the percentage of intermediate $CD4^+$ T cells. Therefore, we postulate that in this patient two processes are coexisting: his inborn error of immunity and immunosenescence, and in his case, a start of immunosenescent phenotype. Second, he is one of the 3 patients that reached a molecular diagnosis that reclassified them to a dysregulated CVID. All 3 of those, with mutations in *LRBA*, *CTLA4* and *IKBKB*, were classified in cluster 2 despite having scores of 13, 9 and 10. Therefore, it could also be that our cluster is effectively separating true complicated CVID (or LOCID) from Dysregulation IEI and non-complicated CVID. However, this also might explain why some differences in the late differentiated phenotype might be diluted within cluster 2. Still, cluster 2 showed higher intermediate T cells. Furthermore, the patient with the highest late T cells was classified in cluster 2. This patient was a 82 year-old patient with a clinical score of 1 that had 41.6% late $CD4^+$ T cells and 40.7% late $CD8^+$ T cells. Exceptionally, he had higher percentage of late $CD4^+$ T cells than $CD8^+$, showing the most senescent state of this cohort, and supporting the senescence burden in cluster 2.

Finally, in our CVID cohort, the molecular diagnosis was reached in 31.8% (n=7) of all patients, a percentage comparable to what has been reported in larger series[96,113,178,179]. Of those, only one was assigned in cluster 1. Of note, only 2 mutations had been previously described and another was affecting an amino acid that had been reported to have other pathogenic mutation at the same site, while the other 4 were reached through extensive functional testing in collaboration with multiple centers. We must emphasize that these are ultra-rare diseases in which we will rarely encounter a previously reported

genetic defect[96,180,181]. Thus, an active collective effort must be made to pursue the molecular defects in these patients while, in the meantime, other characteristics such as lymphocytic phenotype should help us stratify the risk and help guide clinical decisions. On the other hand, identifying molecular diseases that predispose to IEI with worse immunosenescence, will also contribute to shed light to the molecular pathways involved in pathogenic and healthy aging.

6. Conclusions

The conclusions for part I were:

1. During CAP (T0), higher neutrophil and lower lymphocyte percentages were found in non-survivor patients. Also, non-survivors had fewer T and B cells counts than survivors but comparable NK cells, consistent with the shift towards the myeloid and innate immune system described in immunosenescence. Moreover, monocytopenia presented a very high-risk factor for 2-year all-cause mortality. However, neutrophil-to-lymphocyte ratio (NLR) was not useful at T0 while immunoglobulin and complement values showed contradicting results and should not be interpreted on their own to predict 2-year survival in patients with CAP.
2. At the 1-2 months follow-up (T1), survivors returned to normal neutrophil counts and increased their $CD8^+$ T cell and NK cell counts, while non-survivors failed to do so, confirming a shift towards the innate immune system in these patients and consistent with a worse immune-resilience. Consequently, NLR became useful at T1.
3. $CD4^+$ T cell and $CD8^+$ T cell were fundamentally different in their differentiation states. $CD4^+$ T cells were composed of mainly early T cells while $CD8^+$ T cells had comparable percentages of early and late T cells; both at T0 and T1.
4. Total early T cells and $CD4^+$ early T cells were the best predictors for 2-year all-cause mortality, both at T0 and T1. For T0, we proposed a cut-off of 532 cells/μL total early T cells or 416 cells/μL early $CD4^+$ T cells. For T1, we propose a cut-off of 666 cells/μL early total T cells or 523 cells/μL early $CD4^+$ T cells.
5. Sex stratified analysis was essential. Survivor women and non-survivor men were the most different groups and drove most of the found differences in all lymphocytic populations.
6. The T-helper phenotype didn't show an influence of the microbial etiology of CAP, as inferred by their differentiation.
7. The IRP was not useful in regards to an acute infectious event. Lymphopenia in higher-risk patients prevented them from reaching any of the cell-count criteria at T0 and T1, thus, the IRP lost sensitivity with the patients that had higher risk. Among those who met the criteria, the $CD28^{neg}$>300 cells/uL criterion was the most prevalent, confirming the relevance of the differentiated phenotype.

The conclusions for part II were:

1. We have developed a clinical score based on infectious and non-infectious complications of CVID that successfully discriminated complicated CVID at a threshold of 9 points.
2. Non-complicated CVID had higher number and percentage of late-differentiated $CD4^+$ T cells than complicated CVID, suggesting that an immunosenescent state might be more prevalent in this group.

3. The proportion of $CD4^+$ and $CD8^+$ differentiation phenotypes were comparable to those of patients with CAP, in that $CD4^+$ were mainly early, and $CD8^+$ were comparable early and late.
4. The IRP was not useful to discriminate patients with complicated vs non-complicated CVID.
6. Non-complicated CVID patients had a less activated T cell profile, with higher percentage of Th0 cells and lower percentage of activated $CD8^+$ T cells by HLA-DR and CD38.
7. Naive and effector memory T cell subsets, activated T cell subsets and naive and non-switched memory B cell subsets correlated independently with our clinical score.
8. The variables that, combined, distinguished 2 clusters of CVID were the percentage of: NK cells, T-helper Th0, Th2 and Th17, Th1-17, Treg, Teff/Treg ratio, total and $CD4^+$ naive T cells, $CD4^+$ intermediate differentiated T cells, $CD21^{low}$ B cells and transitional B cells.
9. Independent clustering accomplished distinguishing complicated CVID compatible with LOCID findings, but failed to identify complicated CVID caused by dysregulation mutations, potentially mixing these later patients with more truly premature senescent-phenotype CVID. Thus, cluster 1 showed a pro-inflammatory phenotype while cluster 2 showed some immunosenescence characteristics.
10. We found no specific molecular defect that caused CVID and increased immunosenescent phenotype in our cohort.

7. Bibliography

1 United-Nations. World Population Prospects 2024: Summary of Results. New York, 2024.

2 López-Otín C, Blasco MA, Partridge L, Serrano M, Kroemer G. The hallmarks of aging. Cell. 2013; **153**: 1194.

3 López-Otín C, Blasco MA, Partridge L, Serrano M, Kroemer G. Hallmarks of aging: An expanding universe. *Cell* 2023; **186**: 243–278.

4 Fraser HC, Kuan V, Johnen R, Zwierzyna M, Hingorani AD, Beyer A *et al.* Biological mechanisms of aging predict age-related disease co-occurrence in patients. *Aging Cell* 2022; **21**: e13524.

5 Gorgoulis V, Adams PD, Alimonti A, Bennett DC, Bischof O, Bishop C *et al.* Cellular Senescence: Defining a Path Forward. *Cell* 2019; **179**: 813–827.

6 Abbas AK, Litchman A, Pillai S. *Inmunología celular y molecular (10.ª ed.)*. 10th ed. Elsevier España, 2022.

7 Soon MSF, Engel JA, Lee HJ, Haque A. Development of circulating CD4+ T-cell memory. *Immunol Cell Biol* 2019; **97**: 617–624.

8 Surh CD, Sprent J. Homeostasis of Naive and Memory T Cells. Immunity. 2008; **29**. doi:10.1016/j.immuni.2008.11.002.

9 Künzli M, Masopust D. CD4+ T cell memory. *Nat Immunol* 2023; **24**: 903–914.

10 Chen Y, Xu Z, Sun H, Ouyang X, Han Y, Yu H *et al.* Regulation of CD8+ T memory and exhaustion by the mTOR signals. *Cellular & Molecular Immunology 2023 20:9* 2023; **20**: 1023–1039.

11 Walker LSK. Treg and CTLA-4: Two intertwining pathways to immune tolerance. *J Autoimmun* 2013; **45**: 49–57.

12 Deng G, Song X, Fujimoto S, Piccirillo CA, Nagai Y, Greene MI. Foxp3 post-translational modifications and treg suppressive activity. Front. Immunol. 2019; **10**. doi:10.3389/fimmu.2019.02486.

13 Arumugakani G, Wood PMD, Carter CRD. Frequency of Treg Cells Is Reduced in CVID Patients with Autoimmunity and Splenomegaly and Is Associated with Expanded CD21lo B Lymphocytes. *J Clin Immunol* 2010; **30**: 292–300.

14 Cepika AM, Sato Y, Liu JMH, Uyeda MJ, Bacchetta R, Roncarolo MG. Tregopathies: Monogenic diseases resulting in regulatory T-cell deficiency. *Journal of Allergy and Clinical Immunology* 2018; **142**: 1679–1695.

15 Bluestone JA, McKenzie BS, Beilke J, Ramsdell F. Opportunities for Treg cell therapy for the treatment of human disease. *Front Immunol* 2023; **14**: 1166135.

16 Macallan DC, Wallace DL, Zhang V, Ghattas H, Asquith B, De Lara C *et al.* B-cell kinetics in humans: Rapid turnover of peripheral blood memory cells. *Blood* 2005; **105**. doi:10.1182/blood-2004-09-3740.

17 Phad GE, Pinto D, Foglierini M, Akhmedov M, Rossi RL, Malvicini E *et al.* Clonal structure, stability and dynamics of human memory B cells and circulating plasmablasts. *Nat Immunol* 2022; **23**: 1076–1085.

18 Gupta S, Bi R, Su K, Yel L, Chiplunkar S, Gollapudi S. Characterization of naïve, memory and effector CD8 + T cells: Effect of age. In: *Experimental Gerontology*. 2004, pp 545–550.

19 Pawelec G, Akbar A, Beverley P, Caruso C, Derhovanessian E, Fülöp T *et al.* Immunosenescence and Cytomegalovirus: Where do we stand after a decade? *Immunity and Ageing* 2010; **7**: 1–5.

20 Franceschi C, Capri M, Monti D, Giunta S, Olivieri F, Sevini F *et al.* Inflammaging and anti-inflammaging: A systemic perspective on aging and longevity emerged from studies in humans. *Mech Ageing Dev* 2007; **128**: 92–105.

21 Gonçalves MT, Mitchell TJ, Lord JM. Immune ageing and susceptibility to Streptococcus pneumoniae. *Biogerontology* 2016; **17**: 449–465.

22 Murray MA, Chotirmall SH. The Impact of Immunosenescence on Pulmonary Disease. Mediators Inflamm. 2015; **2015**. doi:10.1155/2015/692546.

23 Oh SJ, Lee JK, Shin OS. Aging and the immune system: The impact of immunosenescence on viral infection, immunity and vaccine immunogenicity. *Immune Netw* 2019; **19**: 1–18.

24 Young K, Borikar S, Bell R, Kuffler L, Philip V, Trowbridge JJ. Progressive alterations in multipotent hematopoietic progenitors underlie lymphoid cell loss in aging. *Journal of Experimental Medicine* 2016; **213**. doi:10.1084/jem.20160168.

25 Yousefzadeh MJ, Flores RR, Zhu Y, Schmiechen ZC, Brooks RW, Trussoni CE *et al.* An aged immune system drives senescence and ageing of solid organs. *Nature 2021 594:7861* 2021; **594**: 100–105.

26 Müller L, Di Benedetto S. Aging brain: exploring the interplay between bone marrow aging, immunosenescence, and neuroinflammation. *Front Immunol* 2024; **15**. doi:10.3389/FIMMU.2024.1393324,.

27 Murray JM, Kaufmann GR, Hodgkin PD, Lewin SR, Kelleher AD, Davenport MP *et al.* Naive T cells are maintained by thymic output in early ages but by proliferation without phenotypic change after age twenty. *Immunol Cell Biol* 2003; **81**. doi:10.1046/j.1440-1711.2003.01191.x.

28 Minato N, Hattori M, Hamazaki Y. Physiology and pathology of T-cell aging. *Int Immunol* 2020; **32**: 223–231.

29 Abramson J, Anderson G. Thymic epithelial cells. Annu. Rev. Immunol. 2017; **35**. doi:10.1146/annurev-immunol-051116-052320.

30 Deng Y, Peng Z, Ming K, Qiao X, Ye B, Liu Y *et al.* Single-cell analysis of human thymus and peripheral blood unveils the dynamics of T cell development and aging. *Nature Aging 2025 5:12* 2025; **5**: 2494–2513.

31 Sauce D, Larsen M, Fastenackels S, Roux A, Gorochov G, Katlama C *et al.* Lymphopenia-Driven Homeostatic Regulation of Naive T Cells in Elderly and Thymectomized Young Adults. *The Journal of Immunology* 2012; **189**. doi:10.4049/jimmunol.1201235.

32 Baccala R, Theofilopoulos AN. The new paradigm of T-cell homeostatic proliferation-induced autoimmunity. Trends Immunol. 2005; **26**. doi:10.1016/j.it.2004.11.006.

33 Kato A, Takaori-Kondo A, Minato N, Hamazaki Y. CXCR3 high CD8 + T cells with naïve phenotype and high capacity for IFN-γ production are generated during homeostatic T-cell proliferation. *Eur J Immunol* 2018; **48**: 1663–1678.

34 Sato K, Kato A, Sekai M, Hamazaki Y, Minato N. Physiologic Thymic Involution Underlies Age-Dependent Accumulation of Senescence-Associated CD4 + T Cells . *The Journal of Immunology* 2017; **199**. doi:10.4049/jimmunol.1602005.

35 Bernatz S, Prudente V, Pai S, Attermann AK, Cao Y, Chen J *et al.* Thymic health consequences in adults. *Nature 2026 652:8111* 2026; **652**: 986–994.

36 Strioga M, Pasukoniene V, Characiejus D. CD8+CD28- and CD8+CD57+ T cells and their role in health and disease. Immunology. 2011; **134**: 17–32.

37 Vallejo AN. CD28 extinction in human T cells: Altered functions and the program of T-cell senescence. Immunol. Rev. 2005; **205**. doi:10.1111/j.0105-2896.2005.00256.x.

38 Plunkett FJ, Franzese O, Finney HM, Fletcher JM, Belaramani LL, Salmon M *et al.* The Loss of Telomerase Activity in Highly Differentiated CD8 + CD28 − CD27 − T Cells Is Associated with Decreased Akt (Ser 473) Phosphorylation. *The Journal of Immunology* 2007; **178**: 7710–7719.

39 Buchan SL, Rogel A, Al-Shamkhani A. The immunobiology of CD27 and OX40 and their potential as targets for cancer immunotherapy. *Blood* 2018; **131**: 39–48.

40 Bănică L, Vlaicu O, Jipa R, Abagiu A, Nicolae I, Neaga E *et al.* Exhaustion and senescence of CD4 and CD8 T cells that express co-stimulatory molecules CD27 and CD28 in subjects that acquired HIV by drug use or by sexual route. *Germs* 2021; **11**: 66.

41 Larbi A, Fulop T. From 'truly naïve' to 'exhausted senescent' T cells: When markers predict functionality. Cytometry Part A. 2014; **85**: 25–35.

42 Henson SM, Franzese O, Macaulay R, Libri V, Azevedo RI, Kiani-Alikhan S *et al.* KLRG1 signaling induces defective Akt (ser473) phosphorylation and proliferative dysfunction of highly differentiated CD8+ T cells. *Blood* 2009; **113**: 6619–6628.

43 Mendes AVA, Kallas EG, Benard G, Pannuti CS, Menezes R, Dulley FL *et al.* Impact of cytomegalovirus and grafts versus host disease on the dynamics of CD57+CD28-CD8+ T cells after bone marrow transplant. *Clinics* 2008; **63**. doi:10.1590/S1807-59322008000500016.

44 Weng N ping, Akbar AN, Goronzy J. CD28- T cells: their role in the age-associated decline of immune function. Trends Immunol. 2009; **30**. doi:10.1016/j.it.2009.03.013.

45 Strindhall J, Skog M, Ernerudh J, Bengner M, Löfgren S, Matussek A *et al.* The inverted CD4/CD8 ratio and associated parameters in 66-year-old individuals: The Swedish HEXA immune study. *Age (Omaha)* 2013; **35**: 985–991.

46 Wikby A, Johansson B, Ferguson F. The OCTO and NONA immune longitudinal studies: a review of 11 years studies of Swedish very old humans. In: *Andvances in Cell Aging and Gerontology*. 2002, pp 1–16.

47 Wikby A, Ferguson F, Forsey R, Thompson J, Strindhall J, Löfgren S *et al.* An immune risk phenotype, cognitive impairment, and survival in very late life: impact of allostatic load in Swedish octogenarian and nonagenarian humans. *J Gerontol A Biol Sci Med Sci* 2005; **60**: 556–65.

48 Pangrazzi L, Weinberger B. T cells, aging and senescence. *Exp Gerontol* 2020; **134**: 110887.

49 Grubeck-Loebenstein B, Della Bella S, Iorio AM, Michel JP, Pawelec G, Solana R. Immunosenescence and vaccine failure in the elderly. Aging Clin. Exp. Res. 2009; **21**: 201–209.

50 Ferguson FG, Wikby A, Maxson P, Olsson J, Johansson B. Immune parameters in a longitudinal study of a very old population of swedish people: A comparison between survivors and nonsurvivors. *Journals of Gerontology - Series A Biological Sciences and Medical Sciences* 1995; **50A**. doi:10.1093/gerona/50A.6.B378.

51 Plonquet A, Bastuji-Garin S, Tahmasebi F, Brisacier C, Ledudal K, Farcet JP *et al.* Immune risk phenotype is associated with nosocomial lung infections in elderly in-patients. *Immunity and Ageing* 2011; **8**. doi:10.1186/1742-4933-8-8.

52 Zielinski CE, Corti D, Mele F, Pinto D, Lanzavecchia A, Sallusto F. Dissecting the human immunologic memory for pathogens. *Immunol Rev* 2011; **240**: 40–51.

53 Lanzavecchia A, Sallusto F. Progressive differentiation and selection of the fittest in the immune response. *Nature Reviews Immunology 2002 2:12* 2002; **2**: 982–987.

54 Sallusto F, Zielinski CE, Lanzavecchia A. Human Th17 subsets. *Eur J Immunol* 2012; **42**: 2215–2220.

55 Mahnke YD, Brodie TM, Sallusto F, Roederer M, Lugli E. The who's who of T-cell differentiation: Human memory T-cell subsets. *Eur J Immunol* 2013; **43**: 2797–2809.

56 Kim CH, Rott L, Kunkel EJ, Genovese MC, Andrew DP, Wu L *et al.* Rules of chemokine receptor association with T cell polarization in vivo. *Journal of Clinical Investigation* 2001; **108**: 1331.

57 Zhang Y, Yaguang Zhang, Gu W, Sun B. *Advances in Experimental Medicine and Biology - Th1/Th2 Cell Differentiation and Molecular Signals*. 2014th ed. Dordrecht doi:10.1007/978-94-017-9487-9.

58 Annunziato F, Cosmi L, Santarlasci V, Maggi L, Liotta F, Mazzinghi B *et al.* Phenotypic and functional features of human Th17 cells. *Journal of Experimental Medicine* 2007; **204**: 1849–1861.

59 Aldridge J, Ekwall A-KH, Mark L, Bergström B, Andersson K, Gjertsson I *et al.* T helper cells in synovial fluid of patients with rheumatoid arthritis primarily have a Th1 and a CXCR3+Th2 phenotype. *Arthritis Res Ther* 2020; **22**: 245.

60 Duhen T, Geiger R, Jarrossay D, Lanzavecchia A, Sallusto F. Production of interleukin 22 but not interleukin 17 by a subset of human skin-homing memory T cells. *Nat Immunol* 2009; **10**. doi:10.1038/ni.1767.

61 Dupage M, Bluestone JA. Harnessing the plasticity of CD4+ T cells to treat immune-mediated disease. *Nat Rev Immunol* 2016; **16**: 149–163.

62 Ongrádi J, Kövesdi V. Factors that may impact on immunosenescence: An appraisal. Immunity and Ageing. 2010; **7**. doi:10.1186/1742-4933-7-7.

63 van der Geest KSM, Abdulahad WH, Tete SM, Lorencetti PG, Horst G, Bos NA *et al.* Aging disturbs the balance between effector and regulatory CD4+ T cells. *Exp Gerontol* 2014; **60**. doi:10.1016/j.exger.2014.11.005.

64 Schmitt V, Rink L, Uciechowski P. The Th17/Treg balance is disturbed during aging. *Exp Gerontol* 2013; **48**. doi:10.1016/j.exger.2013.09.003.

65 Sun L, Hurez VJ, Thibodeaux SR, Kious MJ, Liu A, Lin P *et al.* Aged regulatory T cells protect from autoimmune inflammation despite reduced STAT3 activation and decreased constraint of IL-17 producing T cells. *Aging Cell* 2012; **11**. doi:10.1111/j.1474-9726.2012.00812.x.

66 Allen JC, Toapanta FR, Chen W, Tennant SM. Understanding immunosenescence and its impact on vaccination of older adults. Vaccine. 2020; **38**: 8264–8272.

67 Pansarasa O, Pistono C, Davin A, Bordoni M, Mimmi MC, Guaita A *et al.* Altered immune system in frailty: Genetics and diet may influence inflammation. *Ageing Res Rev* 2019; **54**. doi:10.1016/j.arr.2019.100935.

68 Goronzy JJ, Weyand CM. Understanding immunosenescence to improve responses to vaccines. Nat. Immunol. 2013; **14**. doi:10.1038/ni.2588.

69 Ross JB, Myers LM, Noh JJ, Collins MM, Carmody AB, Messer RJ *et al.* Depleting myeloid-biased haematopoietic stem cells rejuvenates aged immunity. *Nature 2024 628:8006* 2024; **628**: 162–170.

70 Moskalev A, Stambler I, Caruso C. Innate and adaptive immunity in aging and longevity: The foundation of resilience. Aging Dis. 2020; **11**: 1363–1373.

71 Mishra V, Hota S, Sahu S, Giri R, Senapati U. Neutrophil-to-lymphocyte ratio as a prognostic factor in oral squamous cell carcinoma – A single-institutional experience from a developing country. *J Oral Maxillofac Pathol* 2021; **25**: 322.

72 Templeton AJ, McNamara MG, Šeruga B, Vera-Badillo FE, Aneja P, Ocaña A *et al.* Prognostic Role of Neutrophil-to-Lymphocyte Ratio in Solid Tumors: A Systematic Review and Meta-Analysis. *JNCI: Journal of the National Cancer Institute* 2014; **106**. doi:10.1093/jnci/dju124.

73 Huang Z, Fu Z, Huang W, Huang K. Prognostic value of neutrophil-to-lymphocyte ratio in sepsis: A meta-analysis. *Am J Emerg Med* 2020; **38**: 641–647.

74 van Duin D, Mohanty S, Thomas V, Ginter S, Montgomery RR, Fikrig E *et al.* Age-Associated Defect in Human TLR-1/2 Function. *The Journal of Immunology* 2007; **178**. doi:10.4049/jimmunol.178.2.970.

75 Zhang J jin, Dong X, Liu G hui, Gao Y dong. Risk and Protective Factors for COVID-19 Morbidity, Severity, and Mortality. *Clin Rev Allergy Immunol* 2023; **64**: 90–107.

76 Méndez R, González-Jiménez P, Latorre A, Mengot N, Zalacain R, Ruiz LA *et al.* Is the long-term mortality similar in COVID-19 and community-acquired pneumonia? *Front Med (Lausanne)* 2023; **10**: 1236142.

77 World Health Organization. Global Health Estimates 2016: Disease burden by Cause, Age, Sex, by Country and by Region. 2018.

78 Mandell LA, Wunderink R. Pneumonia. In: Jameson JL, Fauci AS, Kasper DL, Hauser SL, Longo DL, Loscalzo J (eds). *Harrison's Principles of Internal Medicine, 20e*. McGraw-Hill Education: New York, NY, NY, 2018.

79 Informe Anual del Sistema Nacional de Salud 2024. 2024.

80 Diego G-B, The A, Masi A, Moccia M, García-Bernalt Diego J, Fernández-Soto P *et al.* The Future of Point-of-Care Nucleic Acid Amplification Diagnostics after COVID-19: Time to Walk the Walk. *International Journal of Molecular Sciences 2022, Vol 23, Page 14110* 2022; **23**: 14110.

81 Seok Y, Mauk MG, Li R, Qian C. Trends of respiratory virus detection in point-of-care testing: A review. *Anal Chim Acta* 2023; **1264**: 341283.

82 Incalzi RA, Maini CL, Fuso L, Giordana A, Carbonin PU, Galli G. Effects of aging on mucociliary clearance. *Compr Gerontol A* 1989; **3**: 65–8.

83 Méndez R, Menéndez R, Amara-Elori I, Feced L, Piró A, Ramírez P *et al.* Lymphopenic community-acquired pneumonia is associated with a dysregulated immune response and increased severity and mortality. *Journal of Infection* 2019; **78**: 423–431.

84 Bermejo-Martin JF, Cilloniz C, Mendez R, Almansa R, Gabarrus A, Ceccato A *et al.* Lymphopenic Community Acquired Pneumonia (L-CAP), an Immunological Phenotype Associated with Higher Risk of Mortality. *EBioMedicine* 2017; **24**: 231–236.

85 Viña J, Tarazona-Santabalbina FJ, Pérez-Ros P, Martínez-Arnau FM, Borras C, Olaso-Gonzalez G *et al.* Biology of frailty: Modulation of ageing genes and its importance to prevent age-associated loss of function. Mol. Aspects Med. 2016; **50**. doi:10.1016/j.mam.2016.04.005.

86 Dent E, Kowal P, Hoogendijk EO. Frailty measurement in research and clinical practice: A review. Eur. J. Intern. Med. 2016; **31**. doi:10.1016/j.ejim.2016.03.007.

87 Bonnefoy M, Berrut G, Lesourd B, Ferry M, Gilbert T, Guerin O *et al.* Frailty and nutrition: Searching for evidence. *Journal of Nutrition, Health and Aging* 2015; **19**. doi:10.1007/s12603-014-0568-3.

88 Ho HE, Cunningham-Rundles C. Non-infectious Complications of Common Variable Immunodeficiency: Updated Clinical Spectrum, Sequelae, and Insights to Pathogenesis. *Front Immunol* 2020; **11**: 1–14.

89 Song J, Lleo A, Yang GX, Zhang W, Bowlus CL, Gershwin ME *et al.* Common Variable Immunodeficiency and Liver Involvement. *Clin Rev Allergy Immunol* 2018; **55**: 340–351.

90 Ramirez NJ, Posadas-Cantera S, Caballero-Oteyza A, Camacho-Ordonez N, Grimbacher B. There is no gene for CVID — novel monogenetic causes for primary antibody deficiency. *Curr Opin Immunol* 2021; **72**: 176–185.

91 Ameratunga R, Woon ST. Perspective: Evolving Concepts in the Diagnosis and Understanding of Common Variable Immunodeficiency Disorders (CVID). *Clin Rev Allergy Immunol* 2020; **59**: 109–121.

92 Peng XP, Caballero-Oteyza A, Grimbacher B. Common Variable Immunodeficiency: More Pathways than Roads to Rome. *Annu Rev Pathol* 2023; **18**: 283–310.

93 Abinun M, Albert M, Beaussant Cohen S, Buckland M, Bustamante J, Cant A *et al.* ESID Registry-Working definitions for clinical diagnosis of IEI ESID Registry-Working Definitions for Clinical Diagnosis of PID. 2019.https://esid.org/working-parties/registry-working-party/diagnosis-criteria/ (accessed 15 Jun2026).

94 Baumann U, Routes JM, Soler-Palacín P, Jolles S. The Lung in Primary Immunodeficiencies: New Concepts in Infection and Inflammation. *Front Immunol* 2018; **9**: 1837.

95 Matson EM, Abyazi ML, Bell KA, Hayes KM, Maglione PJ. B Cell Dysregulation in Common Variable Immunodeficiency Interstitial Lung Disease. *Front Immunol* 2021; **11**: 622114.

96 Cunningham-Rundles C, Casanova J-L, Boisson B. Genetics and clinical phenotypes in common variable immunodeficiency. *Front Genet* 2024; **14**. doi:10.3389/fgene.2023.1272912.

97 Ameratunga R, Allan C, Woon S-T. Defining Common Variable Immunodeficiency Disorders in 2020. *Immunol Allergy Clin North Am* 2020; **40**: 403–420.

98 Cunningham-Rundles C, Casanova JL, Boisson B. Common variable immunodeficiency: autoimmune cytopenias and advances in molecular diagnosis. *Hematology* 2024; **2024**: 137–142.

99 Sacco KA, Gazzin A, Notarangelo LD, Delmonte OM. Granulomatous inflammation in inborn errors of immunity. *Front Pediatr* 2023; **11**: 1110115.

100 Smits B, Goldacker S, Seneviratne S, Malphettes M, Longhurst H, Mohamed OE *et al.* The efficacy and safety of systemic corticosteroids as first line treatment for granulomatous lymphocytic interstitial lung disease. *Journal of Allergy and Clinical Immunology* 2023; **152**: 528–537.

101 Rao N, Mackinnon AC, Routes JM. Granulomatous and lymphocytic interstitial lung disease: a spectrum of pulmonary histopathologic lesions in common variable immunodeficiency—histologic and immunohistochemical analyses of 16 cases. *Hum Pathol* 2015; **46**: 1306–1314.

102 Lamers OAC, Smits BM, Leavis HL, de Bree GJ, Cunningham-Rundles C, Dalm VASH *et al.* Treatment Strategies for GLILD in Common Variable Immunodeficiency: A Systematic Review. *Front Immunol* 2021; **12**: 606099.

103 Tessarin G, Baronio M, Gazzurelli L, Rossi S, Chiarini M, Moratto D *et al.* Rituximab Monotherapy Is Effective as First-Line Treatment for Granulomatous Lymphocytic Interstitial Lung Disease (GLILD) in CVID Patients. *J Clin Immunol* 2023; **43**: 2091–2103.

104 Buso H, Firinu D, Gambier RF, Scarpa R, Garzi G, Soccodato V *et al.* Lung function trajectories in common variable immunodeficiencies: An observational retrospective multicenter study. *Journal of Allergy and Clinical Immunology* 2025; **155**: 1027–1035.

105 Salzer E, Kansu A, Sic H, Májek P, Ikincioğullari A, Dogu FE *et al.* Early-onset inflammatory bowel disease and common variable immunodeficiency–like disease caused by IL-21 deficiency. *Journal of Allergy and Clinical Immunology* 2014; **133**: 1651-1659.e12.

106 Nedelea I, Nicoara-Farcau O, Procopet B, Stefanescu H, Radu C, Balan R *et al.* Liver Disease in Common Variable Immunodeficiency: Current Evidence and Knowledge Gaps. *Int J Mol Sci* 2026; **27**. doi:10.3390/ijms27031518.

107 Elmoursi A, DiGiacomo D V., Farmer JR, Barmettler S. Hepatic Manifestations in Common Variable Immunodeficiency Associated With Mortality and Worse Hospital Outcomes in Nationwide Analysis Using National Readmission Database. *Journal of Allergy and Clinical Immunology: In Practice* 2025; **13**: 3118-3128.e3.

108 Silva H, Brito CGX De, Hall A, Eden N, Somers H, Burke N *et al.* Common variable immunodeficiency disorder (CVID)-related liver disease: assessment of the main histological

aspects using novel semiquantitative scoring systems, image analysis and correlation with clinical parameters of liver stiffness and portal hypert…. *J Clin Pathol* 2024; **77**: 709–716.

109 Gullo I, Costa C, Silva SL, Ferreira C, Motta A, Silva SP *et al.* The dysfunctional immune system in common variable immunodeficiency increases the susceptibility to gastric cancer. *Cells* 2020; **9**: 1–21.

110 Resnick ES, Moshier EL, Godbold JH, Cunningham-Rundles C. Morbidity and mortality in common variable immune deficiency over 4 decades. *Blood* 2012; **119**: 1650–1657.

111 Pashangzadeh S, Delavari S, Moeini Shad T, Salami F, Rasouli SE, Yazdani R *et al.* Noninfectious Complications in B-Lymphopenic Common Variable Immunodeficiency. *J Investig Allergol Clin Immunol* 2024; **34**: 233–245.

112 Smith T, Cunningham-Rundles C. Primary B-cell immunodeficiencies. *Hum Immunol* 2019; **80**: 351–362.

113 Abolhassani H, Hammarström L, Cunningham-Rundles C. Current genetic landscape in common variable immune deficiency. *Blood* 2020; **135**: 656–667.

114 Poli MC, Aksentijevich I, Bousfiha AA, Cunningham-Rundles C, Hambleton S, Klein C *et al.* Human inborn errors of immunity: 2024 update on the classification from the International Union of Immunological Societies Expert Committee. *Journal of Human Immunity* 2025; **1**: 20250003.

115 Bousfiha AA, Jeddane L, Moundir A, Poli MC, Aksentijevich I, Cunningham-Rundles C *et al.* The 2024 update of IUIS phenotypic classification of human inborn errors of immunity. *Journal of Human Immunity* 2025; **1**. doi:10.70962/JHI.20250002/277374.

116 López-Nevado M, González-Granado LI, Ruiz-García R, Pleguezuelo D, Cabrera-Marante O, Salmón N *et al.* Primary Immune Regulatory Disorders With an Autoimmune Lymphoproliferative Syndrome-Like Phenotype: Immunologic Evaluation, Early Diagnosis and Management. *Front Immunol* 2021; **12**. doi:10.3389/FIMMU.2021.671755.

117 Gereige JD, Maglione PJ. Current Understanding and Recent Developments in Common Variable Immunodeficiency Associated Autoimmunity. 2019; **10**: 2753.

118 López-Herrera G, Segura-Méndez NH, O'Farril-Romanillos P, Nuñez-Nuñez ME, Zarate-Hernández MC, Mogica-Martínez D *et al.* Low percentages of regulatory T cells in common variable immunodeficiency (CVID) patients with autoimmune diseases and its association with increased numbers of CD4+CD45RO+ T and CD21low B cells. *Allergol Immunopathol (Madr)* 2019; **47**: 457–466.

119 Stuchlý J, Kanderová V, Vlková M, Heřmanová I, Slámová L, Pelák O *et al.* Common Variable Immunodeficiency patients with a phenotypic profile of immunosenescence present with thrombocytopenia. *Scientific Reports 2017 7:1* 2017; **7**: 1–13.

120 Holm AM, Sivertsen EA, Tunheim SH, Haug T, Bjerkeli V, Yndestad A *et al.* Gene expression analysis of peripheral T cells in a subgroup of common variable immunodeficiency shows predominance of CCR7(-) effector-memory T cells. *Clin Exp Immunol* 2004; **138**: 278–289.

121 Wehr C, Kivioja T, Schmitt C, Ferry B, Witte T, Eren E *et al.* The EUROclass trial: defining subgroups in common variable immunodeficiency. *Blood* 2008; **111**: 77–85.

122 Piqueras B, Lavenu-Bombled C, Galicier L, Bergeron-Van Der Cruyssen F, Mouthon L, Chevret S *et al.* Common variable immunodeficiency patient classification based on impaired B cell memory differentiation correlates with clinical aspects. *J Clin Immunol* 2003; **23**: 385–400.

123 Warnatz K, Wehr C, Dräger R, Schmidt S, Eibel H, Schlesier M *et al.* Expansion of CD19 hi CD21 lo/neg B Cells in Common Variable Immunodeficiency (CVID) Patients with Autoimmune Cytopenia. 2002; : 502–513.

124 Torres-Valle A, Neirinck J, Silva SL, de Arriba S, Serrano C, Cordón L *et al.* Immunologic biomarkers of noninfectious complications and overall survival in common variable immunodeficiency. *Journal of Allergy and Clinical Immunology* 2025; **157**. doi:10.1016/j.jaci.2025.10.020.

125 Smits BM, Kleine Budde I, de Vries E, ten Berge IJM, Bredius RGM, van Deuren M *et al.* Immunoglobulin Replacement Therapy Versus Antibiotic Prophylaxis as Treatment for Incomplete Primary Antibody Deficiency. *J Clin Immunol* 2021; **41**: 382.

126 Gouilleux-Gruart V, Chapel H, Chevret S, Lucas M, Malphettes M, Fieschi C *et al.* Efficiency of immunoglobulin G replacement therapy in common variable immunodeficiency: correlations with clinical phenotype and polymorphism of the neonatal Fc receptor. *Clin Exp Immunol* 2013; **171**: 186–194.

127 Fevang B. Treatment of inflammatory complications in common variable immunodeficiency (CVID): current concepts and future perspectives. *Expert Rev Clin Immunol* 2023; **19**: 627–638.

128 Lanz A-L, Riester M, Peters P, Schwerd T, Lurz E, Samer Hajji M *et al.* Abatacept for treatment-refractory pediatric CTLA4-haploinsufficiency. *Clinical Immunology* 2021; **229**: 108779.

129 Yang L, Xue X, Chen X, Wu J, Yang X, Xu L *et al.* Abatacept is effective in Chinese patients with LRBA and CTLA4 deficiency. *Genes Dis* 2021; **8**: 662–668.

130 Lucas CL, Chandra A, Nejentsev S, Condliffe AM, Okkenhaug K. PI3Kδ and primary immunodeficiencies. Nat. Rev. Immunol. 2016; **16**: 702–714.

131 Forbes LR, Vogel TP, Cooper MA, Castro-Wagner J, Schussler E, Weinacht KG *et al.* Jakinibs for the Treatment of Immunodysregulation in Patients with Gain of Function STAT1 or STAT3 Mutations HHS Public Access. *J Allergy Clin Immunol* 2018; **142**: 1665–1669.

132 Baghdassarian H, Blackstone SA, Clay OS, Philips R, Matthiasardottir B, Nehrebecky M *et al.* Variant STAT4 and Response to Ruxolitinib in an Autoinflammatory Syndrome. *N Engl J Med* 2023; **388**: 2241–2252.

133 Ella Murray C, Jannoud E, Prader S, Grimbacher B. How I Treat: STAT3 hyper IgE syndrome. 2026. doi:10.70962/jhi.20260038.

134 Gao Z, Wang X, Wang W, Kang Z, Chen X. Association between neutrophil to lymphocyte ratio and the mortality of patients with sepsis: an update systematic review and meta-analysis. *Front Med (Lausanne)* 2025; **12**: 1637365.

135 An X, Ding PR, Wang FH, Jiang WQ, Li YH. Elevated neutrophil to lymphocyte ratio predicts poor prognosis in nasopharyngeal carcinoma. *Tumour Biol* 2011; **32**: 317–324.

136 Plaza-Florido A, Carrera-Bastos P, Pérez-Prieto I, Fiuza-Luces C, Radom-Aizik S, del Pozo Cruz B *et al.* The long-lived immune system of centenarians. *Nature Reviews Immunology 2026* 2026; : 1–19.

137 Mandell LA, Wunderink R. Pneumonia. In: Jameson JL, Fauci AS, Kasper DL, Hauser SL, Longo DL, Loscalzo J (eds). *Harrison's Principles of Internal Medicine, 20e*. McGraw-Hill Education: New York, NY, NY, 2018http://accessmedicine.mhmedical.com/content.aspx?aid=1155964517.

138 García-Solís B, Van Den Rym A, Martinez-Martínez L, Franco T, Pérez-Caraballo JJ, Markle J *et al.* Inherited human ezrin deficiency impairs adaptive immunity. *Journal of Allergy and Clinical Immunology* 2023; **152**: 997-1009.e11.

139 Körholz J, Tromp SAM, Dalm VASH, de Bie M, de Bree GJ, van Leeuwen EMM *et al.* IKBKB gain of function: An inborn error with clinical heterogeneity progressing toward combined immunodeficiency. *Journal of Allergy and Clinical Immunology* 2025; **156**: 279–293.

140 Salzer U, Grimbacher B. TACI deficiency — a complex system out of balance. *Curr Opin Immunol* 2021; **71**: 81–88.

141 Pulvirenti F, Zuntini R, Milito C, Specchia F, Spadaro G, Danieli MG *et al.* Clinical Associations of Biallelic and Monoallelic TNFRSF13B Variants in Italian Primary Antibody Deficiency Syndromes. *J Immunol Res* 2016; **2016**: 8390356.

142 Alagna L, Meessen JMTA, Bellani G, Albiero D, Caironi P, Principale I *et al.* Higher levels of IgA and IgG at sepsis onset are associated with higher mortality: results from the Albumin Italian Outcome Sepsis (ALBIOS) trial. *Ann Intensive Care* 2021; **11**: 161.

143 Ishchenko A, Van Mechelen M, Pazmino S, Storms L, Neerinckx B, Verschueren P *et al.* Serum calprotectin and complement factor C3 are superior biomarkers of inflammation in early psoriatic arthritis as compared with C-reactive protein. *RMD Open* 2025; **11**. doi:10.1136/RMDOPEN-2025-006019.

144 Leventogiannis K, Kyriazopoulou E, Antonakos N, Kotsaki A, Tsangaris I, Markopoulou D *et al.* Toward personalized immunotherapy in sepsis: The PROVIDE randomized clinical trial. *Cell Rep Med* 2022; **3**: 100817.

145 Machowicz R, Janka G, Wiktor-Jedrzejczak W. Similar but not the same: Differential diagnosis of HLH and sepsis. *Crit Rev Oncol Hematol* 2017; **114**: 1–12.

146 Chaturvedi V, Marsh RA, Zoref-Lorenz A, Owsley E, Chaturvedi V, Nguyen TC *et al.* T-cell activation profiles distinguish hemophagocytic lymphohistiocytosis and early sepsis. *Blood* 2021; **137**: 2337–2346.

147 Beerman I, Maloney WJ, Weissmann IL, Rossi DJ. Stem cells and the aging hematopoietic system. *Curr Opin Immunol* 2010; **22**: 500–506.

148 Yager EJ, Ahmed M, Lanzer K, Randall TD, Woodland DL, Blackman MA. Age-associated decline in T cell repertoire diversity leads to holes in the repertoire and impaired immunity to influenza virus. *Journal of Experimental Medicine* 2008; **205**: 711–723.

149 Goronzy JJ, Lee W-W, Weyand CM. Aging and T-cell diversity. doi:10.1016/j.exger.2006.11.016.

150 Gibson KL, Wu YC, Barnett Y, Duggan O, Vaughan R, Kondeatis E *et al.* B-cell diversity decreases in old age and is correlated with poor health status. *Aging Cell* 2009; **8**. doi:10.1111/j.1474-9726.2008.00443.x.

151 Rodd BG, Tas AA, Taylor KDA. Dysphagia, texture modification, the elderly and micronutrient deficiency: a review. *Crit Rev Food Sci Nutr* 2022; **62**: 7354–7369.

152 Valente Junior CN, Sassi FC, Ritto AP, Pecenin ICSF, Andrade CRF de. Dysphagia in frail elderly: self-reported mealtime symptoms and risk. *Rev Saude Publica* 2025; **59**: e23.

153 Ahuja SK, Manoharan MS, Lee GC, McKinnon LR, Meunier JA, Steri M *et al.* Immune resilience despite inflammatory stress promotes longevity and favorable health outcomes including resistance to infection. *Nat Commun* 2023; **14**: 3286.

154 Pehlivan O, Serin SO, Yesil EE, Demirdag F. Can Monocytopenia Be a New Indicator in Determining Survival in Covid-19 Disease? *Clin Lab* 2021; **67**: 2339–2346.

155 Wu M, Li HL, Luan YY, Feng Y, Yao YM. Monocytopenia and Its Impact on Outcomes in Patients with Severe Sepsis Including Septic Shock: A Case-control Study. *Shock* 2020; **54**: 272–273.

156 Charlier C, Perrodeau É, Leclercq A, Cazenave B, Pilmis B, Henry B *et al.* Clinical features and prognostic factors of listeriosis: the MONALISA national prospective cohort study. *Lancet Infect Dis* 2017; **17**: 510–519.

157 Chung H, Lee JH, Jo YH, Hwang JE, Kim J. Circulating Monocyte Counts and its Impact on Outcomes in Patients With Severe Sepsis Including Septic Shock. *Shock* 2019; **51**: 423–429.

158 Pei B, Zhang J, Lai L, Chen H. Neutrophil-to-lymphocyte ratio as a predictive biomarker for hyperprogressive disease mediated by immune checkpoint inhibitors: a systematic review and meta-analysis. *Front Immunol* 2024; **15**: 1393925.

159 Abensur Vuillaume L, Le Borgne P, Alamé K, Lefebvre F, Bérard L, Delmas N *et al.* Neutrophil-to-lymphocyte ratio and early variation of nlr to predict in-hospital mortality and severity in ed patients with sars-cov-2 infection. *J Clin Med* 2021; **10**: 2563.

160 Wang Y, Dong C, Han Y, Gu Z, Sun C. Immunosenescence, aging and successful aging. *Front Immunol* 2022; **13**: 942796.

161 Lakshmikanth T, Consiglio C, Sardh F, Forlin R, Wang J, Tan Z *et al.* Immune system adaptation during gender-affirming testosterone treatment. *Nature 2024 633:8028* 2024; **633**: 155–164.

162 Kleina SL, Marriott I, Fish EN. Sex-based differences in immune function and responses to vaccination. *Trans R Soc Trop Med Hyg* 2015; **109**: 9–15.

163 Lei Q, Wang D, Sun K, Wang L, Zhang Y. Resistance Mechanisms of Anti-PD1/PDL1 Therapy in Solid Tumors. Front. Cell Dev. Biol. 2020; **8**: 672.

164 Esensten JH, Helou YA, Chopra G, Weiss A, Bluestone JA. CD28 Costimulation: From Mechanism to Therapy. *Immunity* 2016; **44**: 973–988.

165 Plunkett FJ, Franzese O, Finney HM, Fletcher JM, Belaramani LL, Salmon M *et al.* The Loss of Telomerase Activity in Highly Differentiated CD8 + CD28 − CD27 − T Cells Is Associated with Decreased Akt (Ser 473) Phosphorylation. *The Journal of Immunology* 2007; **178**: 7710–7719.

166 Franco-Leyva T, Torres OH, Saez Prieto ME, Boera-Carnicero G, Santos Á, Clotet S *et al.* Early differentiated CD28+ CD27+ T lymphocytes as a biomarker for short and long-term outcomes in older patients with pneumonia. *J Leukoc Biol* 2022; **112**: 1183–1190.

167 Wikby A, Ferguson F, Forsey R, Thompson J, Strindhall J, Löfgren S *et al.* An immune risk phenotype, cognitive impairment, and survival in very late life: impact of allostatic load in Swedish octogenarian and nonagenarian humans. *J Gerontol A Biol Sci Med Sci* 2005; **60**: 556–65.

168 Sopena-Rios M, Ripoll-Cladellas A, Omidi F, Ballouz S, Alquicira-Hernandez J, Oelen R *et al.* Single-cell analysis of the human immune system reveals sex-specific dynamics of immunosenescence. *Nat Aging* 2026; **6**: 932–949.

169 Liu G, Jiang X, Zeng X, Pan Y, Xu H. Analysis of Lymphocyte Subpopulations and Cytokines in COVID-19-Associated Pneumonia and Community-Acquired Pneumonia. *J Immunol Res* 2021; **2021**. doi:10.1155/2021/6657894.

170 Mravec Bencúrová D, Mandíková Š, Daňková P. Age and sex-specific differences in interleukin 4, interferon gamma, macrophage migration inhibitory factor, and vascular endothelial growth factor levels in the tears of healthy subjects. *Eur J Ophthalmol* 2022; **32**: 1900–1906.

171 Zhu J. T Helper Cell Differentiation, Heterogeneity, and Plasticity. *Cold Spring Harb Perspect Biol* 2018; **10**: a030338.

172 European Society for Immunodeficiencies. Common Variable Immunodeficiency (CVI) diagnosis criteria. 2022.https://esid.org/Education/Common-Variable-Immunodeficiency-CVI-diagnosis-criteria.

173 Gruver AL, Hudson LL, Sempowski GD. Immunosenescence of ageing. 2007.

174 Bateman EAL, Ayers L, Sadler R, Lucas M, Roberts C, Woods A *et al.* T cell phenotypes in patients with common variable immunodeficiency disorders: associations with clinical phenotypes in comparison with other groups with recurrent infections. *Clin Exp Immunol* 2012; **170**: 202–211.

175 Klocperk A, Friedmann D, Schlaak AE, Unger S, Parackova Z, Goldacker S *et al.* Distinct CD8 T Cell Populations with Differential Exhaustion Profiles Associate with Secondary Complications in Common Variable Immunodeficiency. *J Clin Immunol* 2022; **42**: 1254–1269.

176 Warnatz K, Denz A, Dräger R, Braun M, Groth C, Wolff-Vorbeck G *et al.* Severe deficiency of switched memory B cells (CD27+IgM−IgD−) in subgroups of patients with common variable immunodeficiency: a new approach to classify a heterogeneous disease. *Blood* 2002; **99**: 1544–1551.

177 Unger S, Seidl M, van Schouwenburg P, Rakhmanov M, Bulashevska A, Frede N *et al.* The TH1 phenotype of follicular helper T cells indicates an IFN-γ–associated immune dysregulation in patients with CD21low common variable immunodeficiency. *Journal of Allergy and Clinical Immunology* 2018; **141**: 730–740.

178 Walsh ZH, Frangieh CJ, Kothapalli N, Levy J, Heck CK, Melms JC *et al.* Scalable generation and functional classification of genetic variants in inborn errors of immunity to accelerate clinical diagnosis and treatment. *Cell* 2025; **188**: 4861-4879.e27.

179 Aygun A, Topyıldız E, Geyik M, Karaca NE, Durmaz A, Aksu G *et al.* Current genetic defects in common variable immunodeficiency patients on the geography between Europe and Asia: a single-center experience. *Immunol Res* 2023; **1**: 1–9.

180 Christiansen M, Offersen R, Jensen JMB, Petersen MS, Larsen CS, Mogensen TH. Identification of Novel Genetic Variants in CVID Patients With Autoimmunity, Autoinflammation, or Malignancy. *Front Immunol* 2020; **10**: 486420.

181 Aggarwal V, Banday AZ, Jindal AK, Das J, Rawat A. Recent advances in elucidating the genetics of common variable immunodeficiency. *Genes Dis* 2020; **7**: 26–37.

8. Annex

T0 (x̄ ± SD)	Men	Women	p	Surv			Non surv			p
				Men	Women	Total	Men	Women	Total	
	n = 72	n = 42		n = 33	n = 26	n = 59	n = 39	n = 16	n = 55	
IgG (mg/dL)	1141.47 ± 374.86	1052.86 ± 389.64	0.1403	1022.39 ± 336.64	1039.38 ± 419.5	1029.88 ± 372.09	1242.23 ± 379.97	1074.75 ± 347.62	1193.51 ± 375.58	0.0393
IgA (mg/dL)	376.16 ± 212.66	352.89 ± 216.68	0.3237	354.21 ± 191.11	344.78 ± 213.97	350.05 ± 199.77	394.72 ± 230.15	366.06 ± 227.44	386.39 ± 227.63	0.602
IgM (mg/dL)	106.97 ± 77.11	183.89 ± 321.93	0.1824	96.4 ± 64.64	143.9 ± 182.44	117.33 ± 131.22	115.92 ± 86.09	248.89 ± 469.6	154.6 ± 264.93	0.375
IgE UI/mL	230.51 ± 314.91	218.94 ± 646.57	0.1882	252.6 ± 332.48	181.85 ± 281.81	221.42 ± 310.6	211.82 ± 302.37	279.2 ± 1002.03	231.43 ± 586.68	0.034
CH50 UI/mL	60.11 ± 17.99	65.49 ± 22.46	0.2317	65.64 ± 17.48	63.32 ± 21.3	64.58 ± 19.17	55.72 ± 17.38	69.01 ± 24.52	59.58 ± 20.41	0.0881
C3 (mg/dL)	103.4 ± 31.03	119.17 ± 39.04	0.0368	113.77 ± 22.17	128.62 ± 41.04	120.31 ± 32.44	94.62 ± 34.81	103.83 ± 30.85	97.3 ± 33.69	0.0017
C4 (mg/dL)	24.47 ± 8.81	25.13 ± 10.06	0.8325	25.21 ± 7.69	26.32 ± 10.64	25.7 ± 9.04	23.85 ± 9.71	23.2 ± 9.04	23.66 ± 9.44	0.783

T1 (x̄ ± SD)	Men	Women	p	Surv			Non surv			p
				Men	Women	Total	Men	Women	Total	
	n = 53	n = 41		n = 32	n = 33	n = 65	n = 21	n = 8	n = 29	
IgG (mg/dL)	1293.36 ± 687.57	1155.85 ± 384.82	0.3889	1107.09 ± 325.93	1174.7 ± 393.57	1141.42 ± 360.64	1577.19 ± 961.46	1078.12 ± 359.91	1439.52 ± 862.67	0.0363
IgA (mg/dL)	354.25 ± 175.37	349.41 ± 294.88	0.1884	342.34 ± 168.25	348.9 ± 287.63	345.67 ± 234.71	372.38 ± 188.45	351.5 ± 344.49	366.62 ± 234.79	0.421
IgM (mg/dL)	131.48 ± 123.92	135.31 ± 163.65	0.8132	138.43 ± 146.59	138.49 ± 174.7	138.46 ± 160.21	120.9 ± 80.13	122.16 ± 115.18	121.25 ± 88.9	0.946
IgE UI/mL	140.71 ± 207.21	110.11 ± 182.01	0.4212	144.71 ± 212.41	132.54 ± 196.56	138.53 ± 203	134.62 ± 204.05	17.6 ± 23.06	102.34 ± 180.85	0.0814
CH50 UI/mL	66.35 ± 17.54	72.51 ± 18.44	0.1373	70.34 ± 18.18	70.52 ± 18.74	70.44 ± 18.32	60.45 ± 15.08	80.7 ± 15.59	66.04 ± 17.55	0.0404
C3 (mg/dL)	103.35 ± 18.89	108.97 ± 22.46	0.2387	107.36 ± 18.83	107.96 ± 23.06	107.66 ± 20.93	97.23 ± 17.69	113.16 ± 20.64	101.62 ± 19.56	0.243
C4 (mg/dL)	23.9 ± 7.48	24.8 ± 6.58	0.6148	23.88 ± 7.18	23.65 ± 5.88	23.76 ± 6.51	23.94 ± 8.08	29.53 ± 7.59	25.48 ± 8.22	0.29

Supplementary Table 1. Immunoglobulin and complement values from T0 and T1 by survival and sex stratification, expressed as mean and standard deviation. Significant p values are highlighted in green.

T0 (Median [IQR])	Men	Women	p	Surv			Non surv			p
				Men	Women	Total	Men	Women	Total	
	n = 72	n = 42		n = 33	n = 26	n = 59	n = 39	n = 16	n = 55	
Leukocytes $x10^6$/L	9775 [7592.5 – 12487.5]	8985 [7190 – 11480]	0.3735	10320 [7930 – 14900]	8845 [7190 – 9738]	9230 [7565 –	9610 [7060 – 11760]	10880 [7668 – 12178]	9750 [7085 – 11885]	0.2680
Neutrophils %	77 [70 – 85]	69 [61 – 82]	0.0105	77 [66 – 83]	62 [60 – 76]	71 [61 – 82]	78 [73 – 86]	72 [66 – 82]	77 [70 – 85]	0.0228
Monocytes %	8 [5 – 9]	8 [6 – 11]	0.2251	8 [6 – 10]	7 [6 – 10]	8 [6 – 10]	7 [4 – 9]	9 [7 – 11]	8 [4 – 10]	0.2210
Lymphocytes %	11 [6 – 16]	19 [9 – 27]	0.0034	12 [7 – 19]	23 [14 – 28]	17 [8 – 25]	11 [5 – 14]	13 [8 – 21]	11 [6 – 16]	0.0038
Neutrophils $x10^6$/L	7660 [5165 – 9887.5]	5750 [4545 – 8912.5]	0.1031	8390 [5220 – 11280]	5250 [4440 – 7565]	6300 [4720 –	7330 [5065 – 8840]	7250 [5640 – 9480]	7330 [5180 – 8935]	0.1760
Monocytes $x10^6$/L	750 [450 – 957.5]	715 [560 – 927.5]	1	810 [600 – 1160]	645 [560 – 827.5]	720 [575 – 965]	680 [355 – 880]	835 [542.5 –	760 [400 – 920]	0.0742
Lymphocytes $x10^6$/L	1135 [677.5 – 1587.5]	1430 [940 – 2227.5]	0.0167	1370 [850 – 1760]	1530 [1295 – 2398]	1490 [1075 – 2020]	940 [505 – 1435]	1000 [783 – 1608]	970 [555 – 1515]	0.0008

Supplementary Table 2. Leukocyte values from T0 by survival and sex stratification, expressed as median and interquartile range (IQR). Significant p values are highlighted in green.

T1 (Median [IQR])	Men	Women	p	Surv			Non surv			p
	n = 53	n = 41		Men n = 32	Women n = 33	Total n = 65	Men n = 21	Women n = 8	Total n = 29	
Leukocytes x10^6/L	7250 [5860 – 8730]	7210 [6000 – 9520]	0.7059	6645 [5728 – 7988]	6930 [6160 – 9420]	6850 [5890 – 8340]	7990 [6720 – 10500]	7840 [5645 – 10598]	7990 [6590 – 10500]	0.0984
Neutrophils %	65 [58 – 74]	65 [58 – 68]	0.2465	61 [53 – 69]	63 [57 – 67]	61 [55 – 69]	73 [70 – 78]	67 [66 – 71]	72 [66 – 78]	0.0001
Monocytes %	9 [7 – 10]	8 [7 – 10]	0.4234	9 [7 – 11]	8 [8 – 9]	8 [7 – 10]	9 [7 – 10]	10 [7 – 11]	9 [7 – 10]	0.4620
Lymphocytes %	21 [14 – 30]	23 [20 – 29]	0.1094	26 [20 – 32]	24 [21 – 29]	25 [21 – 31]	14 [12 – 18]	20 [17 – 23]	16 [12 – 20]	<0.0001
Neutrophils x10^6/L	4580 [3720 – 6400]	4620 [3730 – 6220]	0.8908	4150 [2733 – 5335]	4470 [3730 – 6010]	4160 [3150 – 5520]	5550 [4580 – 7900]	5305 [3753 – 7175]	5550 [4540 – 7900]	0.0091
Monocytes x10^6/L	660 [470 – 820]	590 [510 – 800]	0.7545	645 [460 – 775]	570 [500 – 720]	590 [480 – 760]	700 [500 – 840]	765 [560 – 895]	720 [550 – 860]	0.4110
Lymphocytes x10^6/L	1480 [1070 – 1880]	1670 [1350 – 2160]	0.0284	1665 [1330 – 2025]	1800 [1370 – 2160]	1690 [1350 – 2090]	1070 [840 – 1490]	1430 [1347 – 1775]	1340 [910 – 1570]	0.0020

Supplementary Table 3. Leukocytes values from T1 by survival and sex stratification, expressed as median and interquartile range (IQR). Significant p values are highlighted in green.

	Survivors (n = 28)			Non-survivors (n = 18)		
Median [IQR]	T0	T1	p	T0	T1	p
Leukocytes x10^6/L	9140 [7468 – 10813]	7450 [6398 – 8928]	0.0071	11500 [9063 – 11970]	8745 [6765 – 10950]	0.0539
Neutrophils %	71 [61 – 77]	64 [58 – 70]	0.1256	77 [72 – 81]	73 [64 – 79]	0.0432
Monocytes %	8 [7 – 10]	8 [7 – 10]	0.3386	8 [5 – 8]	9 [7 – 10]	0.0268
Lymphocytes %	19 [8 – 28]	24 [20 – 30]	0.0662	12 [9 – 15]	14 [12 – 18]	0.0814
Neutrophils x10^6/L	5875 [4635 – 8853]	4450 [4008 – 6370]	0.0118	7890 [7108 – 9478]	6025 [4558 – 8335]	0.0468
Monocytes x10^6/L	800 [600 – 985]	600 [543 – 855]	0.0962	775 [568 – 890]	710 [573 – 878]	0.7938
Lymphocytes x10^6/L	1625 [1103 – 2293]	1830 [1415 – 2160]	0.2844	1125 [918 – 1525]	1325 [980 – 1750]	0.9133

	Men (n = 26)			Women (n = 20)		
Median [IQR]	T0	T1	p	T0	T1	p
Leukocytes x10^6/L	10470 [8640 – 11978]	7700 [6623 – 9505]	0.0031	8985 [7418 – 11195]	7665 [6713 – 9990]	0.1327
Neutrophils %	77 [74 – 80]	71 [60 – 75]	0.0008	62 [60 – 71]	66 [58 – 70]	0.9854
Monocytes %	8 [6 – 9]	9 [8 – 11]	0.0010	8 [7 – 11]	8 [7 – 9]	0.6477
Lymphocytes %	11 [7 – 15]	17 [14 – 26]	0.0029	24 [18 – 28]	23 [21 – 28]	0.6477
Neutrophils x10^6/L	8065 [6460 – 10333]	4860 [4315 – 6808]	0.0014	5465 [4635 – 7600]	4995 [4008 – 6910]	0.3300
Monocytes x10^6/L	775 [555 – 900]	725 [565 – 890]	0.8086	815 [630 – 935]	580 [558 – 668]	0.0420
Lymphocytes x10^6/L	1110 [805 – 1555]	1440 [1100 – 1810]	0.0619	2040 [1505 – 2453]	1985 [1435 – 2165]	0.6813

Supplementary Table 4. Paired analysis of leukocytes by survival and sex stratification, expressed as median and interquartile range (IQR). Significant p values are highlighted in green.

	Cluster 1	Cluster 2	Cluster 3	Cluster 4	Cluster 5	p
Early T cells %	38.5 [21.7 – 42.9]	69.4 [54.1 – 77.1]	64.9 [49.2 – 73]	52.5 [43.2 – 64.6]	68.7 [59 – 78.5]	0.0005
Int T cells %	7.3 [5.8 – 12.5]	7 [6 – 10.4]	8.4 [6.9 – 10.5]	10.4 [8.1 – 14.3]	6.6 [5.4 – 8.7]	0.0120
Late T cells %	48.5 [40.2 – 66.9]	16.2 [8.2 – 28.8]	21.3 [14.9 – 33.3]	27.4 [14.8 – 37.7]	14.6 [12 – 20.1]	0.0012
$CD4^+$ Early T cells %	53.3 [34.3 – 63.6]	83.1 [78.2 – 86.2]	79.9 [68.3 – 85.4]	71.7 [60.2 – 75.6]	84.8 [75.9 – 88.4]	0.0001
$CD4^+$ Int T cells %	13.3 [9.2 – 16.3]	9.2 [7.6 – 12.1]	8.7 [7.4 – 13.6]	14.9 [10.9 – 17.6]	6.9 [5.4 – 9.9]	0.0005
$CD4^+$ Late T cells %	26.6 [18.6 – 52.4]	2.3 [0.5 – 9.1]	7.2 [2.9 – 16]	9.3 [7.6 – 18.4]	3.8 [2 – 5.2]	<0.0001
$CD8^+$ Early T cells %	18.4 [11.7 – 30]	42.1 [21.2 – 55.6]	32 [17.9 – 46.7]	35.4 [19.2 – 43.9]	34.2 [22.2 – 46.4]	0.1410
$CD8^+$ Int T cells %	4.2 [3.2 – 7.5]	4.2 [3.1 – 8.2]	4.8 [3.1 – 7]	4.7 [3.2 – 7.7]	4.4 [3.3 – 6.2]	0.9920
$CD8^+$ Late T cells %	68.8 [53 – 73]	38.1 [22.4 – 60.2]	49.5 [36.2 – 62.8]	48.1 [25 – 60.5]	44.5 [33.7 – 59.6]	0.0875

Supplementary Table 5. T differentiated cell values by T-helper clusters.

	n	IL2	IL4	IL6	IL10	TNF	IFNg	IL17A
Cluster 1	7	1.26	**4.29**	1.77	0.77	0.69	-0.21	-0.39
x̃ (IQR)		(1.32)	**(1.8)**	(5.41)	(0.9)	(0.97)	(1.33)	(1.38)
Cluster 2	24	-0.44	0.4	1.26	-0.21	0.14	-0.08	0.08
x̃ (IQR)		(1.11)	(1.84)	(6.36)	(2.03)	(1.46)	(1.14)	(1.3)
Cluster 3	27	0.08	0.07	1.93	0.17	-0.23	0.13	-0.2
x̃ (IQR)		(2.02)	(2.66)	(4.8)	(1.94)	(1.23)	(1.91)	(1.6)
Cluster 4	20	-0.35	**-0.33**	1.04	-0.65	-0.4	-0.38	1.1
x̃ (IQR)		(1.65)	**(1.46)**	(5.45)	(0.79)	(1.41)	(1.47)	(2.34)
Cluster 5	17	-0.29	0.08	1.98	0.44	0.69	-0.37	0.05
x̃ (IQR)		(1.89)	(2.81)	(7.49)	(0.97)	(2.6)	(1.25)	(2.15)
Kruskal-Wallis (p)		ns	*	ns	ns	ns	ns	ns

Supplementary Table 6. Cytokine median and interquartilic range of each of the 5 clusters defined by T-helper profiles.. *p<0.05, ns=non-significant

	Men n = 63	Women n = 32	p	Surv Men n = 29	Surv Women n = 18	Surv Total n = 47	Non surv Men n = 34	Non surv Women n = 14	Non surv Total n = 48	p
IL-2	-0,3148 [-0,76 - 0,97]	0,2194 [-0,69 - 1,62]	ns	-0,3148 [-0,86 - 0,54]	-0,2475 [-0,93 - 1,39]	-0,3148 [-0,83 - 0,65]	-0,319 [-0,74 - 1,21]	0,3699 [0,01 - 7,84]	0,0644 [-0,68 - 1,74]	ns
IL-4	**0,0107 [-0,90 - 1,71]**	**0,989 [-0,20 - 4,23]**	**0,0319**	**0,0107 [-0,82 - 1,77]**	**-0,0136 [-0,36 - 2,17]**	**0,0107 [-0,67 - 1,84]**	**-0,04435 [-0,93 - 1,90]**	**2,861 [0,79 - 13,66]**	**0,5461 [-0,39 - 1,18]**	*
IL-6	1,766 [0,32 - 6,43]	2,042 [-0,17 - 6,20]	ns	1,929 [0,26 - 5,54]	0,934 [-0,62 - 3,72]	1,536 [-0,33 - 4,48]	1,385 [0,31 - 6,79]	4,166 [0,97 - 14,18]	2,19 [0,42 - 7,04]	ns
IL-10	-0,1067 [-0,76 - 0,88]	-0,2751 [-1,11 - 0,98]	ns	0,1117 [-0,68 - 0,64]	-0,6855 [-1,20 - 0,64]	-0,3101 [-0,93 - 0,61]	-0,1915 [-0,81 - 1,08]	0,3033 [-0,95 - 1,73]	-0,1124 [-0,83 - 1,35]	ns
TNF	0,1488 [-0,75 - 0,97]	-0,161 [-0,73 - 0,93]	ns	0,2953 [-0,62 - 0,75]	-0,4429 [-0,82 - 0,73]	-0,0454 [-0,68 - 0,69]	0,106 [-0,92 - 1,67]	0,1295 [-0,36 - 1,62]	0,106 [-0,78 - 1,60]	ns
IFN	-0,1546 [-0,62 - 1,16]	-0,2618 [-0,75 - 0,67]	ns	-0,2075 [-0,84 - 0,70]	-0,334 [-0,99 - 0,76]	-0,2075 [-0,94 - 0,67]	-0,0772 [-0,55 - 1,54]	-0,1638 [-0,43 - 0,69]	-0,1037 [-0,53 - 1,10]	ns
IL17A	**0,4281 [-0,33 - 1,75]**	**-0,5578 [-0,91 - 0,74]**	**0,004**	**0,1131 [-0,27 - 1,90]**	**-0,5258 [-0,90 - 0,43]**	**0,0491 [-0,77 - 1,44]**	**0,5755 [-0,44 - 1,76]**	**-0,6341 [-0,96 - 0,97]**	**0,4983 [-0,77 - 1,57]**	*

Supplementary Table 7. Cytokine levels of men, women, survivors and non-survivors. *p<0.05, **<0.01, ***p<0.001, ns=non-significant

T0 (Median [IQR])	Men	Women	p	Surv			Non surv			p
	n = 72	n = 42		Men n = 33	Women n = 26	Total n = 59	Men n = 39	Women n = 16	Total n = 55	
Early T cells %	61.0 [47.5 – 75.0]	64.9 [43.4 – 72.6]	0.4451	61.9 [44.0 – 78.4]	68.1 [51.3 – 74.3]	67.9 [45.5 – 76.7]	60.4 [51.8 – 71.6]	48.4 [35.5 – 66.2]	59.7 [43.9 – 70.9]	0.1280
Int T cells %	8.4 [6.1 – 11.8]	7.9 [6.7 – 10.7]	0.7026	8.1 [6.4 – 9.8]	7.3 [5.2 – 11.9]	7.3 [6.2 – 10.6]	8.9 [6.0 – 13.4]	8.2 [7.5 – 9.7]	8.4 [6.3 – 12.0]	0.5630
Late T cells %	20.1 [10.8 – 33.9]	21.3 [14.7 – 33.8]	0.461	18.8 [11.2 – 40.5]	18.1 [9.6 – 25.7]	18.8 [10.0 – 34.0]	22.4 [10.6 – 31.5]	32.3 [20.4 – 52.7]	23.0 [14.4 – 33.8]	0.0286
CD4+ Early T cells %	79.8 [67.8 – 85.9]	78.1 [60.1 – 85.5]	0.4956	82.4 [70.4 – 86.9]	80.7 [64.0 – 87.5]	81.5 [65.9 – 87.2]	78.7 [67.5 – 84.7]	68.2 [59.3 – 82.9]	76.6 [66.3 – 84.5]	0.3540
CD4+ Int T cells %	9.4 [7.1 – 15.5]	10.6 [8.1 – 14.7]	0.7223	8.9 [7.4 – 11.9]	9.2 [6.0 – 15.5]	8.9 [6.9 – 14.2]	9.7 [6.9 – 17.2]	11.3 [9.2 – 13.3]	11.0 [8.2 – 15.7]	0.3300
CD4+ Late T cells %	7.1 [1.5 – 12.2]	6.7 [3.4 – 17.3]	0.1711	8.1 [2.0 – 10.9]	6.1 [1.9 – 12.1]	6.8 [1.9 – 12.1]	5.1 [1.0 – 12.4]	16.2 [5.7 – 25.7]	7.2 [2.9 – 17.1]	0.0581
CD8+ Early T cells %	35.4 [19.2 – 48.1]	32.0 [20.3 – 43.8]	0.4468	36.4 [17.9 – 48.9]	37.9 [22.9 – 48.6]	36.4 [20.5 – 48.9]	35.0 [19.7 – 46.7]	21.3 [13.0 – 41.3]	29.0 [19.1 – 44.1]	0.1160
CD8+ Int T cells %	4.6 [3.4 – 8.2]	3.8 [2.7 – 5.5]	0.0471	4.6 [3.4 – 6.2]	3.6 [2.5 – 6.2]	4.4 [3.1 – 6.5]	4.6 [3.4 – 8.5]	4.0 [3.1 – 5.4]	4.4 [3.3 – 8.1]	0.2160
CD8+ Late T cells %	47.3 [29.4 – 61.7]	47.7 [36.8 – 61.8]	0.4882	51.0 [26.8 – 64.9]	38.9 [29.5 – 56.1]	44.5 [28.0 – 61.1]	40.9 [31.0 – 61.5]	61.1 [45.4 – 72.1]	51.9 [33.7 – 62.5]	0.0210
Early T cells/uL	422 [239 – 680]	577 [288 – 928]	0.1069	569 [348 – 896]	756 [466 – 1313]	616 [390 – 1026]	304 [196 – 577]	372 [240 – 513]	333 [208 – 555]	0.0005
Int T cells /uL	67 [36 – 104]	80 [51 – 142]	0.0982	76 [38 – 101]	103 [55 – 171]	82 [47 – 124]	60 [26 – 110]	64 [45 – 100]	62 [33 – 110]	0.1180
Late T cells /uL	122 [56 – 351]	202 [111 – 388]	0.0461	203 [93 – 376]	188 [119 – 248]	189 [94 – 354]	116 [46 – 192]	234 [108 – 529]	123 [65 – 349]	0.0445
CD4+ Early T cells /uL	336 [188 – 574]	440 [253 – 784]	0.1274	421 [252 – 712]	634 [317 – 1026]	541 [274 – 829]	241 [160 – 473]	272 [205 – 400]	260 [170 – 431]	0.0012
CD4+ Int T cells /uL	50 [27 – 81]	64 [38 – 113]	0.0785	60 [30 – 75]	83 [45 – 131]	64 [36 – 103]	50 [18 – 86]	51 [33 – 71]	50 [22 – 86]	0.0766
CD4+ Late T cells /uL	32 [5 – 70]	49 [16 – 93]	0.0352	38 [10 – 88]	46 [16 – 80]	46 [10 – 83]	21 [2 – 51]	65 [16 – 126]	31 [10 – 76]	0.0486
CD8+ Early T cells/uL	76 [31 – 143]	101 [48 – 151]	0.1702	94 [51 – 173]	113 [68 – 167]	111 [56 – 171]	58 [23 – 110]	59 [35 – 137]	58 [25 – 117]	0.0094
CD8+ Int T cells /uL	10 [7 – 20]	13 [9 – 24]	0.3368	12 [8 – 24]	12 [7 – 23]	12 [8 – 24]	10 [5 – 16]	15 [9 – 23]	11 [6 – 19]	0.3800
CD8+ Late T cells /uL	90 [37 – 214]	139 [78 – 258]	0.0254	135 [55 – 289]	129 [78 – 189]	132 [65 – 265]	76 [30 – 127]	169 [86 – 411]	100 [37 – 180]	0.0343

Supplementary Table 8. Sex-stratified analysis of differentiated T cell subpopulations at T0.

T1 (Median [IQR])	Men	Women	p	Surv			Non surv			p
				Men	Women	Total	Men	Women	Total	
	n = 53	n = 41		n = 32	n = 33	n = 65	n = 21	n = 8	n = 29	
Early T cells %	62.6 [48.7 – 72.9]	60.0 [48.4 – 71.4]	0.6750	64.4 [47.4 – 73.9]	61.3 [48.4 – 71.4]	62.2 [48.0 – 73.4]	62.3 [52.6 – 69.2]	57.9 [48.0 – 63.2]	60.0 [50.5 – 68.1]	0.7020
Int T cells %	9.9 [7.5 – 13.9]	8.3 [5.6 – 10.1]	0.0597	9.1 [7.3 – 12.5]	8.3 [5.8 – 10.1]	8.8 [6.6 – 12.0]	10.4 [7.7 – 15.0]	7.7 [5.3 – 10.1]	10.2 [5.7 – 14.9]	0.1280
Late T cells %	19.1 [9.8 – 32.3]	22.7 [14.7 – 30.4]	0.5752	16.9 [9.7 – 32.4]	21.5 [14.0 – 28.7]	19.6 [11.3 – 31.8]	21.0 [9.8 – 30.5]	26.1 [16.3 – 33.4]	22.2 [14.8 – 31.0]	0.8050
CD4+ Early T cells %	78.9 [65.3 – 88.4]	76.5 [60.8 – 87.0]	0.5023	82.4 [68.0 – 89.6]	78.3 [60.8 – 87.7]	81.2 [65.0 – 89.3]	78.4 [65.3 – 83.0]	75.2 [70.4 – 80.8]	77.8 [65.3 – 81.0]	0.4510
CD4+ Int T cells %	12.5 [8.1 – 17.4]	10.3 [7.5 – 13.7]	0.1145	9.6 [7.9 – 15.0]	10.0 [7.3 – 13.5]	9.8 [7.5 – 14.3]	14.2 [11.5 – 18.7]	12.4 [8.3 – 13.9]	13.7 [8.7 – 17.7]	0.1220
CD4+ Late T cells %	2.7 [0.4 – 12.2]	6.4 [3.2 – 17.5]	0.1036	1.9 [0.6 – 13.2]	6.4 [3.2 – 17.5]	5.5 [0.8 – 16.4]	3.1 [0.4 – 12.2]	6.4 [4.1 – 11.9]	5.1 [1.0 – 12.2]	0.3980
CD8+ Early T cells %	35.1 [25.8 – 50.3]	36.2 [21.2 – 41.6]	0.3683	33.8 [24.2 – 58.3]	36.2 [22.2 – 42.8]	34.8 [22.2 – 51.8]	36.3 [30.4 – 44.1]	30.0 [20.6 – 40.2]	36.3 [23.5 – 41.2]	0.7150
CD8+ Int T cells %	5.8 [3.1 – 9.2]	3.4 [2.6 – 5.8]	0.0163	6.0 [4.0 – 9.2]	3.9 [2.6 – 5.8]	5.0 [2.8 – 7.4]	4.0 [3.0 – 8.2]	3.1 [2.3 – 5.8]	3.9 [2.7 – 7.2]	0.0934
CD8+ Late T cells %	40.6 [19.1 – 59.1]	44.9 [32.9 – 58.1]	0.2196	41.9 [18.4 – 60.8]	44.1 [31.8 – 57.4]	43.4 [23.1 – 58.1]	39.3 [30.2 – 46.3]	53.7 [39.6 – 62.1]	40.6 [34.9 – 59.0]	0.5460
Early T cells/uL	712 [466 – 928]	691 [566 – 943]	0.2998	759 [604 – 975]	748 [587 – 957]	755 [592 – 967]	466 [318 – 712]	602 [565 – 681]	565 [381 – 712]	0.0027
Int T cells /uL	114 [66 – 150]	106 [68 – 155]	0.7488	117 [86 – 174]	106 [68 – 156]	114 [71 – 160]	101 [53 – 131]	103 [82 – 112]	101 [53 – 129]	0.3920
Late T cells /uL	189 [109 – 372]	273 [152 – 393]	0.0877	205 [135 – 415]	274 [161 – 393]	239 [142 – 407]	135 [96 – 303]	259 [149 – 417]	182 [108 – 303]	0.2430
CD4+ Early T cells /uL	494 [366 – 689]	559 [434 – 768]	0.1028	572 [426 – 721]	585 [448 – 790]	582 [436 – 785]	366 [255 – 575]	478 [379 – 550]	390 [270 – 575]	0.0022
CD4+ Int T cells /uL	81 [47 – 113]	81 [56 – 117]	0.6583	86 [55 – 114]	85 [56 – 124]	85 [55 – 118]	75 [43 – 109]	75 [61 – 81]	75 [45 – 95]	0.4440
CD4+ Late T cells /uL	13 [3 – 87]	54 [22 – 119]	0.0109	13 [5 – 90]	57 [22 – 124]	38 [8 – 119]	13 [2 – 58]	41 [21 – 84]	29 [3 – 80]	0.0766
CD8+ Early T cells/uL	139 [67 – 215]	122 [87 – 192]	0.9271	146 [106 – 252]	137 [86 – 192]	144 [97 – 248]	105 [62 – 159]	119 [89 – 135]	106 [63 – 155]	0.1400
CD8+ Int T cells /uL	22 [11 – 33]	15 [10 – 25]	0.1273	25 [15 – 45]	15 [10 – 25]	20 [11 – 34]	16 [9 – 24]	16 [12 – 22]	16 [9 – 24]	0.0569
CD8+ Late T cells /uL	133 [60 – 252]	188 [95 – 294]	0.1518	148 [62 – 271]	188 [88 – 294]	173 [86 – 294]	129 [54 – 211]	202 [129 – 359]	133 [72 – 256]	0.3970

Supplementary Table 9. Sex-stratified analysis of differentiated T cell subpopulations at T1.

	Cluster 1	Cluster 2	p
Lymphocytes (cells/uL)	3444.2	1257	0.7105
T cells %	83.69	69.88	0.0755
T CD4 cells %	53.02	40.64	0.3301
T CD8 cells %	28.12	25.52	0.9399
B cells %	10.71	10.48	0.9399
NK cells %	5.31	19.02	0.0336
CD4 DR- CD38+ %	24.45	31.86	0.7105
CD4 DR- CD38- %	46.63	57.98	0.7105
CD8 DR+ CD38- %	17.9	12.88	0.5035
CD8 DR+ CD38+ %	24.01	4.57	0.0056
CD8 DR- CD38+ %	19.96	14.7	0.5035
CD8 DR- CD38- %	38.13	66.74	0.0056
CD4 T effector %	84.53	75.93	0.414
CD4 T reg %	1.5	6.04	0.0336
Ratio Teff/Treg	136.06	17.32	0.0336
CD3 early diff %	56.55	67.33	0.6042
CD3 inter diff %	16.1	10.52	0.1063
CD3 terminally diff %	20.83	19.43	0.8252
CD4 early diff %	74.79	83.01	0.0503
CD4 inter diff %	24.44	9.55	0.0028
CD4 terminally diff %	0.74	7.42	0.5035
CD8 early diff %	40.87	53.11	0.414
CD8 inter diff %	2.9	9.57	0.1483
CD8 terminally diff %	38.6	30.4	0.6042
CD3 T naive %	7.01	25.17	0.0196
CD3 central mem %	22.64	23.45	0.8252
CD3 T eff mem %	42.75	23.86	0.2601
CD3 TEMRA %	27.6	26.74	1
CD4 T naive %	6.85	29.9	0.0336
CD4 central mem %	41.51	31.4	0.3301
CD4 T eff mem %	47.49	30.61	0.1986
CD4 TEMRA %	4.15	8.08	0.8252
CD8 T naive %	18.55	21.97	0.6881
CD8 central mem %	4.89	9.23	0.5035
CD8 T eff mem %	20.49	17.31	0.414
CD8 TEMRA %	56.07	51.49	0.7105
Th0 %	8.07	33.07	0.0028
Th1 %	43.14	21.8	0.0755
Th1-2 %	16.4	15.14	0.8252
Th2 %	0.66	3.94	0.0028
Th17 %	1.25	8.73	0.0112
Th1-17 %	25.53	11.37	0.0336
Th9 %	22.51	18.03	0.6042
Th22 %	0.71	2.85	0.1483
B naive %	79.99	56.48	0.0755
B class non switched %	9.17	19.7	0.2601
B class switched %	1.7	4.84	0.6741
B marginal zone %	14.93	22.4	0.7105
B IgD CD27 %	2.85	7.31	0.5035
B $CD19^{low}$ %	1.22	1	0.7105
B $CD21^{low}$ %	50.37	13.36	0.0028
B plasmablasts %	0.28	0.36	0.8196
B transicionales %	13.61	3.05	0.0336

Supplementary Table 10. Mean and U-Mann Whitney test for each variable included in CVID derivation cohort clustering.